Angewandte Chemie
Eine Zeitschrift der Gesellschaft Deutscher Chemiker

Supporting Information

Nonconventional Fluorescent Non-Isocyanate Polyurethane Foams for Multipurpose Sensing Applications

M. Mahapatra, M. Bourguignon, B. Grignard, M. Vandevenne, M. Galleni, C. Detrembleur**

Supporting Information

Nonconventional Fluorescent Non-Isocyanate Polyurethane Foams for Multipurpose Sensing Applications

Manas Mahapatra, Maxime Bourguignon, Bruno Grignard, Marylène Vandevenne, Moreno Galleni, and Christophe Detrembleur**

Dr. Manas Mahapatra*, Dr. Maxime Bourguignon, Dr. Bruno Grignard, Dr. Christophe Detrembleur*

Center for Education and Research on Macromolecules (CERM), CESAM Research Unit, Department of Chemistry, University of Liege, Liege, Belgium.

E-mail: christophe.detrembleur@uliege.be

Dr. Christophe Detrembleur

WEL Research Institute, avenue Pasteur, 6, 1300 Wavre, Belgium.

Dr. Bruno Grignard

FRITCO$_2$T Platform, CESAM Research Unit, University of Liege, Liege, Belgium.

Dr. Marylène Vandevenne, Dr. Moreno Galleni

Laboratory of Enzymology and Protein Folding, Centre for Protein Engineering, InBioS, University of Liege, Liege, Belgium.

1. Experimental

1.1. Materials

Trimethylol propane triglycidyl ether (TMPTE, Aldrich, technical grade); m-xylylenediamine (XDA, Aldrich, 99%); 1,2-bis(2-aminoethoxy)ethane (EDR, TCI, >98%); 1,3-cyclohexanedimethanamine (BAC, TCI, >98%); polyethyleneimine (PEI 25,000, branched, Aldrich, 99%, average M_n = 10,000 GPC); tetrabutylammonium iodide (TBAI, Aldrich, 99%); 1,8-diazabicyclo[5.4.0]undec-7-ene (DBU, Sigma-Aldrich, 98%); and potassium hydroxide (KOH, VWR, 90%) were used without further modification. Calcium chloride dehydrate ($CaCl_2$. H_2O, Sigma-Aldrich, >99%); Potassium chloride (KCl, Sigma-Aldrich, >99%); Nickel(II) acetate tetrahydrate ($Ni(OCOCH_3)_2{\cdot}4H_2O$, Merck), Barium nitrate ($BaNO_3$), Copper(II) acetate monohydrate ($Cu(CO_2CH_3)_2{\cdot}H_2O$, Merck), copper(II) sulfate ($CuSO_4$, VWR, 98%), copper(II) bromide, ($CuBr_2$, Aldrich), Iron(III) nitrate nonahydrate ($Fe(NO_3)_3 \cdot 9\ H_2O$, Sigma, >98%), Manganese(II) acetate tetrahydrate ($(CH_3COO)_2Mn{\cdot}4H_2O$, Janssen chimica); Magnesium chloride ($MgCl_2 \cdot 6H_2O$, Sigma); Cobalt(II) acetate, ($(CH_3CO_2)_2Co$, ABCR, 98%), Zinc chloride ($ZnCl_2$, UCB), Iron(II) sulfate heptahydrate ($FeSO_4{\cdot}7H_2O$, Sigma, 99%), Aluminium nitrate nonahydrate ($Al(NO_3)_3{\cdot}9\ H_2O$, Aldrich, 98%) and Mercury(II) acetate ($Hg(CH_3COO)_2$, Sigma-Aldrich) were used for sensing-quantification-exclusion study. The Ciprofloxacin (Fluka, >98%, HPLC), erythromycin (Fluka, >95%, NT), ampicillin sodium salt (Gentaur), Bacitracin (Fluka), Kanamycin monosulfate (USP grade, MP Biomedical), Neomycin sulfate (Sigma), tetracycline chloride (Fluka, >98%) and cephalexin (Sigma) antibiotics were purchased and used for antibiotic sensing without modification.

1.2. Synthesis procedures

1.2.1a. Trimethylolpropane tri-cyclic carbonate (TMPTC) synthesis

In a 250 mL high pressure reactor, trimethylolpropane triglycidyl ether (TMPTE, 60 g, 198.4 mmol) and tetrabutylammonium iodide (1830 mg, 2.73 mmol) were introduced. At 80 °C and 100 bar of CO_2, the cell was then brought to equilibrium. Under stirring, the reaction continued for 24 h. The product was then recovered upon depressurization, and any remaining CO_2 was eliminated under vacuum for 16 h at 60 °C. The full conversion of epoxide into five membered cyclic carbonate was checked by ^1H and ^{13}C NMR spectroscopy in $CDCl_3$ [1].

1.2.1b. TMPTC synthesis in kilogram scale

In a 2.0 L high pressure cell reactor, 1.157 kg of TMPTE and 35.29 g of tetrabutylammonium iodide (TBAI, 2.5 mol% vs TMPTE) were added. Then the high-pressure cell was equilibrated at 110 °C for 24 h at constant pressure of 90 bar keeping stirring rate of 200 rpm. Finally, the stirring was stopped, and the cell was slowly depressurized at 110 °C. The as obtained viscous crude TMPTC of about 1,400 kg was obtained having yield of >98% as confirmed from the ^1H NMR in $CDCl_3$ [2]. Before introducing into formulation, product was degassed by thermal treatment at 80 °C for 16 h and then by vacuum treatment at 60 °C for 16 h.

Reference

[1] M. Bourguignon, B. Grignard, C. Detrembleur, *Angew. Chem. Int. Ed.* **2022**, *61*, e202213422.

[2] M. Bourguignon, B. Grignard, C. Detrembleur, *J. Am. Chem. Soc.* **2024**, *146*, 988.

1.2.2. Synthesis of foams using water induced foaming stagey

NIPUF1 (Table S1a, entry 1) was synthesized according to the following procedure: TMPTC (5 g, 5CC = 34.7 mmol), water (300 mg, 16.67 mmol), mXDA (1750 mg, NH_2 = 25.70 mmol) and KOH (90 mg, 1.60 mmol) were added thoroughly in a 4 × 4 cm^2 silicon mold and were mixed for 1 min at room temperature (~20 °C) to create a homogeneous mixture. After that the homogeneous mixture was placed in a pre-heated oven at 100 °C for 4 h. The foam was demolded after cooling to room temperature and finally stored at room temperature under ambient condition. The following foams were synthesized according to the same procedure.

Table S1a Synthesis conditions and properties of self-blown foams synthesized using three different strategies

Entry	Name	Amine	Catalyst	Foaming agent	Condition
1	**NIPUF1**	mXDA (1.77 g)	KOH/ 0.09 g	H_2O/ 0.30 g	100 °C/ 4 h
2	**NIPUF2**	EDR (1.91 g)	KOH/ 0.09 g	H_2O/ 0.60 g	100 °C/ 4 h
3	**NIPUF3**	EDR (1.91 g) + PEI (0.20 g)	KOH/ 0.09 g	H_2O/ 0.60 g	100 °C/ 4 h

TMPTC used for the synthesis of all foams = 5 g; mXDA: *m*-xylylene diamine; EDR: 1,2-bis(2-aminoethoxy)ethane; and PEI: polyethyleneimine branched

Adopting the same water induced foaming procedure and replacing the mXDA by EDR, the **NIPUF2** was synthesized.

NIPUF2 (Table S1a, entry 2): TMPTC (5 g, 5CC = 34.7 mmol), water (600 mg, 33.33 mmol), EDR (1910 mg, NH_2 = 25.78 mmol) and KOH (90 mg, 1.60 mmol) at 100 °C for 4 h.

NIPUF2 of variable densities: The **NIPUF2** foams of different densities were prepared from of formulation of identical chemical composition in a same closed mold (volume of 40 mL) by varying the total mass of the formulation as reported in Table S1b.

Table S1b Preparation of **NIPUF2** of different densities

Entry	Foam	TMPTC	Amine	Catalyst	Foaming agent	Condition
1	NIPUF2 (160)	5.0 g	EDR/ 1.91 g	KOH/ 0.090 g	H_2O/ 0.30 g	100 °C / 4 h
2	NIPUF2 (300)	7.5 g	EDR/ 2.89 g	KOH/ 0.146 g	H_2O/ 0.47 g	100 °C / 4 h
3	NIPUF2 (410)	10.0 g	EDR/ 3.86 g	KOH/ 0.195 g	H_2O/ 0.60 g	100 °C / 4 h

1.2.3. Synthesis of polyethyleneimine functionalized foam

NIPUF3 (Table S1a, entry 3) was synthesized according to the following procedure:

TMPTC (5 g, 5CC = 34.5 mmol) and polyethyleneimine (200 mg) were added in a 4 × 4 cm^2 silicon mold and were mixed at room temperature (~20 °C) for 5 min to get a homogeneous viscous mixture. Then, water (600 mg, 33.33 mmol), EDR (1910 mg, NH_2 = 25.78 mmol) and KOH (90 mg, 1.60 mmol) were added to the TMPTC-polyethyleneimine homogeneous mixture, and the formulation was mixed well for 1 min to obtain homogeneous mixture. Then the formulation (homogeneous mixture) was positioned in a preheated oven at 100 °C for 4 h.

1.2.4. Synthesis of foam containing 1,3-cyclohexanedimethanamine

Foam containing 1,3-cyclohexanedimethanamine was synthesized according to the following procedure: TMPTC (5 g, 5CC = 34.7 mmol), water (300 mg, 16.67 mmol), BAC (1850 mg, NH_2 = 26.00 mmol) and KOH (90 mg, 1.60 mmol) were added thoroughly in a 4 × 4 cm^2 silicon mold and were mixed for 1 min at room temperature (~20 °C) to create a homogeneous mixture. After that the homogeneous mixture was placed in a pre-heated oven at 80 °C for 5 h. The

foam was demolded after cooling to room temperature and finally stored at room temperature under ambient condition.

1.3. Characterization techniques

1.3.1. ATR-Infrared analysis

Attenuated transmission reflectance (ATR) Infrared (IR) spectra were recorded by a Nicolet IS5 spectrometer (Thermo Fisher Scientific) equipped with a transmission or with a diamond ATR device. Spectra were obtained in transmission or ATR mode as a result of 32 spectra in the range of 4000-500 cm^{-1} with a nominal resolution of 4 cm^{-1}. Spectra were further processed by the OriginPro 9.0 software.

1.3.2. Nuclear magnetic resonance (NMR) spectroscopy

^{1}H NMR analyses were performed on a Bruker 400 MHz spectrometer at 25 ^{o}C in the Fourier transform mode. Sixteen scans for ^{1}H spectra and 512 scans for ^{13}C spectra were recorded. Crosspolarization magic angle spinning (CP-MAS) solid-state ^{13}C NMR spectra were collected using a Bruker Avance DSX-400 instrument. Samples were packed in 4 mm zirconia rotors and spun at 10 kHz.

1.3.3. Thermogravimetric analysis (TGA)

TGA analysis was performed on a TGA2 instrument from Mettler Toledo. Around ~8 mg of sample was flushed with nitrogen (20 mL min^{-1}) for 10 min at 25 ^{o}C. The sample was then heated at 10 ^{o}C min^{-1} until 600 ^{o}C under a nitrogen atmosphere (20 mL min^{-1}).

1.3.4. Dynamic scanning calorimetry (DSC)

DSC study was performed on a DSC Q2000 differential calorimeter (TA Instruments). All the experiments were performed under ultrapure nitrogen flow. All samples (loaded and unloaded) were dried at 60°C for 2 h prior to the DSC measurement. We used only one heating cycle for the T_g measurements to avoid any aging/evolution of the sample during multiple heating cycles. Samples of ~5 mg were used and placed in sealed aluminum pans. The samples were first cooled down to −80 ^{o}C at a rate of 10 ^{o}C min^{-1} and then heated to 100 ^{o}C at 10 ^{o}C min^{-1}.

1.3.5. Scanning electron microscopy (SEM)

Scanning electron microscopy (SEM) was recorded with a QUANTA 600 apparatus microscope from FEI with a piece of foam dried in a desiccator.

1.3.6. Energy dispersive X-ray spectroscopy (EDX)

EDX spectra of all Fe^{2+}, Cu^{2+}, Fe^{3+} and Hg^{2+} loaded samples were analyzed using ZEISS EVO-MA-10 and JEOL JSM-7600F having 3 and 1 nm resolution, respectively, attached with W filament and Sb sources.

1.3.7. Compression test

Compression tests were performed on an INSTRON (model 34TM-10) device integrated with Aide Bluehill Universal software. Compression was performed at a rate of 2 mm min^{-1} on cubic foam samples of ~1 cm^3. Compression modulus was calculated by the slope at the beginning (i.e. 2-8 strain %) of the stress-strain curve. The experiment was performed with three replicates.

1.3.8. Inductively coupled plasma (ICP) optical emission spectrometer

The concentrations of used metal ions were determined using an inductively coupled plasma optical emission spectrometer (ICP-OES: Varian 720-ES) at the characteristic wavelengths. For Cu and Fe, working concentrations were measured at 212.604/ 213.598/ 217.941/

221.458/ 327.395 nm and 234.350/ 238.204/ 239.563/ 240.489/ 259.837 nm of wavelengths, respectively.

1.3.9. Fluorescence spectroscopy

Fluorescence spectra of photoluminescent foams and metal ions-/formaldehyde/-tetracycline-loaded foams were recorded within 350–800 nm using the spectrofluorometer (Tecan Infinite 200Pro) using 350–450 nm of excitation wavelengths (λ_{ex}s). UV-star® microplate, 96 well, half area, μclear®, transparent, 10 ST/BTL of Greiner Bio-One GmbH, Germany (REF: 675801) was used as sample holder. The fluorescence spectra were recorded from the bottom of the well with manual gain of 60, number of flashes of 10, integration time of 20 μs, 0 μs of lag time. The excitation and emission slit widths were 10 and 20 nm for source and detector, respectively. All experiment was performed with three replicates and most reproducible data were resented.

1.3.10. Fluorescence quantum yield measurement

Fluorescence quantum yields (FQY) of **NIPUF1**, **NIPUF2** and **NIPUF3** (grinded to powder) were measured with an integrating sphere (K-Sphere, HORIBA) mounted inside the FluoroMax-4 spectrometer, equipped with a 450 W xenon lamp. All spectra were analized by FluorEssence Software (Version 3.9). The spectral emission corrections were carried out with a HORIBA emission correction kit. A neutral density filter (ND210B, THORLABS) was used for light intensity adjustment. For FQY calculations the corrected emission spectra were expressed in relative quantum units. All measurements were repeated five time to have reproducible results. For more details please visit: https://static.horiba.com/fileadmin/Horiba/Products/Scientific/Molecular_and_Microanalysis/PTI_QuantaMaster/QM_K-sphere_PLQY_FL-2019-07-17.pdf

1.3.11. Fluorescence lifetime imaging (FLIM) study

Fluorescence lifetime images were recorded with Fluotime100 fluorescence spectrophotometer (Picoquant, Berlin, Germany) based on a picoHarp300 unit and using a pulsed diode laser (LDH-440; center wavelength 440 nm; pulse width 54 ps; repetition frequency 10 MHz) as an excitation source. Raw images were recorded by raster scanning an area of 830×830 nm with are solution of 512×512 pixels. The photons of each pixel were temporally sorted with respect to the excitation pulse in the histograms with a time resolution of 29 ps/channel.

1.3.12. Analysis of FLIM results by MATLAB

All the FILM data were analysed by the open source Pulsed Interleaved Excitation (PIE) analysis by PAM, a versatile software package offering a variety of analysis tools, including phasor analysis by the help of MATLAB-R2022b software. The pico quanta universal file format file was used to open .ptu in detector 1 or detector 2. The .phr file was saved with respect to reference Atto-425 and subsequently the phasor was analysed by advanced analysis followed by phasor. The lifetime of foam was calculated keeping lifetime of Atto-425 as internal reference. All the phasor plots were shown in the supporting information. The software is available as a source code, requiring MATLAB to run, or as compiled standalone software compatible with Windows or MacOS at http://www.cup.uni-muenchen.de/pc/lamb/software/pam.html or hosted in Git repositories under http://www.gitlab.com/PAM-PIE/PAM and http://www.gitlab.com/PAM-PIE/PAMcompiled.

1.3.13. Fluorescence imaging

The fluorescence imaging of the foams was carried out by Confocal Zeiss LSM 880. The images were analyzed using the advanced PicoQuanta software. The laser sources of 454, 488, 514, 543, 594 and 633 nm were used for the measurements.

1.4. Methodology

1.4.1. Swelling experiments of the NIPU foams

Foam was dried in an over at 50 °C for 2 h or in desiccator for 24 h. The initial mass (m_i) of the dried NIPU foam was measured. Then, swelling of the foam was performed by immersing of the dried foam in tetrahydrofuran for 24 h. After 24 h, swollen foam was weighted and mass (m_t) were recorded. The swelling of the NIPU foams after 24 h was measured by the formula:

$$Swelling\ (\%) = (m_t - m_i)/m_i \times 100$$

1.4.2. Gel content

As synthesized NIPU foam was cut into small portions and initial mass (m_1) was taken. Then, the foam was dissolved in in tetrahydrofuran for 24 h. After that, tetrahydrofuran was removed and foam was dried at room temperature and under vacuum at 60 °C for 48 h and 16 h, respectively, and final mass (m_2) was taken. Finally, gel content (GC) was calculated by the formula:

$$GC = (m_2/m_1) \times 100$$

1.4.3. Graphics based analyses

All graphics-based analyses were carried out by Origin 9.0, ChemDraw Ultra 12.0, Gaussian 16, GaussSum 6.0, Multiwfn_3.8, IrfanView 64, VMD1.9.4a53 and design expert 7.0 softwares.

2. Characterization of NIPU foams

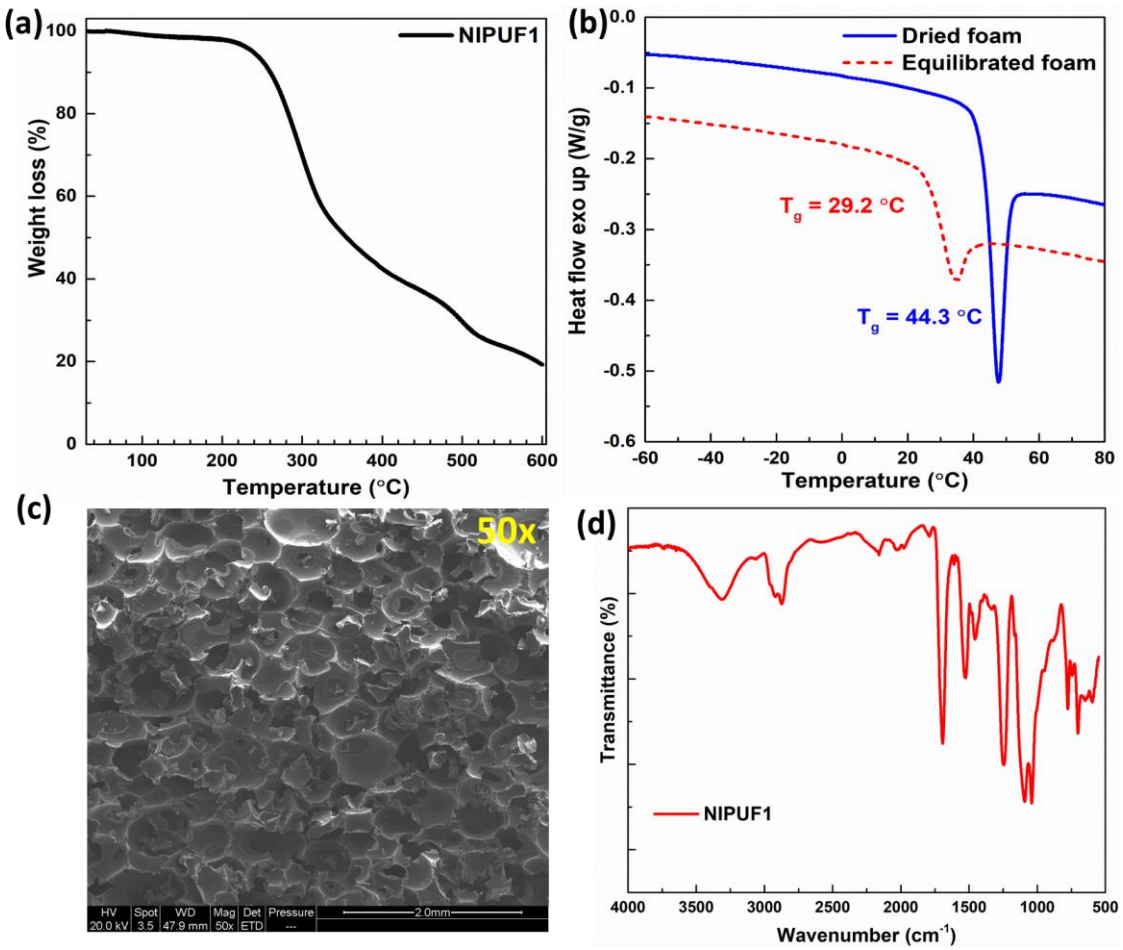

Entry	Wavenumber (cm^{-1})	Assignment
1	3310	O-H *str.* -CH_2OH and >CHOH; the hydrogen bonding O-H…OH and O-H…N-H make the spectrum broad
2	2918	>C-H *str.*
3	2870	-CH_2- *str.*
4	1791	>C=O *str.* of cyclic carbonate
5	1693	>C=O *str.* of -OCONH-
6	1525	combined N-H *deformation* and C-N *str.* of -OCONH-
7	1455	C-H *deformation* of -CH_2-
8	1246	combined C-N and C-O *str.*
9	1095	C-O *str.*
10	1036	C-O *str.*

Figure S1. (a) TGA curve of dried **NIPUF1**; temperature at 10% mass loss ($T_{d10\%}$ = 267 °C); (b) DSC thermogram of equilibrated and dried **NIPUF1**; (c) SEM photomicrographs of **NIPUF1** at 50x magnifications; (d) ATR-infrared spectrum and ATR-infrared spectrum analysis of **NIPUF1**

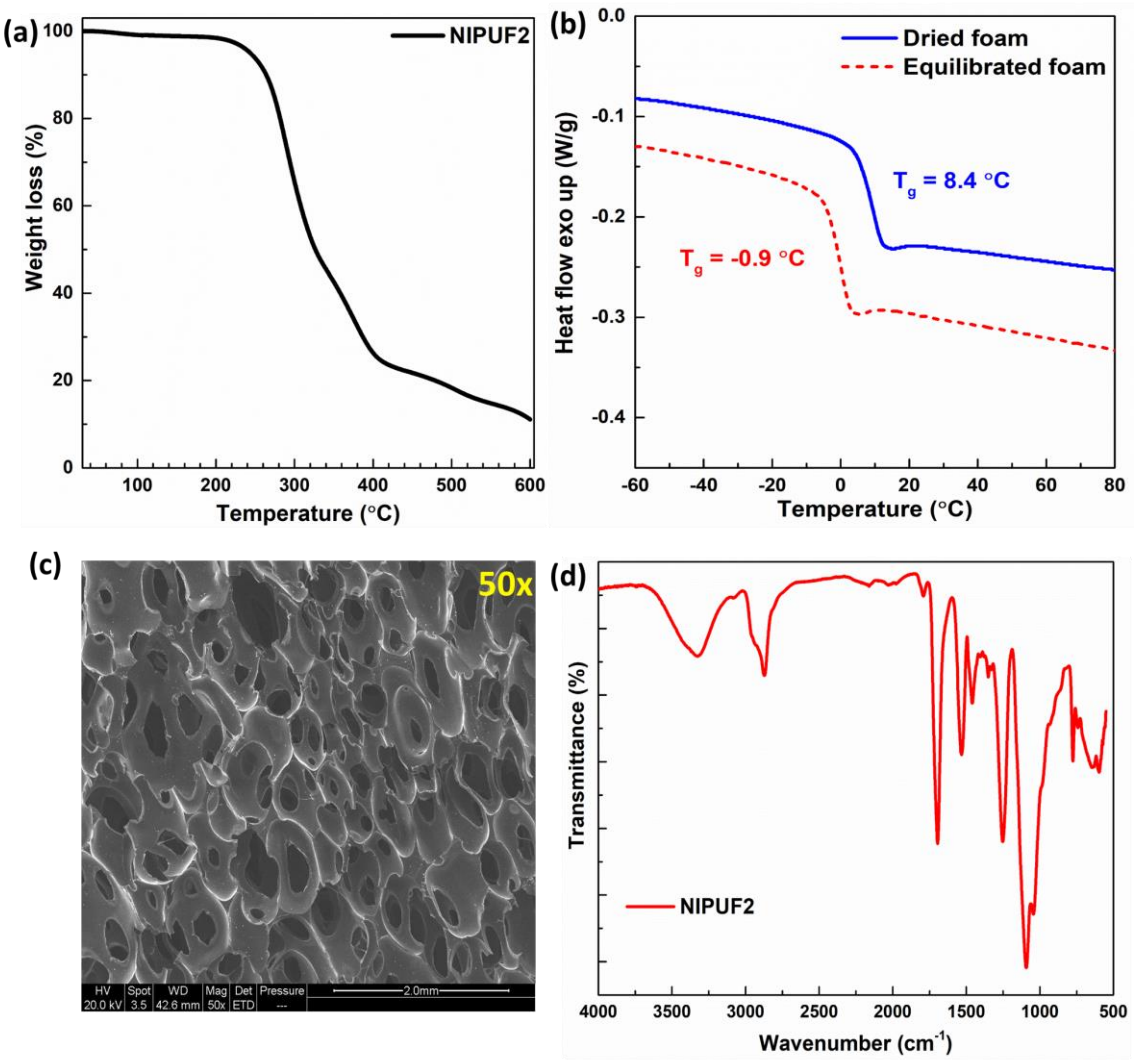

Entry	Wavenumber (cm^{-1})	Assignment
1	3325	O-H *str.* -CH_2OH and >CHOH; the hydrogen bonding O-H…OH and O-H…N-H make the spectrum broad
2	2936	>C-H *str.*
3	2871	-CH_2- *str.*
4	1791	>C=O *str.* of cyclic carbonate
5	1694	>C=O *str.* of -OCONH-
6	1531	combined N-H *deformation* and C-N *str.* of -OCONH-
7	1460	C-H *deformation* of -CH_2-
8	1252	combined C-N and C-O *str.*
9	1092	C-O *str.*
10	1042	C-O *str.*

Figure S2. (a) TGA curve of dried **NIPUF2**; temperature at 10% mass loss ($T_{d10\%}$ = 265 °C); (b) DSC thermogram of equilibrated and dried **NIPUF2**; (c) SEM photomicrographs of **NIPUF2** at 50x magnifications; (d) ATR-infrared spectrum and ATR-infrared spectrum analysis of **NIPUF2**

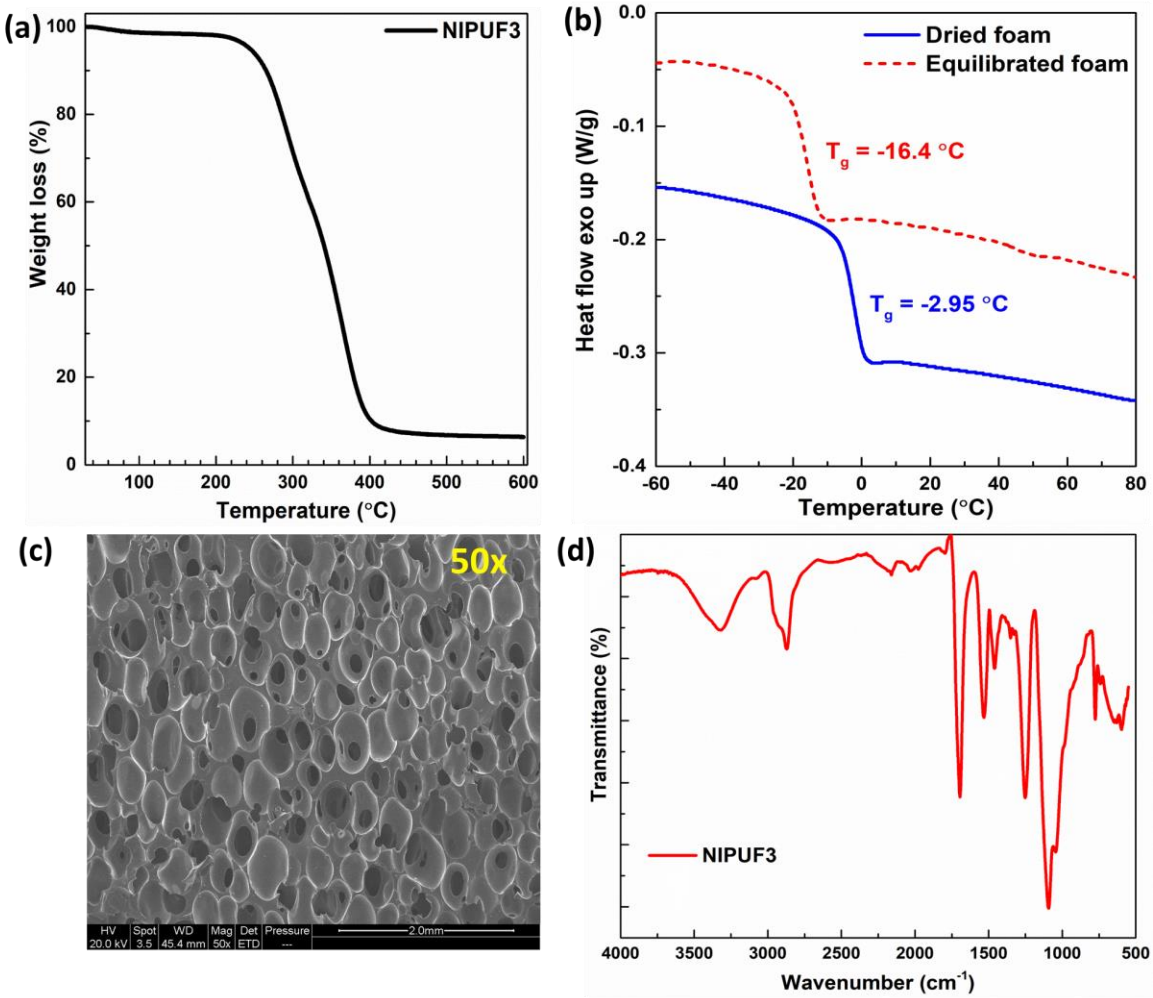

Entry	Wavenumber (cm^{-1})	Assignment
1	3326	O-H *str.* -CH_2OH and >CHOH; the hydrogen bonding O-H…OH and O-H…N-H make the spectrum broad
2	2921	>C-H *str.*
3	2871	-CH_2- *str.*
4	1795	>C=O *str.* of cyclic carbonate
5	1694	>C=O *str.* of -OCONH-
6	1532	combined N-H *deformation* and C-N *str.* of -OCONH-
7	1460	C-H *deformation* of -CH_2-
8	1251	combined C-N and C-O *str.*
9	1092	C-O *str.*
10	1042	C-O *str.*

Figure S3. (a) TGA curve of dried **NIPUF3**; temperature at 10% mass loss ($T_{d10\%}$ = 265 °C); (b) DSC thermogram of equilibrated and dried **NIPUF3**; (c) SEM photomicrographs of **NIPUF3** at 50x magnifications; (d) ATR-infrared spectrum and ATR-infrared spectrum analysis of **NIPUF3**

3. Nontraditional fluorescence of NIPU foams

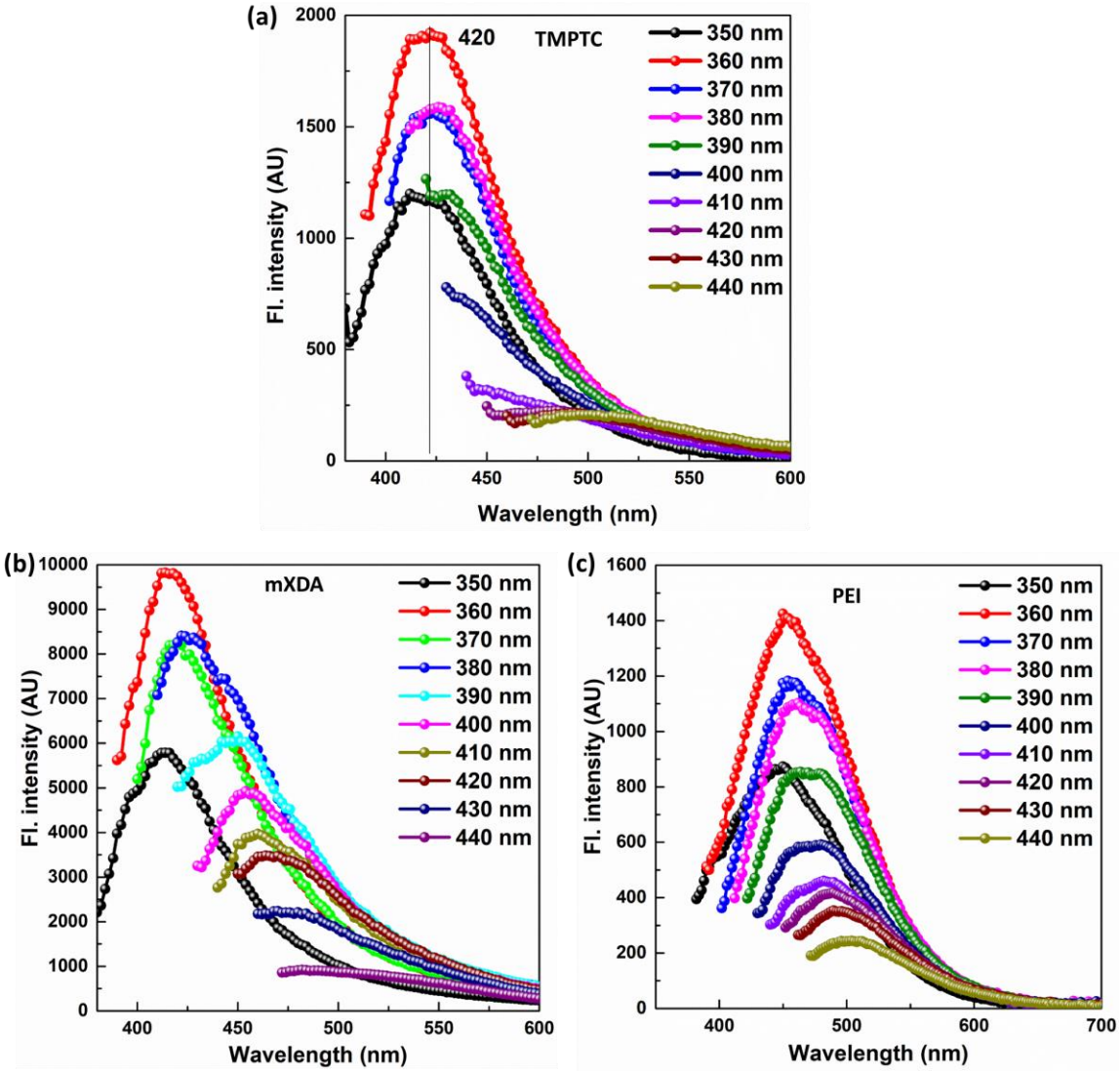

Figure S4. Fluorescence spectra of (a) TMPTC, (b) mXDA and (c) PEI using excitation wavelengths (λ_{ex}) = 350, 360, 370, 380, 390, 400, 410, 420, 430 and 440 nm

Table S2. CIE coordinates of **NIPUF1**, **NIPUF2** and **NIPUF3**

Wavelength (nm)	Coordinates of NIPUF1		Coordinates of NIPUF2		Coordinates of NIPUF3	
	x	y	x	y	x	y
330 nm	0.18881	0.19362	0.19966	0.20783	-	-
350 nm	0.18862	0.19292	0.19307	0.19339	0.17391	0.17173
360 nm	0.18670	0.19135	0.19177	0.19435	0.17320	0.17980
370 nm	0.18662	0.19486	0.19147	0.19955	0.17441	0.19273
380 nm	0.18829	0.20824	0.19246	0.21190	0.17691	0.21057
390 nm	0.19264	0.23502	0.19506	0.23134	0.18123	0.23533
400 nm	0.20073	0.27841	0.20095	0.26481	0.18750	0.26835
410 nm	0.21467	0.34193	0.21299	0.31985	0.19937	0.32145
420 nm	0.23170	0.40581	0.23248	0.38888	0.22041	0.39477
430 nm	0.24854	0.46586	0.25686	0.45961	0.24684	0.46980
440 nm	0.26731	0.52651	0.28973	0.52792	0.28012	0.53707
450 nm	0.28895	0.57602	0.32327	0.57101	0.31691	0.57371
460 nm	0.31332	0.60745	0.35526	0.58781	0.34018	0.59649
470 nm	0.34056	0.61638	0.38486	0.58518	0.36992	0.59601
480 nm	0.37568	0.60331	0.41556	0.56951	0.40269	0.58041
490 nm	0.41121	0.57849	0.44292	0.54922	0.43372	0.55769
500 nm	0.44804	0.54688	0.47239	0.52348	0.46611	0.52948
520 nm	0.52427	0.47447	0.53610	0.46275	0.53529	0.46355

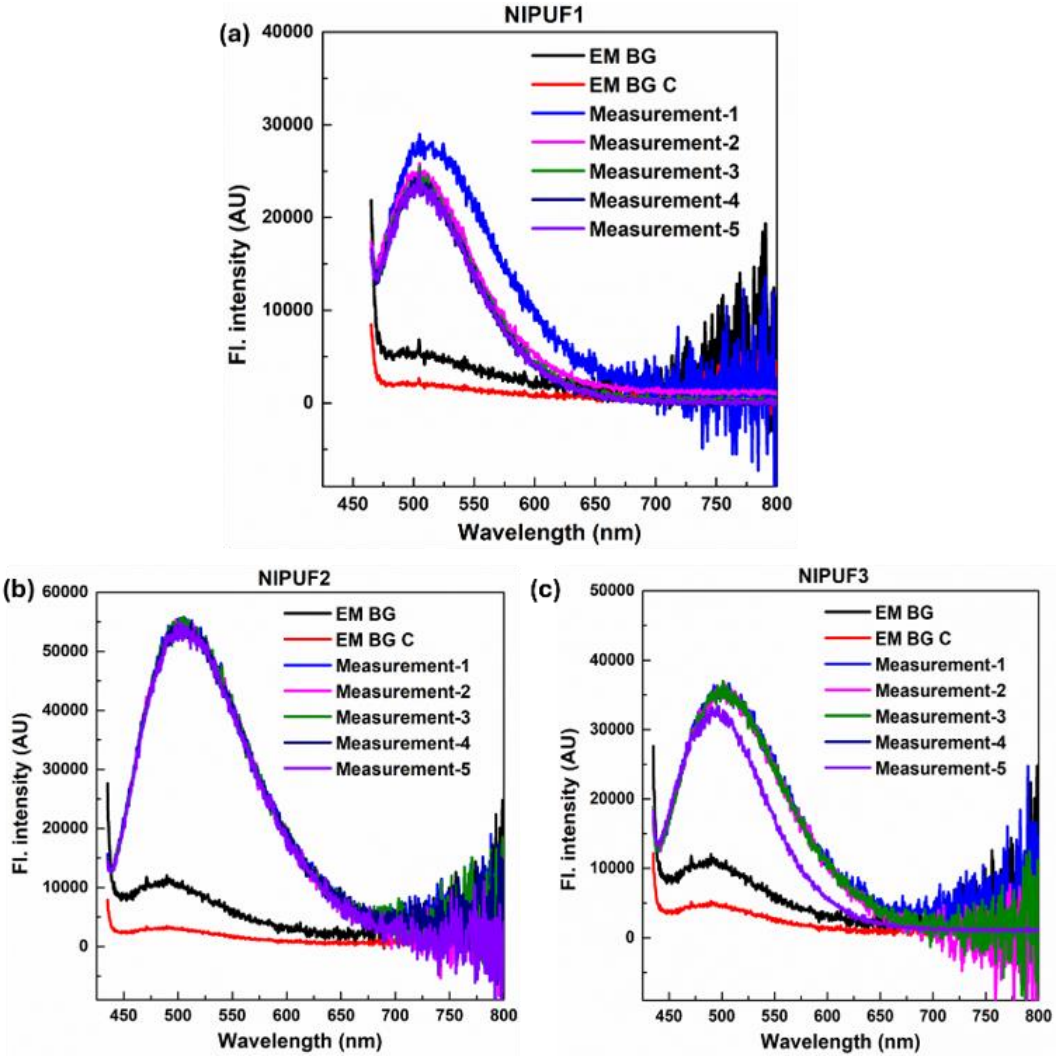

Figure S5. Fluorescence spectra of (a) **NIPUF1** (at λ_{ex} = 460 nm), (b) **NIPUF2** (at λ_{ex} = 430 nm) and (c) **NIPUF3** (at λ_{ex} = 430 nm) were used to calculate fluorescence quantum yields. Foams were grinded to powder and measured with an integrating sphere (K-Sphere, HORIBA) mounted inside the FluoroMax-4 spectrometer, equipped with a 450 W xenon lamp. All spectra were analized by FluorEssence Software (Version 3.9). The spectral emission corrections were carried out with a HORIBA emission correction kit. A neutral density filter (ND210B, THORLABS) was used for light intensity adjustment.

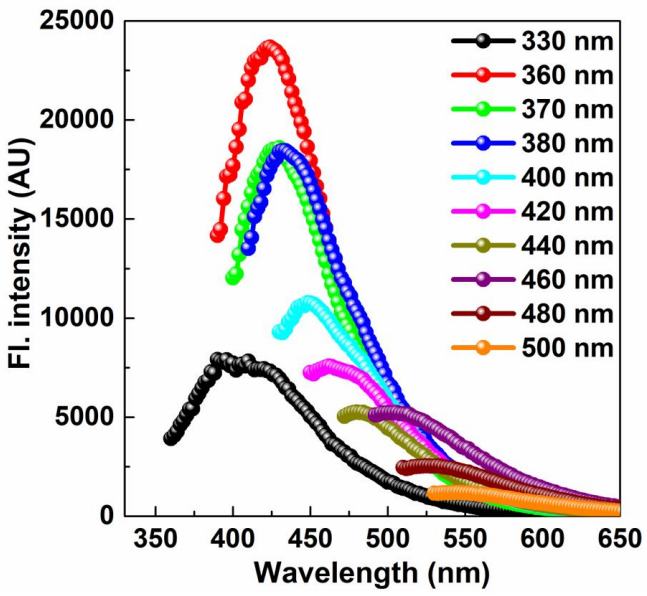

Figure S6. Fluorescence spectra of foam containing 1,3-cyclohexanedimethanamine using excitation wavelengths (λ_{ex}) = 330, 360, 370, 380, 400, 420, 440, 460, 480 and 500 nm

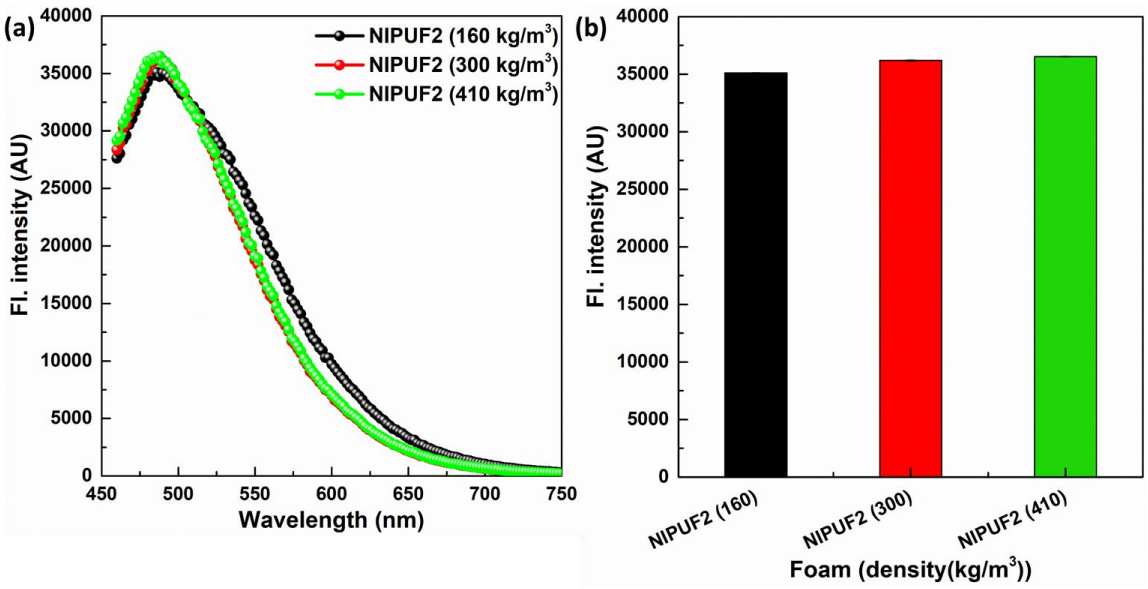

Figure S7. (a) Fluorescence spectra of **NIPUF2** (160 kg/m^3), **NIPUF2** (300 kg/m^3) and **NIPUF2** (410 kg/m^3) at λ_{ex} = 430 nm; and (b) fluorescence intensities of **NIPUF2** (160 kg/m^3), **NIPUF2** (300 kg/m^3) and **NIPUF2** (410 kg/m^3); foams of variable densities were achieved using closed mold keeping chemical composition same. (See synthesis section and Table S1b for more details)

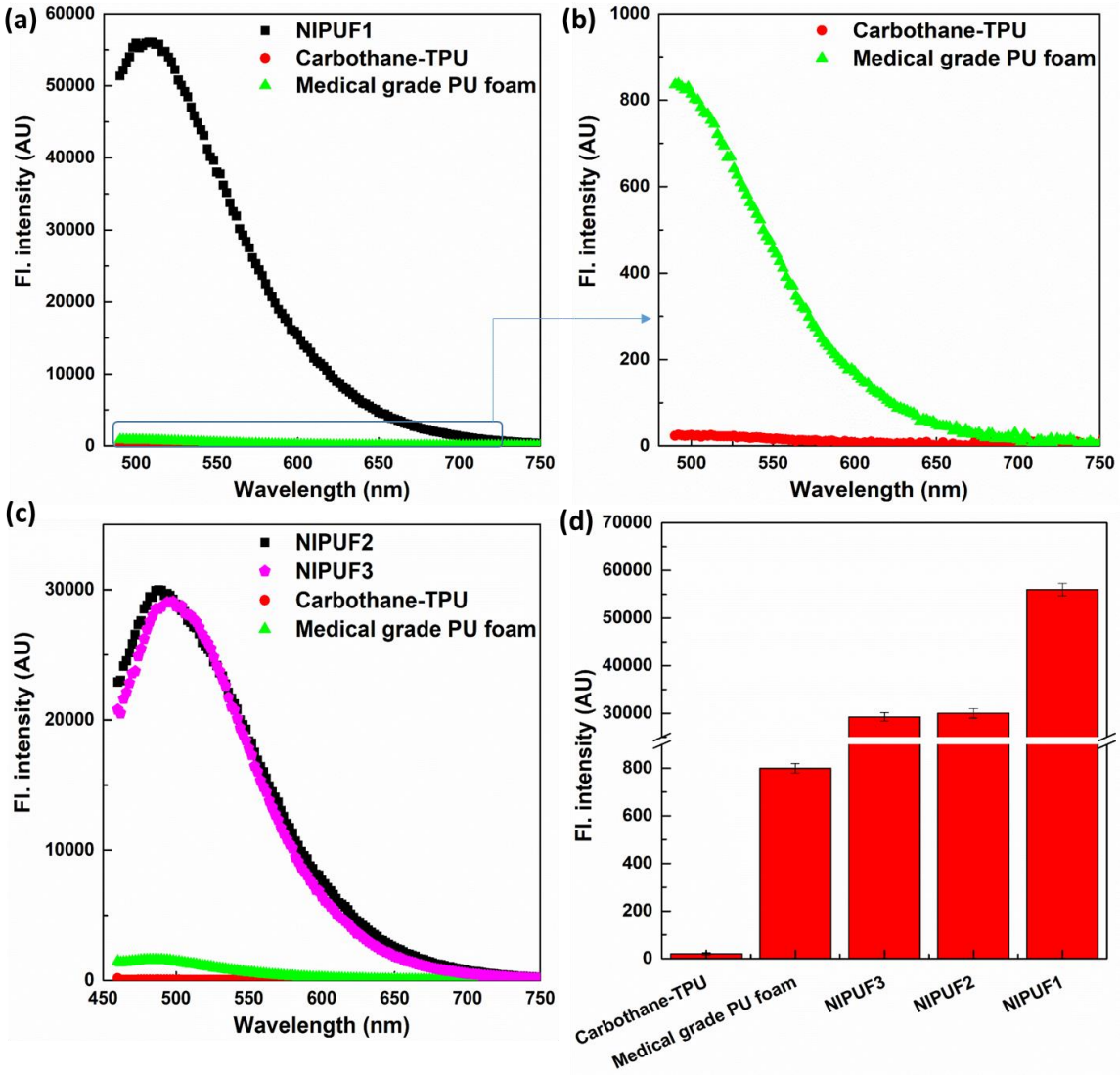

Figure S8. (a) Fluorescence spectra of **NIPUF1**, carbothane-TPU, medical grade PU foam; (b) zoomed fluorescence spectra of carbothane-TPU, medical grade PU foam; (c) fluorescence spectra of **NIPUF2**, **NIPUF3**, carbothane-TPU, medical grade PU foam; and (d) comparison of fluorescence intensities of carbothane-TPU, medical grade PU foam, **NIPUF3**, **NIPUF2** and **NIPUF1**.

Fluorescence Lifetime Imaging Microscopy (FILM)

FLIM examines a fluorophore's fluorescence decay rate on a timescale ranging from sub nanoseconds to hundreds of nanoseconds. FLIM has several distinct benefits over intensity-based fluorescence microscopy. Fluorescence intensity imaging can distinguish between fluorophores with different spectrum features and offers information on their geographical distribution. However, intensity alone is unable to distinguish fluorescent substances with similar spectra or distinct chemical surroundings around the same fluorophore. Using the fluorescence lifetime, FLIM can routinely distinguish spectrally overlapping fluorophores. Overall, FLIM is beneficial in its capacity to identify alterations in the molecular surroundings of fluorescent substances and offer information on fluorophore function and behaviour that intensity studies alone could not provide. FLIM, as opposed to intensity-based measures, is generally independent of fluorophore concentration. FLIM can thus detect whether a change in the intensity of fluorescence is caused by changes in quantum yield (e.g., fluorescence quenching), a difference in fluorophore concentration overall, or both. FLIM studies are also less susceptible to inner filter effects, which are absorption and scattering events that alter the recorded fluorescence intensity. As a result, FLIM is highly suited for precise measurements of quenching dynamics. The phasor analysis was performed to calculate the fluorescence lifetimes. The advantages of phasor are fit-free, intuitive representation of lifetime estimates, useful for large time-domain or frequency-domain datasets and visualization of lifetime heterogeneity. The atto-425 with lifetime of 3.60 ns was used as reference for calculating the phasor of all loaded and unloaded foams and films. For more information please see “R. Datta, T. M. Heaster, J. T. Sharick, A. A. Gillette, and M. C. Skala, Fluorescence lifetime imaging microscopy: fundamentals and advances in instrumentation, analysis, and applications. J. Biomed. Opt. 25(7), 071203 (2020), DOI: 10.1117/1.JBO.25.7.071203.

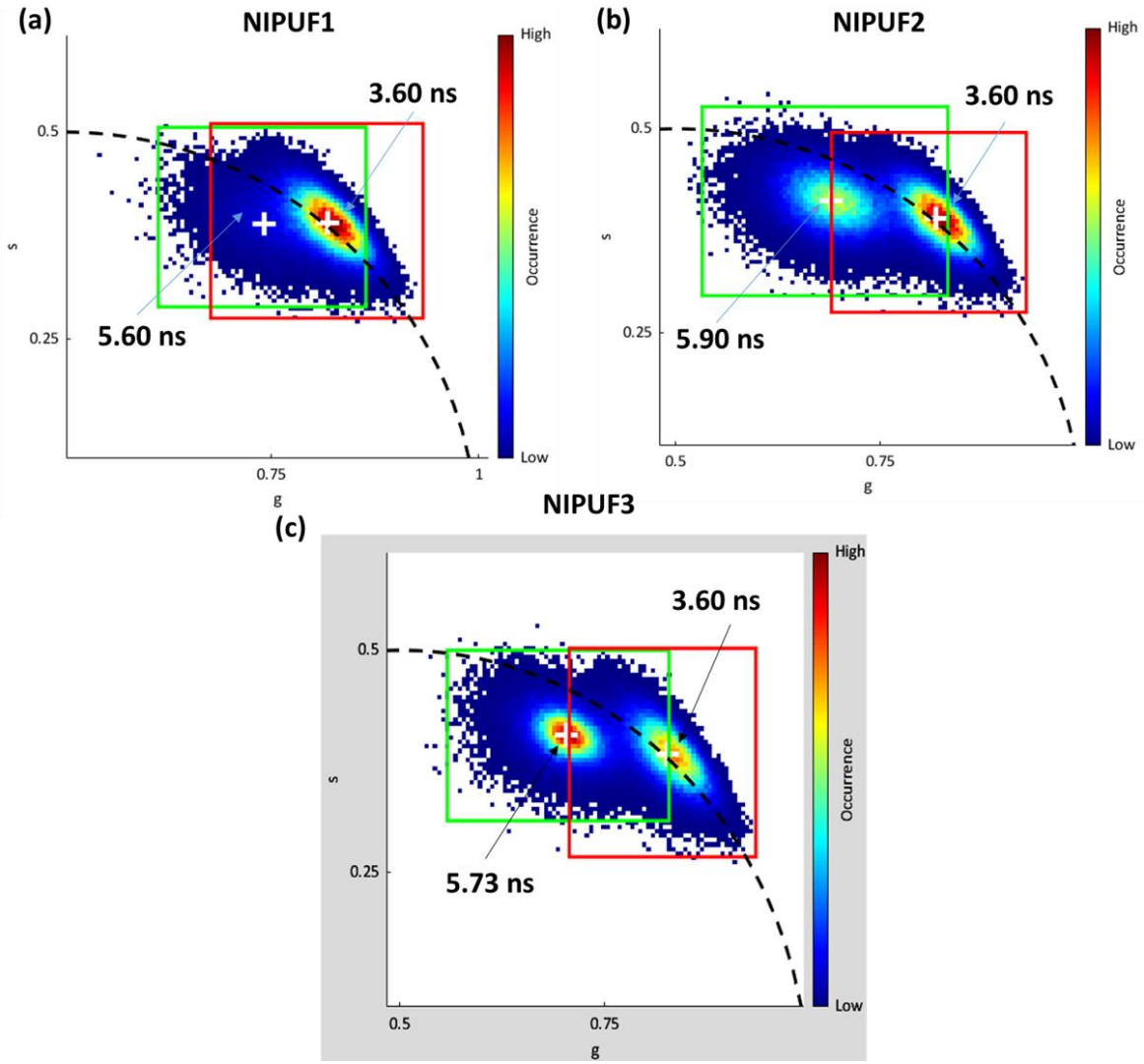

Figure S9. Phasor histogram plots of (a) **NIPUF1**, (b) **NIPUF2** and (c) **NIPUF3**, showing lifetimes; the atto-425 having 3.60 ns lifetime is used as the reference; the black dotted line corresponds to the universal circle highlighting all possible phasors for monoexponential decays; JET colormaps are used for generating the p**hasor colormaps; the threshold minimum/maximum = 100/ 5000 is used**

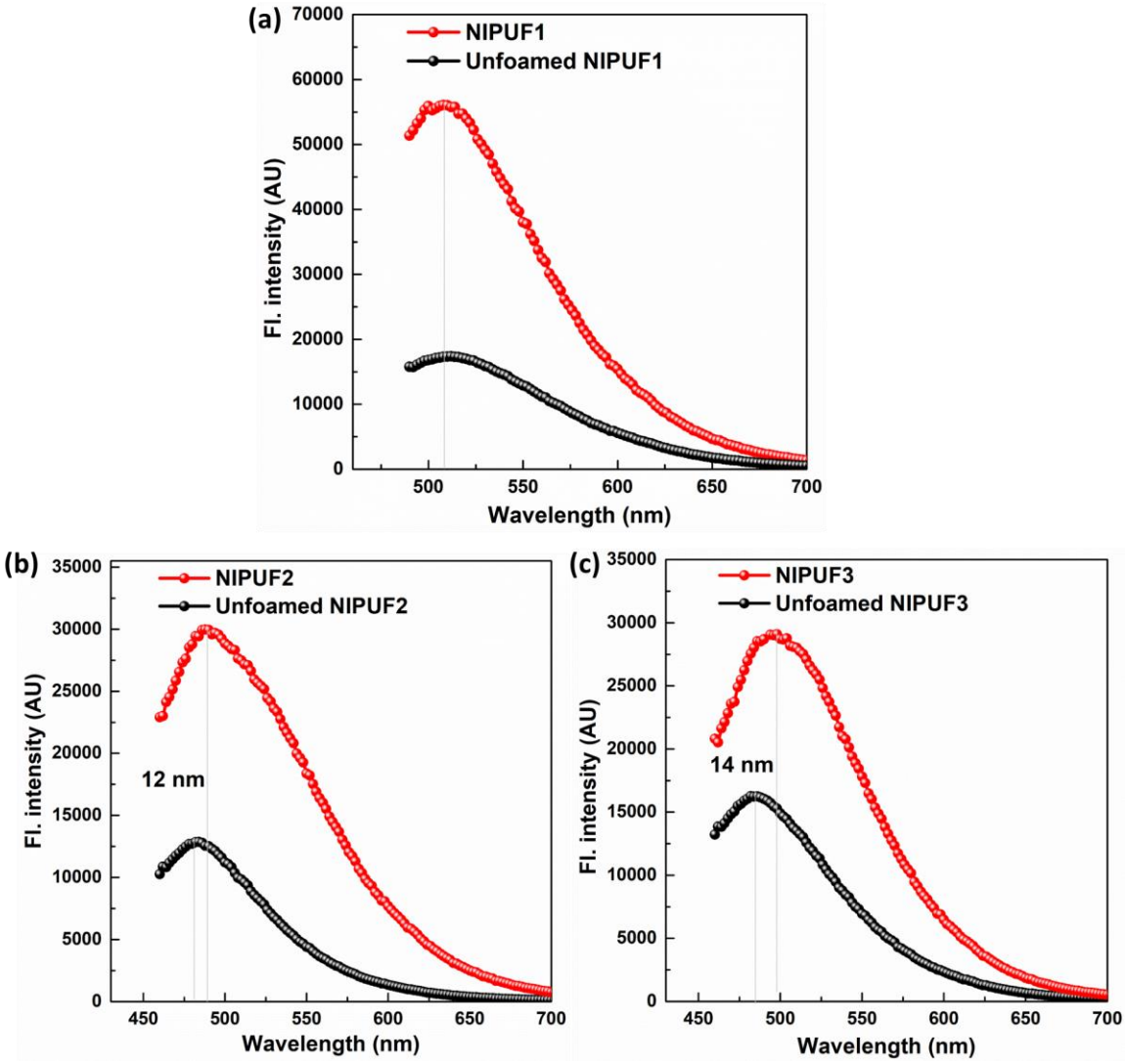

Figure S10. (a) Fluorescence spectra of **NIPUF1** and unfoamed **NIPUF1** at λ_{ex} = 460 nm, (b) fluorescence spectra of **NIPUF2** and unfoamed **NIPUF2** at λ_{ex} = 430 nm and (c) fluorescence spectra of **NIPUF3** and unfoamed **NIPUF3** at λ_{ex} = 430 nm; unfoamed materials were synthesized using the same recipe in Table S1a without water

In order to highlight the influence of the hydroxyl groups on the fluorescence behavior of the polymer matrix, we have modulated the content of hydroxyl groups by curing the same NIPU formulations without water. In that case, there was no hydrolysis of the cyclic carbonate groups, thus avoiding the introduction of the pending vicinal diol groups. As CO_2 was not released, the NIPU were not foamed but contained less hydroxyl groups. The comparative fluorescence studies of **NIPUF1**, **NIPUF2**, **NIPUF3** and their corresponding unfoamed materials are presented in **Figure S8**. In all cases, the unfoamed materials presented a lower fluorescence intensity, and in the case of unfoamed **NIPUF2** and **NIPUF3,** a lower emission wavelength was also observed compared to their foamed counter-parts bearing vicinal diols. The presence of hydroxyl groups seems thus to have an important influence on the fluorescence properties of the foams. But this observation should be taken with caution as we compare a foamed and unfoamed material, and other factors might also contribute to this change of fluorescence behavior.

4. Computational study

Amine	Structures of the model compounds		
EDR	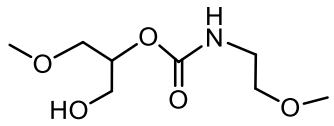 **Model compound-1a**	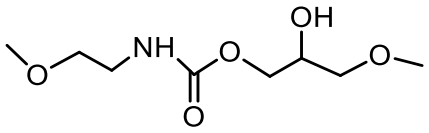 **Model compound-2a**	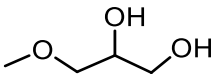 **Model compound-3**
mXDA	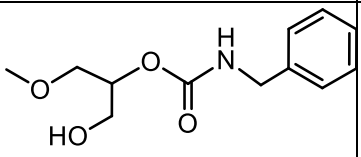 **Model compound-1b**	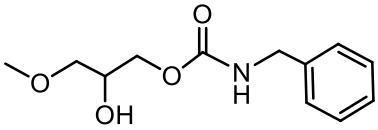 **Model compound-2b**	
	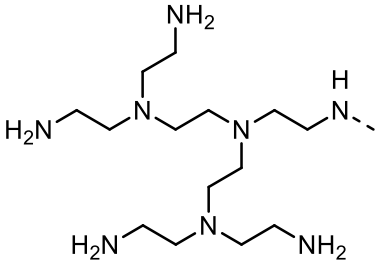 **PEI**		

Protocols

To make the analysis more convenient molecules were fragmented to model compounds. For the water induced system, the backbones were represented by model compound-1a, model compound-2a (EDR) and model compound-1b, model compound-2b (mXDA) and model compound-3 which were the main component of the molecules. All best possible configurations of each model compound were optimized in the ground state with Gaussian 16 (Consortium des Équipements de Calcul Intensif: CÉCI clusters) by density functional theory (DFT) using B3LYP functional and 6-311G basis set with default spin, zero charge and singlet spin. Subsequently, the lowest energy configuration was screened. The ground state and lowest energy singlet-excited state (S_1) geometries of the best configurations were further optimized by B3LYP functional and 6-311+G(d,p) basis set. The frequency optimization was performed for all configurations using the same functional and basis set in which no imaginary frequency at the energy minima was found establishing the stability of those configurations. The time-dependent DFT (TDDFT) was performed with the method TD-SCF on PBEPBE functional and 6-311+G(d, p) basis set and N = 30 to get absorption details. The energy levels of HOMOs/ LUMOs were calculated using GaussSum2.2. The orbitals were extracted using GaussView6.0.16.

To investigate the mechanism of fluorescence and explore the inter chain interactions between chains, model NIPUFs were created by making aggregation of model compounds. The **NIPUF1**, **NIPUF2** and **NIPUF3** were made by the “1b+2b+3”, “1a+2a+3”, and “1a+2a+3+PEI”, respectively. All the aggregates were computed theoretically via density functional theory (DFT) using B3LYP functional and 6-311G basis set with default spin, zero charge and singlet spin. For each aggregate, all best possible configurations were optimized and subsequently the lowest energy configuration was screened for further calculations. The ground state and lowest energy singlet-excited state (S_1) geometries of the best configurations

were further optimized by B3LYP functional and 6-311+G(d,p) basis set basis set. The time-dependent DFT (TDDFT) was performed with the method TD-SCF on PBEPBE functional and 6-311+G(d, p) basis set considering N = 30 transitions to get the absorption details. The energy levels of HOMOs/ LUMOs were calculated using GaussSum2.2. The orbitals were extracted using GaussView6.0.16.

For small, medium and large aggregates, the DFT calculations were performed only using 1a+2a+3, 2 x (1a+2a+3) and 3 x (1a+2a+3) model compounds, respectively, optimized by B3LYP functional and 6-311+G basis set. The energy levels of HOMOs/ LUMOs were calculated using GaussSum2.2. The orbitals were extracted using GaussView6.0.16.

The ground state optimization of metal complex with foams were carried out by B3LYP functional and LanL2DZ basis set. The frequency optimization was performed for the configuration using the same functional and basis set in which no imaginary frequency at the energy minima was found establishing the stability of configuration. The orbitals were extracted using GaussView6.0.16.

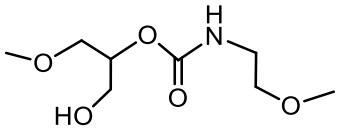

Model compound-1a

Optimized: B3LYP+6-311G

Configuration	Structure	Energy (Hartree)	HOMO (eV)	LUMO (eV)	$\Delta E_{HOMO-LUMO}$
Configuration-1	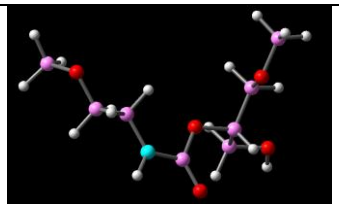	-746.1690	-7.21	-0.18	7.03
Configuration-2	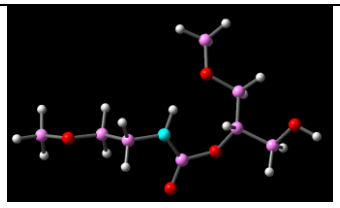	-746.1652	-7.03	-0.33	6.70
Configuration-3	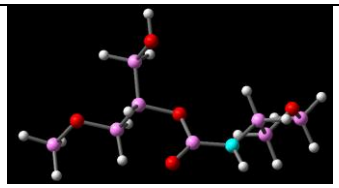	-746.1688	-7.19	-0.11	7.08
Configuration-4	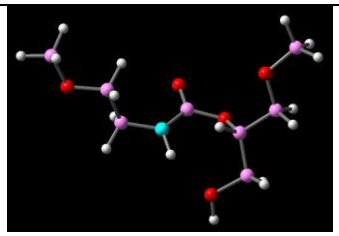	-746.1617	-7.04	-0.53	6.51

Configuration-5	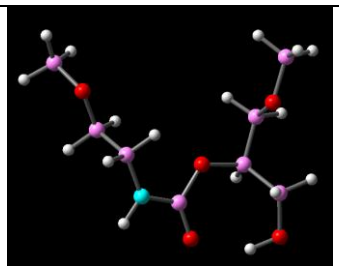	-746.1726	-7.16	-0.22	6.94
Configuration-6	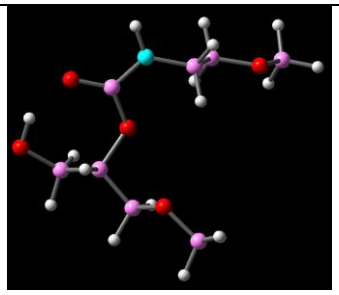	-746.1728	-7.28	-0.17	7.11
Configuration-7	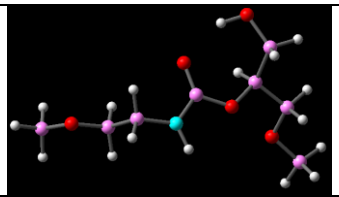	-746.174695	-7.27	-0.12	7.15
Configuration-8	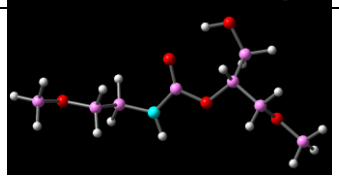	-746.174539	-7.16	-0.18	6.98
Configuration-9		-746.174539	-7.16	-0.18	6.98
Configuration-10	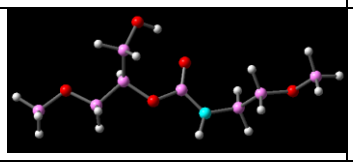	**-746.174770**	**-7.18**	**-0.25**	**6.93**
Configuration-11	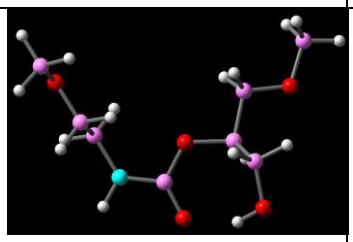	-746.172826	-7.18	-0.24	6.94
Configuration-12	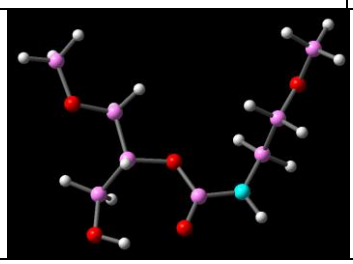	-746.172683	-7.17	-0.26	6.91

Coordinates of model compound-1a (configuration-10) in ground state (S_0)

Optimized by B3LYP+6-311+G(d, p)

N	1.34148	-1.20048	-0.21747
C	0.40101	-0.24477	-0.4083
O	0.60533	0.85411	-0.96478
O	-0.81461	-0.64756	0.10491
C	-2.0451	0.15379	-0.17178
H	1.05163	-2.05238	0.23189
C	2.73351	-1.0245	-0.63702
H	3.1665	-2.0059	-0.8233
H	2.75336	-0.46178	-1.56754
C	3.57396	-0.29291	0.40756
H	3.20391	0.72907	0.54126
H	3.52886	-0.81273	1.37307
O	4.92909	-0.28614	-0.1022
C	5.86618	0.45857	0.71525
H	5.94642	0.02846	1.71944
H	6.82773	0.39012	0.21497
H	5.57141	1.50971	0.79695
C	-2.04583	1.5037	0.54123
H	-3.08155	1.80506	0.68155
H	-1.57926	1.37898	1.52715
O	-1.42582	2.56172	-0.21828
H	-0.56684	2.23994	-0.56603
H	-2.11966	0.31151	-1.24762
O	-4.4069	-0.17476	-0.07776
C	-5.57304	-0.94705	0.30401
H	-6.43509	-0.38256	-0.038
H	-5.56851	-1.93224	-0.17368
H	-5.62618	-1.07369	1.39038
C	-3.1498	-0.78217	0.3014
H	-3.09572	-0.91562	1.3886
H	-3.02943	-1.75933	-0.17604

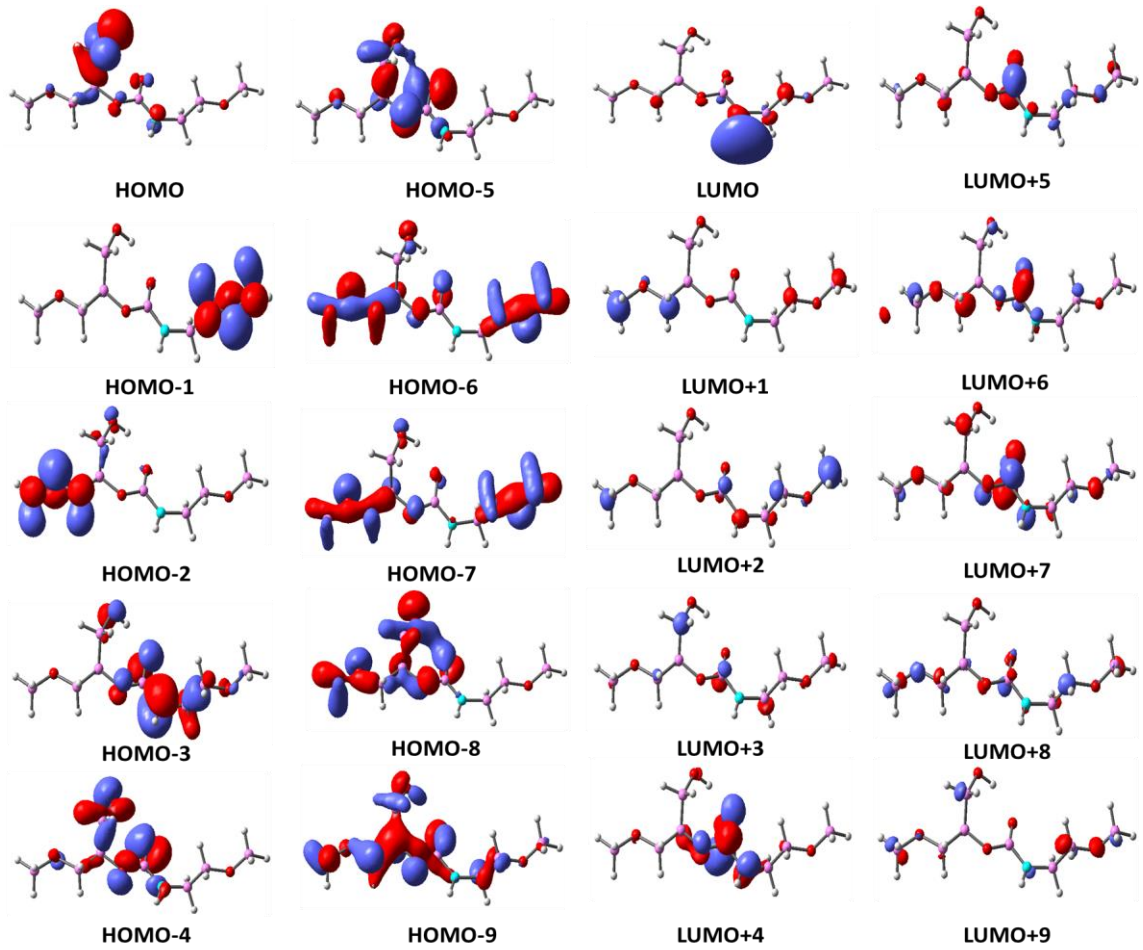

Figure S11. HOMOs and LUMOs of model compound-1a (configuration 10) in ground state (S_0)

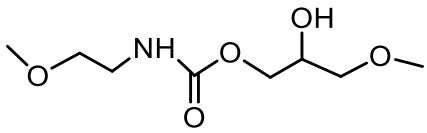

Model compound-2a

Optimized by B3LYP+6-311G

Configuration	Structure	Energy (Hartree)	HOMO (eV)	LUMO (eV)	$\Delta E_{HOMO-LUMO}$
Configuration-1	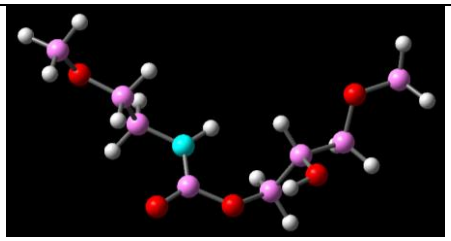	-745.885009	-7.18	0.16	7.34
Configuration-2	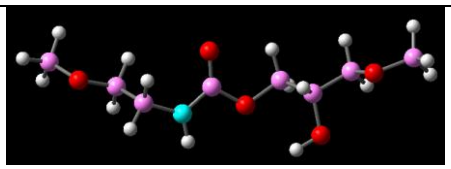	-745.900770	-6.97	0.59	7.74
Configuration-3	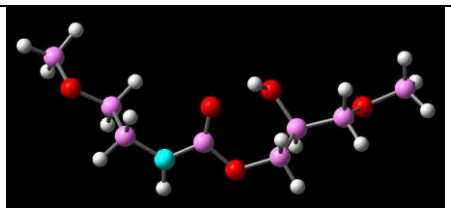	-745.901676	-6.91	0.38	7.29
Configuration-4	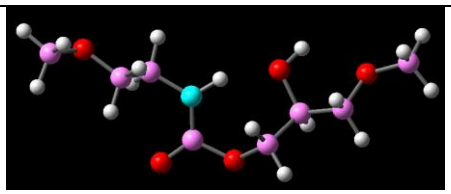	-745.901021	-6.81	0.51	7.32
Configuration-5	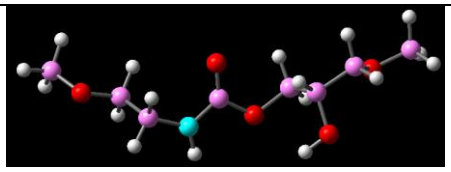	-745.903453	-7.05	0.64	7.69
Configuration-6	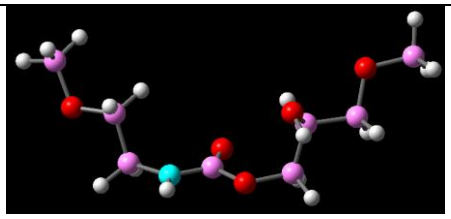	-745.895064	-7.05	0.61	7.66
Configuration-7	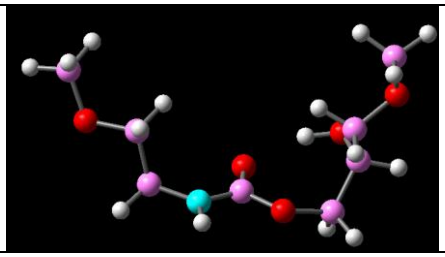	-745.903500	-6.85	0.22	7.07

Configuration-8	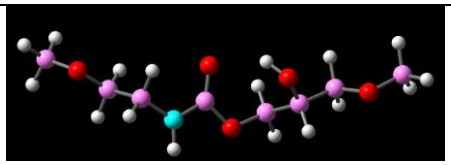	**-746.172255**	**-7.18**	**0.13**	**7.31**
Configuration-9	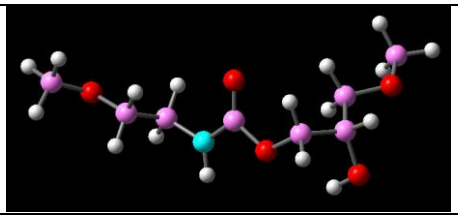	-745.900421	-6.93	0.46	7.39

Coordinates of model compound-2a (configuration-8) in ground state (S_0)

Optimized by B3LYP+6-311+G(d, p)

C	5.61597	-0.62201	-0.73114
O	4.61078	-0.51004	0.25885
C	3.46463	0.18852	-0.18549
C	2.44537	0.16879	0.95243
N	1.24297	0.92386	0.63287
C	0.16226	0.35975	0.0436
O	0.07915	-0.80323	-0.31179
H	6.44452	-1.17423	-0.28746
H	5.25086	-1.16786	-1.6117
H	5.97442	0.36613	-1.05209
H	3.72268	1.22681	-0.44819
H	3.0354	-0.29015	-1.07695
H	2.16222	-0.86163	1.16834
H	2.89524	0.59234	1.85283
H	1.18107	1.90215	0.86624
O	-0.83076	1.27823	-0.10148
O	-2.50439	-0.83933	0.93672
H	-1.8199	-1.3009	0.42822
C	-3.0347	0.19836	0.15859
H	-3.42397	0.93063	0.87846
C	-2.01562	0.83976	-0.78665
H	-1.75409	0.1287	-1.57156
H	-2.44446	1.73502	-1.23347
C	-6.24729	-1.09095	-1.10896
H	-7.15221	-1.42608	-0.64668
H	-6.45626	-0.24556	-1.7307
H	-5.83802	-1.87963	-1.7051
C	-4.07132	-0.22358	-0.69961
H	-3.76363	-1.0405	-1.31837
H	-4.27865	0.62917	-1.31176
O	-5.23318	-0.69023	-0.02149

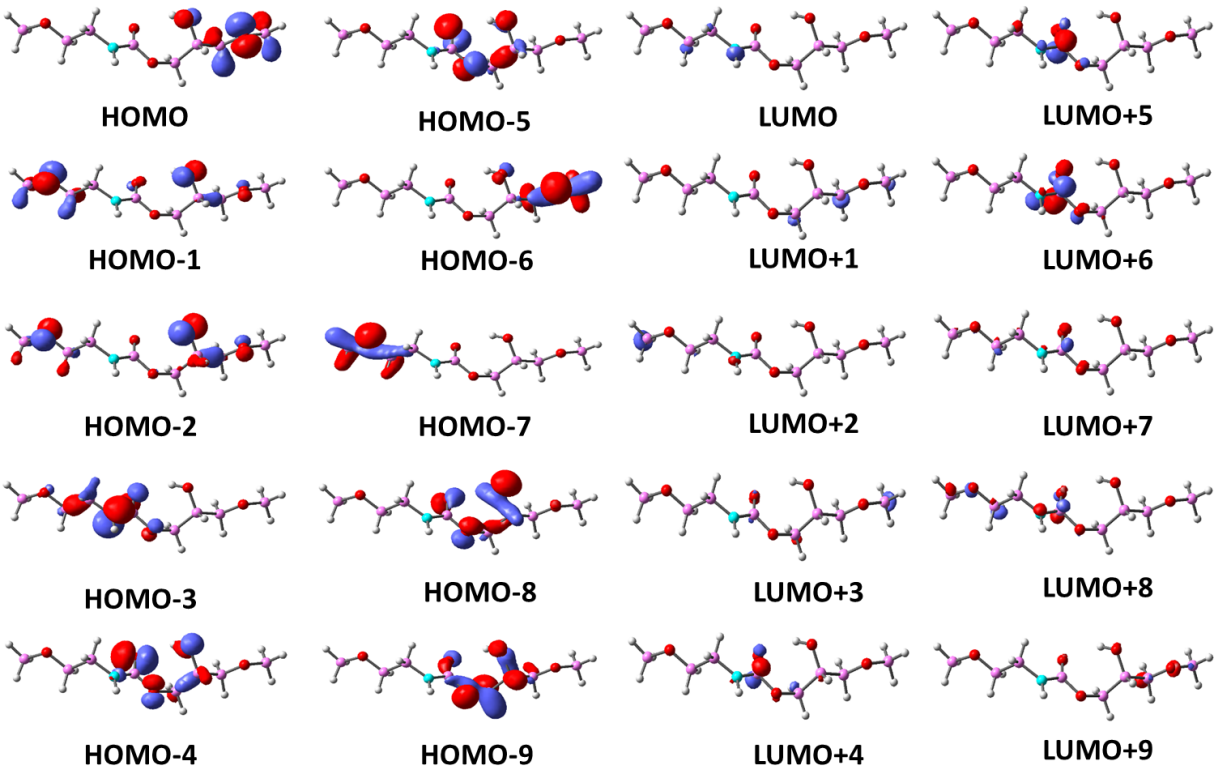

Figure S12. HOMOs and LUMOs of compound-2a (configuration-8) in ground state (S_0)

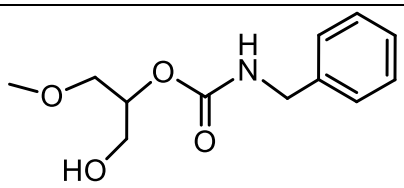

Model compound-1b

Optimized by B3LYP+6-311G

Configuration	**Structure**	**Energy (Hartree)**	**HOMO (eV)**	**LUMO (eV)**	**$\Delta E_{HOMO-LUMO}$**
Configuration-1	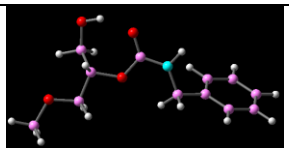	-823.1295	-6.78	-0.72	6.06
Configuration-2	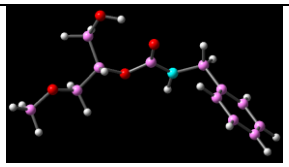	**-823.1321**	**-7.08**	**-0.84**	**6.24**
Configuration-3	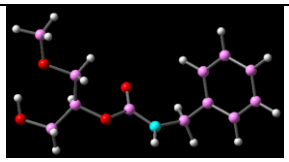	-823.1315	-7.01	-0.57	6.44
Configuration-4	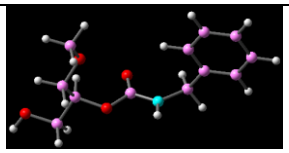	-823.1255	-6.73	-0.32	6.41
Configuration-5	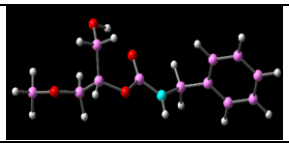	-823.1316	-6.93	-0.67	6.26

Coordinates of model compound-1b (configuration-2) in ground state (S_0)

Optimized by B3LYP+6-311+G(d, p)

O	4.50369	1.27936	0.39489
C	0.22484	-0.80387	-0.37778
O	0.21305	-1.64451	0.54821
O	1.32749	-0.05838	-0.73789
C	2.55036	-0.06543	0.12074
C	3.28467	-1.40379	0.09635
O	2.82158	-2.33751	1.09341
C	3.3608	1.08099	-0.47013
C	5.38884	2.34414	-0.03464
H	2.25563	0.16798	1.14374
H	3.22003	-1.81997	-0.91739
H	4.33005	-1.21346	0.32915
H	1.84171	-2.37362	1.06038
H	3.68339	0.83245	-1.48836
H	2.74207	1.98248	-0.51086
H	6.19276	2.38195	0.69412
H	5.80392	2.13834	-1.02683
H	4.86839	3.30727	-0.05466
C	-2.14108	-1.1612	-1.02483
H	-1.9698	-2.06809	-0.44745
H	-2.49065	-1.45646	-2.01525
C	-3.17565	-0.28246	-0.34482
C	-4.24532	0.25806	-1.06925
C	-3.06662	0.00648	1.02506
C	-5.19054	1.07615	-0.44208
H	-4.34355	0.03557	-2.12532
C	-4.0083	0.82314	1.65189
H	-2.24747	-0.4159	1.593
C	-5.07249	1.36097	0.91945
H	-6.01298	1.48566	-1.01359
H	-3.917	1.0354	2.70887
H	-5.80317	1.99187	1.40776
N	-0.83082	-0.50933	-1.1708
H	-0.72108	0.24302	-1.83047

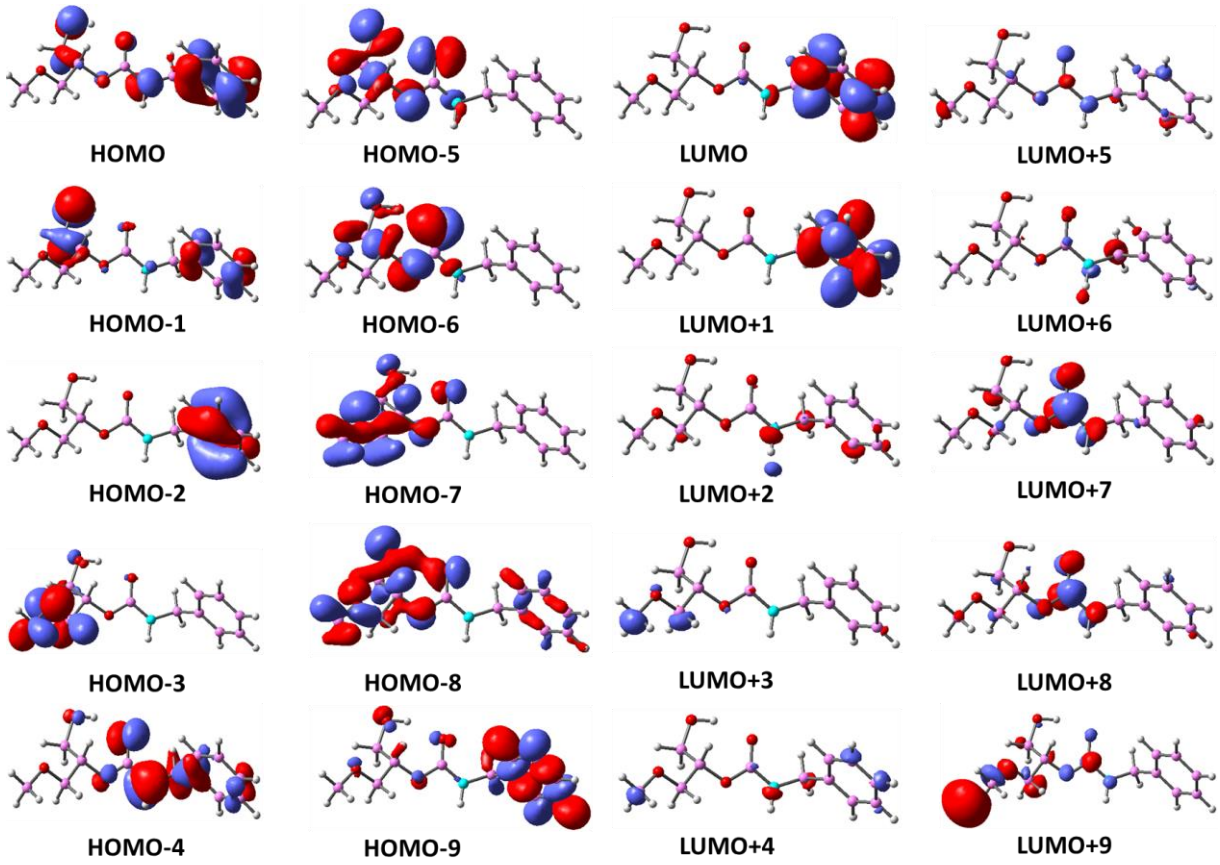

Figure S13. HOMOs and LUMOs of model compound-1b (configuration-2) in ground state (S_0)

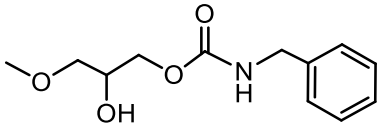

Model compound-2b

Configuration	Structure	Energy (Hartree)	HOMO (eV)	LUMO (eV)	$\Delta E_{HOMO-LUMO}$
Configuration-1	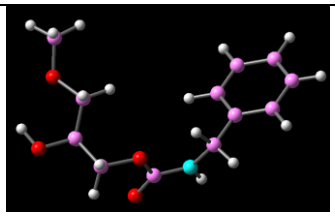	-823.129010	-6.96	-0.57	6.39
Configuration-2	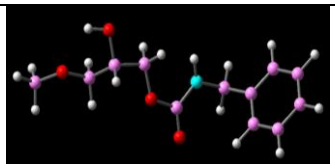	-823.120167	-6.95	-0.50	6.45
Configuration-3	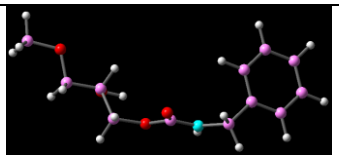	-823.125994	-6.95	-0.59	6.36
Configuration-4	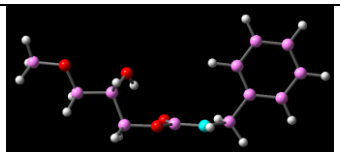	**-823.404485**	**-6.97**	**-0.71**	**6.26**
Configuration-5	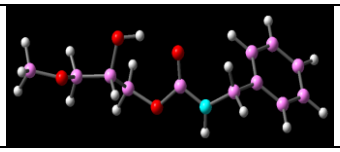	-823.128513	-6.74	-0.61	6.13

Coordinates of model compound-2b (configuration-4) in ground state (S_0)

Optimized by B3LYP+6-311+G(d, p)

N	-0.6602	-1.39879	-0.38161
C	0.59996	-1.23465	0.08403
O	0.92368	-1.18062	1.25872
H	-0.78523	-1.39494	-1.38269
O	1.47518	-1.14141	-0.95381
C	-1.82927	-1.4591	0.48646
H	-2.30946	-2.43801	0.39067
H	-1.45285	-1.38176	1.50844
C	-2.84154	-0.36533	0.20254
C	-2.4518	0.97847	0.16051
C	-4.18649	-0.68353	0.00235
C	-3.39024	1.97942	-0.07373
H	-1.41008	1.24089	0.3114
C	-5.12962	0.31826	-0.22965
H	-4.50086	-1.72234	0.02819
C	-4.73298	1.65229	-0.26875
H	-3.07467	3.01641	-0.10129
H	-6.16991	0.05437	-0.38403
H	-5.46268	2.43302	-0.45134
C	2.86619	-1.02591	-0.6123
H	3.41145	-1.43752	-1.45981
H	3.08406	-1.61177	0.28169
C	3.29151	0.42687	-0.38368
H	3.21422	1.01335	-1.30883
O	2.49444	1.10436	0.55058
H	2.203	0.47745	1.23058
C	6.76579	1.26975	0.51374
H	7.2172	0.62264	-0.20902
H	7.32203	2.18191	0.57249
H	6.76479	0.79036	1.47035
C	4.64222	0.32722	0.00705
H	5.08622	-0.3197	-0.72045
H	4.74026	-0.10884	0.97923
O	5.31696	1.57821	0.09263

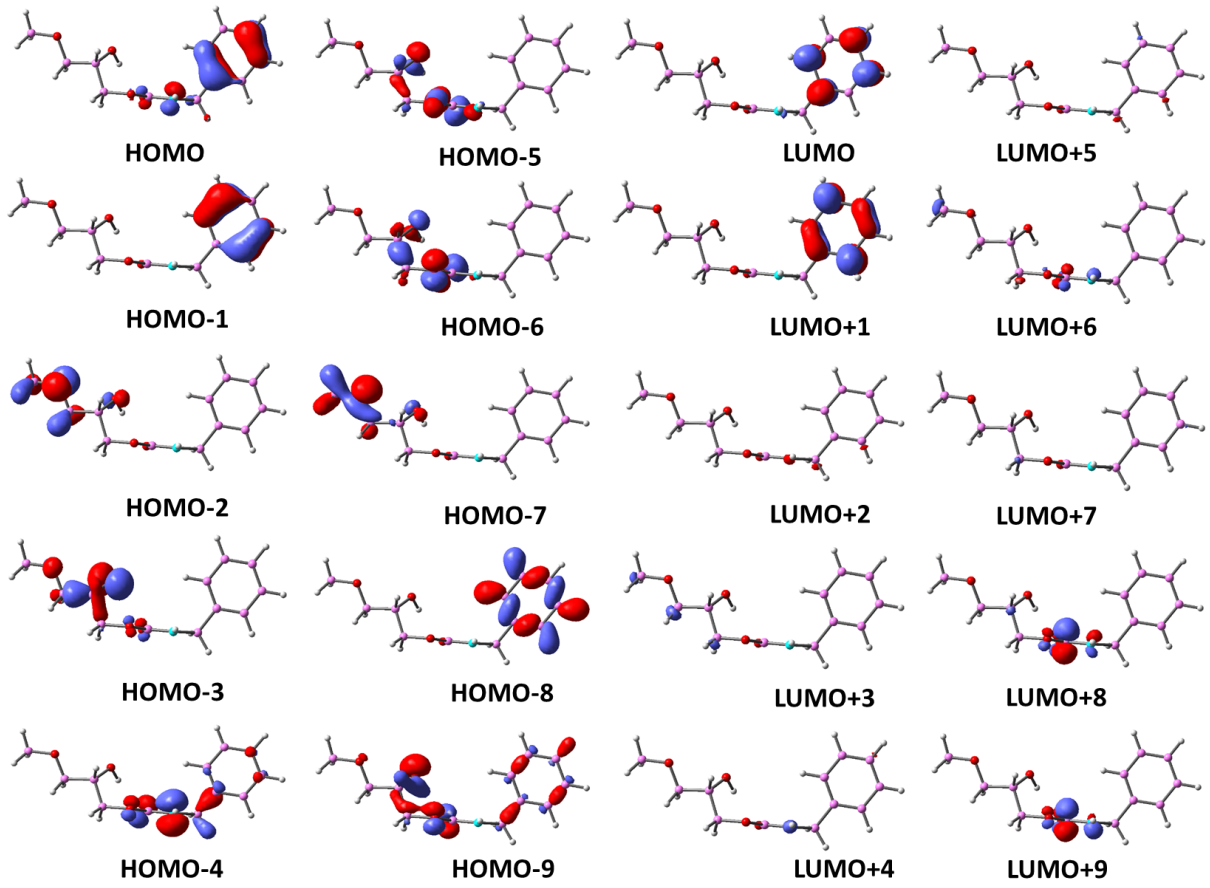

Figure S14. HOMOs and LUMOs of model compound-2b (configuration-4) in ground state (S_0)

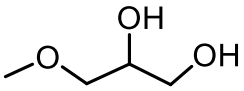

Model compound-3

Optimized by B3LYP+6-311G

Configuration	**Structure**	**Energy (Hartree)**	**HOMO (eV)**	**LUMO (eV)**	$\Delta E_{HOMO-LUMO}$
Configuration-1	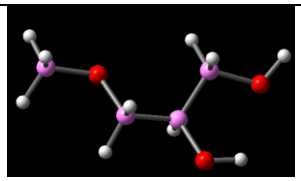	-384.0716	-7.12	0.56	7.68
Configuration-2	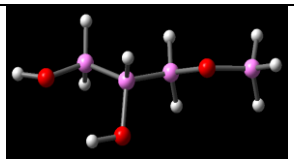	-384.0663	-6.87	0.50	7.37
Configuration-3	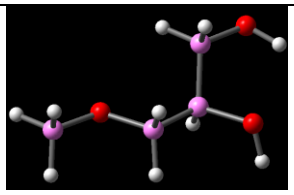	-384.0703	-7.15	0.39	7.54
Configuration-4	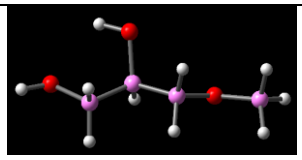	-384.0663	-6.87	0.50	7.37
Configuration-5	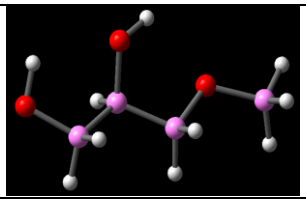	**-384.0743**	**-7.19**	**0.81**	**8.00**

Coordinates of optimized model compound-3 (configuration-5) in ground state (S_0)
Optimized by B3LYP+6-311+G(d, p)

C	0.76524	-0.65469	0.1329
C	-0.55202	-0.03299	-0.29207
C	-1.78864	-0.76727	0.19987
O	-2.98147	-0.04378	-0.19095
O	-0.66021	1.30732	0.28483
H	0.80556	-0.75641	1.22309
H	-0.58117	0.04207	-1.38287
H	-1.86505	-1.75437	-0.25207
H	-1.73809	-0.87233	1.28887
H	-2.8417	0.89173	0.05072
H	0.15805	1.79446	0.07973
H	0.90793	-1.6388	-0.32843
O	1.79867	0.26846	-0.31466
C	3.14638	-0.10973	0.06466
H	3.42483	-1.06954	-0.38113
H	3.80055	0.66886	-0.31656
H	3.24743	-0.17354	1.15273

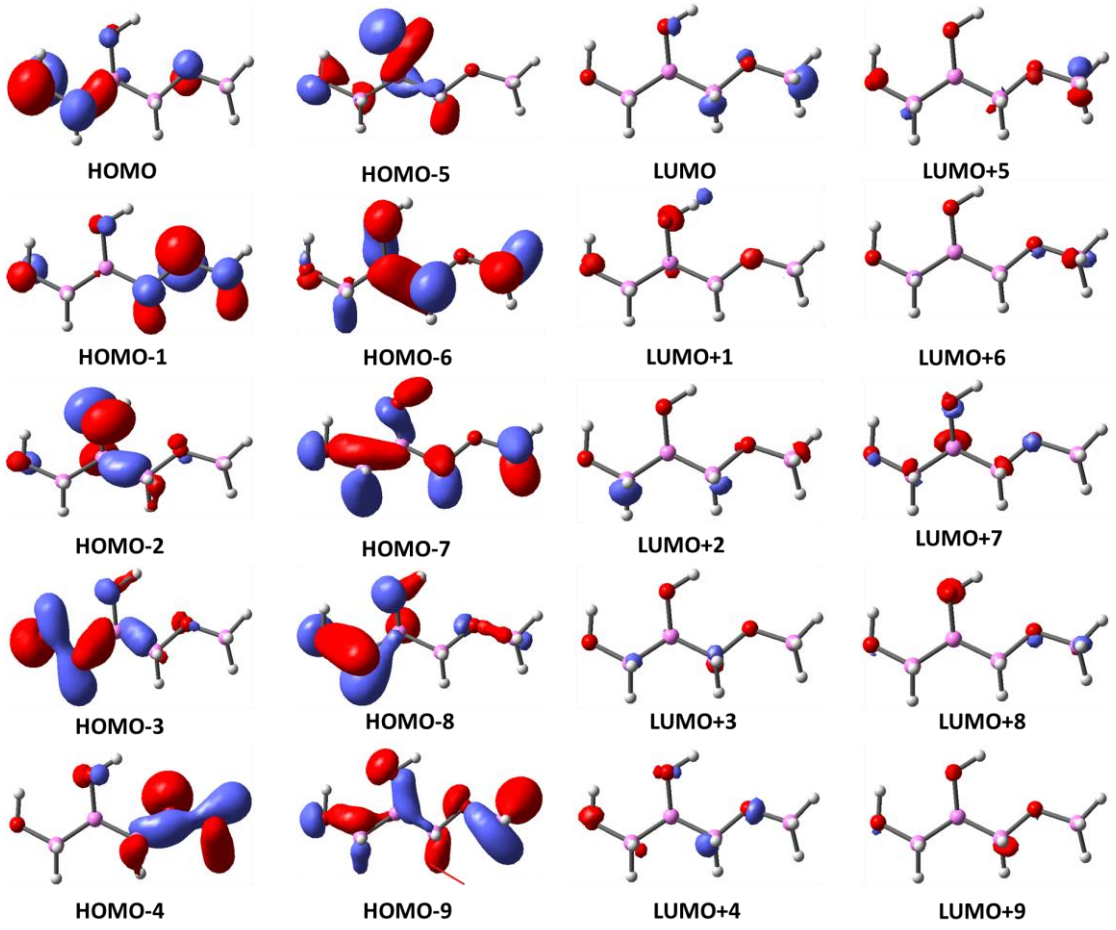

Figure S15. HOMOs and LUMOs of model compound-3 (configuration-5) in ground state (S_0)

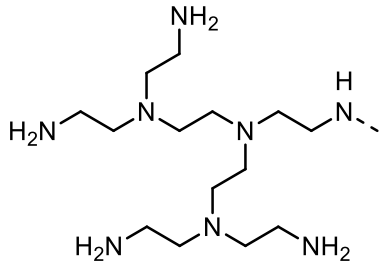

Model PEI

Optimized by B3LYP+6-311G

Configuration	Structure	Energy (Hartree)	HOMO (eV)	LUMO (eV)	$\Delta E_{HOMO-LUMO}$
Configuration-1	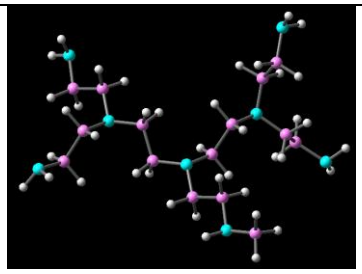	-1033.920359	-5.61	-0.20	5.41

Coordinates of optimized model PEI in ground state (S_0)

Optimized by B3LYP+6-311+G(d, p)

N	-10.77709	-5.9615	0.76157
C	-9.38846	-5.49773	0.92428
C	-9.35133	-3.97766	1.17197
N	-7.99399	-3.43363	1.21776
C	-8.03238	-1.97394	1.09609
C	-6.64759	-1.29507	0.9914
N	-6.73172	0.14849	0.7618
C	-5.45418	0.78392	1.09178
C	-5.43975	2.31965	0.98321
N	-4.17919	2.85151	1.50598
C	-4.10361	4.30987	1.46001
C	-7.26841	-3.87624	2.40896
C	-5.86257	-4.39363	2.06125
N	-5.14882	-4.82061	3.27628
C	-7.17283	0.46485	-0.5991
C	-8.26921	1.55203	-0.60198
N	-8.92611	1.74365	-1.89519
C	-10.12054	2.57645	-1.75839
C	-7.9931	2.22938	-2.90936
C	-8.61326	2.45902	-4.29916
N	-7.56412	2.74142	-5.29422
C	-9.89469	4.0471	-1.36603
N	-11.18226	4.75915	-1.29194
H	-10.80037	-6.9909	0.65765
H	-11.325	-5.76224	1.61658
H	-8.8133	-5.74704	0.00157
H	-8.93934	-6.07516	1.76268
H	-9.91141	-3.7237	2.1031

H	-9.91731	-3.52062	0.32369
H	-8.62375	-1.71084	0.18946
H	-8.5876	-1.52689	1.95571
H	-6.12154	-1.47792	1.95756
H	-6.03952	-1.77937	0.19099
H	-5.19076	0.54604	2.15189
H	-4.63471	0.36609	0.45874
H	-5.55197	2.64182	-0.07796
H	-6.28749	2.73424	1.57859
H	-4.06747	2.53981	2.50306
H	-3.12312	4.64484	1.86864
H	-4.19048	4.68351	0.41428
H	-4.90838	4.7656	2.08023
H	-7.7934	-4.7056	2.9345
H	-7.21415	-3.07475	3.18063
H	-5.25091	-3.61413	1.55581
H	-5.93916	-5.25957	1.36217
H	-4.18512	-5.1148	3.04017
H	-5.03775	-4.02317	3.92649
H	-7.60248	-0.42254	-1.1167
H	-6.30124	0.7432	-1.23185
H	-7.85004	2.51282	-0.232
H	-9.02939	1.22803	0.15066
H	-10.8054	2.11665	-1.00547
H	-10.71284	2.5404	-2.70219
H	-7.19108	1.46984	-3.06538
H	-7.48286	3.16199	-2.57313
H	-9.30743	3.33029	-4.29496
H	-9.18453	1.55742	-4.62292
H	-7.99011	2.96891	-6.20954
H	-7.03015	3.58601	-5.02491
H	-9.26214	4.57136	-2.1175
H	-9.39278	4.13434	-0.37567
H	-11.02547	5.76728	-1.11832
H	-11.6724	4.7131	-2.20221

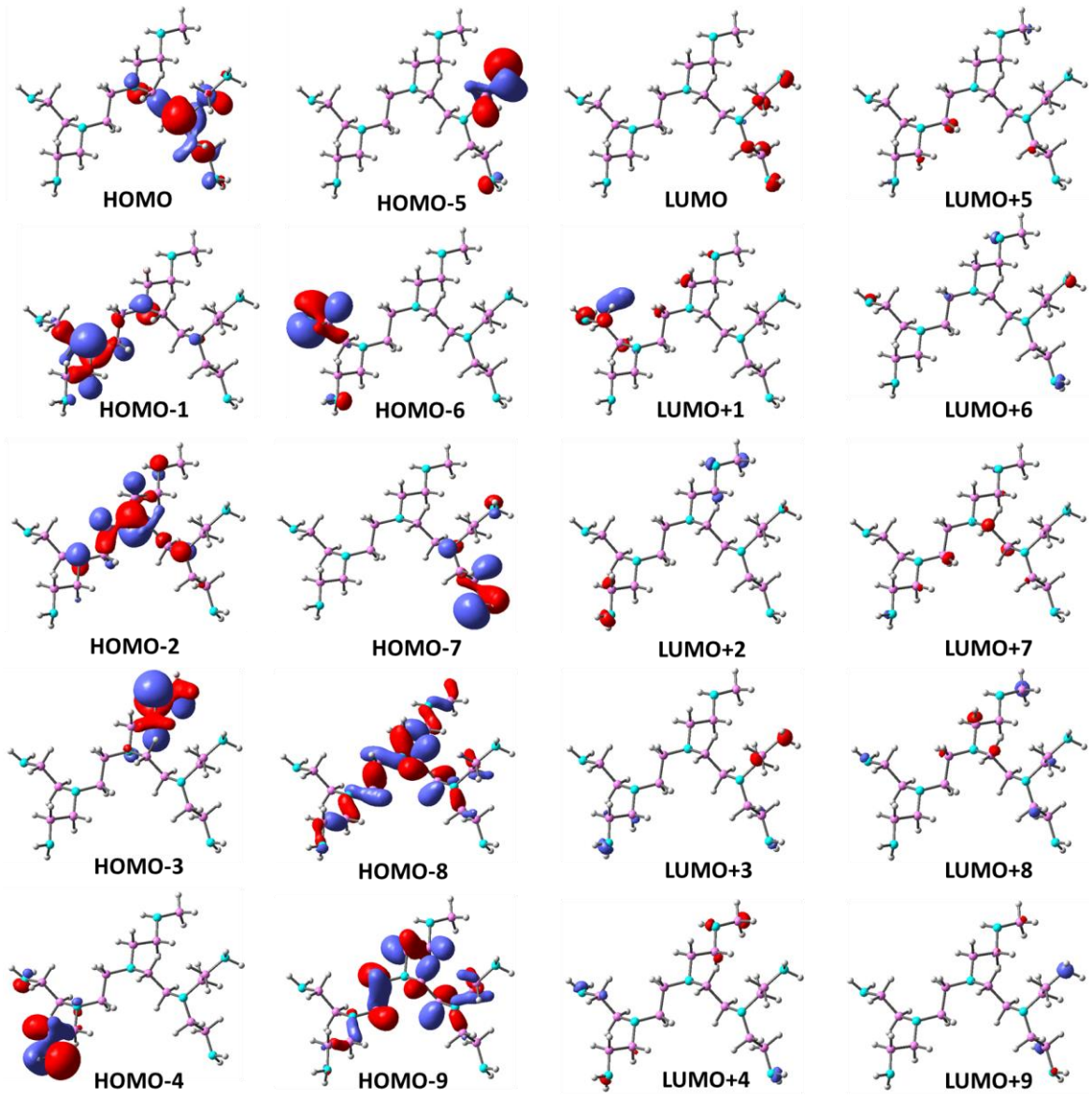

Figure S16. HOMOs and LUMOs of PEI in ground state (S_0)

Reduced density gradient (RDG)

RDG is an important computational tools for identifying and quantifying the noncovalent interactions, like hydrogen bonding, van der Waals interaction and steric repulsion.[1,2] The noncovalent interaction indices are usually calculated by using software VMD version 1.9.4a53 [3] integrated with Multiwfn version 3.8 [4] program and gnuplot version 5.2. The formatted .chk file of any optimized structure is used as input for calculation. Generally, noncovalent interactions are analyzed from the plots of RDG (s) versus the sign of second Hessian eigenvalue multiplied by electron density [Sign(λ_2)ρ(r)], using the noncovalent interaction index based visualization technique.[1,2] In this context, attractive ($\lambda_2 < 0$) and repulsive ($\lambda_2 > 0$) interactions are confirmed from the higher absolute values of electron densities at interaction of critical points. Additionally, the mapping of [Sign(λ_2)ρ(r)] onto a three-dimensional RDG isosurfaces produces red, green and blue color scattering points correlated to steric repulsions, van der Waals forces and hydrogen bonding, respectively, signifying the nature/strength of noncovalent interactions.[5]

[1] J. Contreras-García, E. R. Johnson, S. Keinan, R. Chaudret, J.-P. Piquemal, D. N. Beratan, W. Yang, NCIPLOT: A Program for Plotting Noncovalent Interaction Regions. J. Chem. Theory Comput. 2011, 7, 625.

[2] E. R. Johnson, S. Keinan, P. Mori-Sanchez, J. Contreras-García, A. J. Cohen, W. Yang, Revealing Noncovalent Interactions. J. Am. Chem. Soc. 2010, 132, 6498.

[3] W. Humphrey, A. Dalke and K. Schulten, VMD-Visual Info Molecular Dynamics, J. Molec. Graphics 1996, 14.1, 33-38.

[4] T. Lu, F. Chen, Multiwfn: A Multifunctional Wave Function Analyzer. J. Comput. Chem., 2012, 33, 580-592.

[5] G. Saleh, C. Gatti, L. L. Presti, J. Contreras-Garc, Revealing Non-covalent Interactions in Molecular Crystals through Their Experimental Electron Densities. Chem. - Eur. J. 2012, 18, 15523.

Aggregate of 1b+2b+3

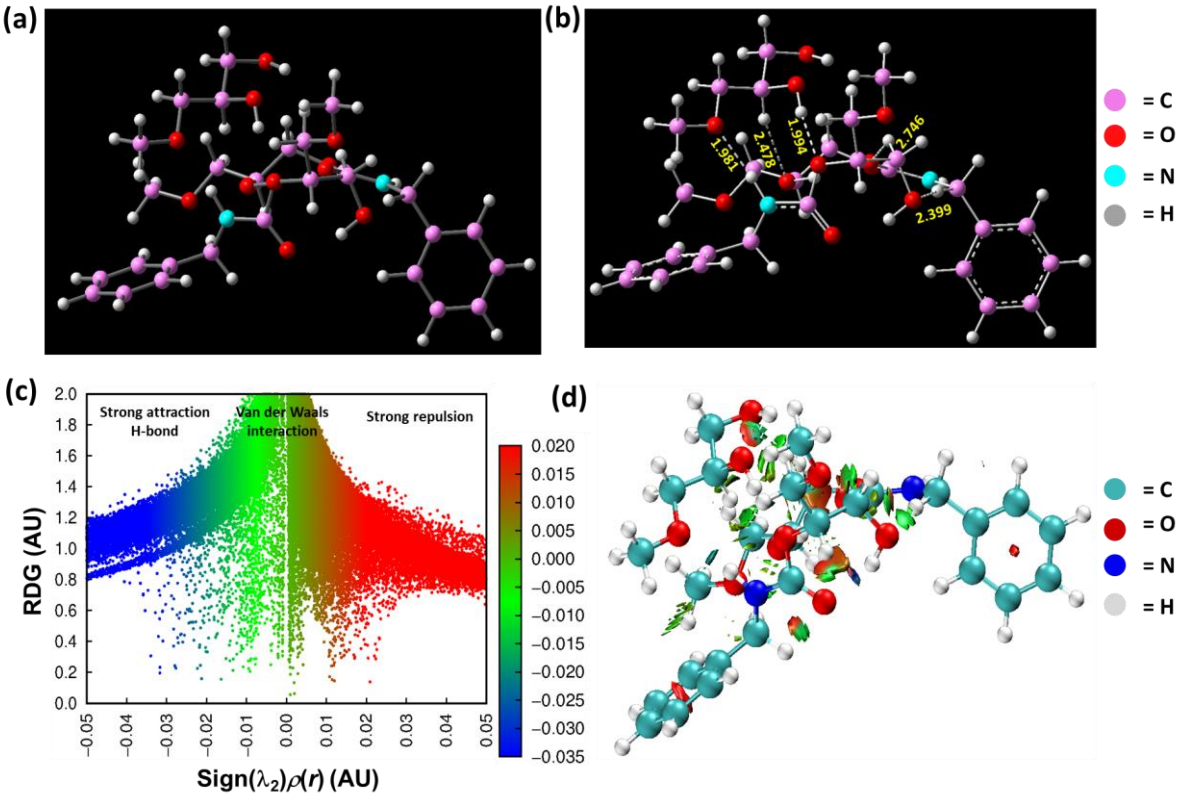

Figure S17. (a) Optimized structure of aggregate of 1b+2b+3; (a) structure of aggregate of 1b+2b+3 showing hydrogen bonding; (c) reduced density gradient (RDG) versus electron density × sign of second Hessian eigenvalue [sign(λ_2)ρ(r)] plots for aggregate of 1b+2b+3; (d) independent gradient model showing different interaction index for aggregate of 1b+2b+3

Coordinates of aggregate 1b+2b+3 in S_0

Optimized by B3LYP+6-311+G(d, p)

C	2.17924	4.90732	-0.77864
O	1.63654	3.62202	-1.06618
C	0.29976	3.46562	-0.58878
C	-0.31722	2.23518	-1.24828
N	-1.66892	1.99076	-0.74858
O	-3.96915	2.32902	-0.82251
C	-2.72188	2.68718	-1.26999
O	-2.62423	3.57413	-2.0857
H	3.20029	4.91812	-1.15887
H	1.59589	5.6925	-1.27321
H	2.1943	5.09774	0.30204
H	0.30221	3.35636	0.50448
H	-0.29129	4.35069	-0.84888
H	-0.3362	2.38145	-2.33095
H	0.27591	1.34609	-1.03026
H	-1.85764	1.08252	-0.34203
C	-4.2099	1.67573	0.43219
H	-5.19905	2.01434	0.73784
H	-3.47727	1.98443	1.18283
C	-4.24401	0.14628	0.29852
H	-4.58495	-0.11736	-0.70993
O	-2.95798	-0.44553	0.42939
H	-2.68848	-0.44856	1.37618
N	1.49973	-0.38369	1.70889
C	5.69902	-2.8928	-1.00442
O	4.64022	-2.04379	-0.58593
C	2.63994	-0.01138	2.34777
O	2.69546	0.541	3.42394
O	3.79696	-0.3294	1.66486
C	3.92362	0.08855	0.28862
C	4.19586	1.60053	0.22281
O	4.05477	2.08248	-1.10431
C	5.05945	-0.70306	-0.32427
H	5.27362	-3.88183	-1.17541
H	6.15372	-2.52862	-1.93434
H	6.47276	-2.96339	-0.23053
H	3.00412	-0.11787	-0.26379
H	3.51357	2.11131	0.90996
H	5.21588	1.81031	0.56022
H	3.1604	2.44939	-1.20296
H	5.36299	-0.21958	-1.26084
H	5.90966	-0.70979	0.36983
C	0.19186	0.01995	2.1847
H	-0.41238	0.29579	1.31997
H	0.3114	0.89594	2.82199
C	-0.54248	-1.08015	2.9486
H	-0.45286	-2.03956	2.42354
H	-0.13219	-1.19299	3.95848
O	-1.92211	-0.69564	3.02268
C	-2.68198	-1.47034	3.94376
H	-2.30066	-1.34086	4.96286
H	-3.70972	-1.11135	3.89253
H	-2.65349	-2.53595	3.68313

H	1.54373	-1.06147	0.948
C	-0.92211	-2.7614	-2.75685
C	-0.20747	-2.58344	-1.4221
C	1.30196	-2.57881	-1.59639
O	1.91319	-2.56392	-0.31214
O	-0.58054	-1.35765	-0.80379
H	-0.68297	-1.92053	-3.42477
H	-0.47621	-3.42662	-0.77034
H	1.60086	-3.47562	-2.15488
H	1.59626	-1.69566	-2.17953
H	2.88116	-2.50906	-0.41873
H	-1.53944	-1.35384	-0.65435
H	-0.60093	-3.6958	-3.24193
O	-2.31604	-2.79738	-2.49762
C	-3.10229	-2.83565	-3.67479
H	-2.88728	-3.7333	-4.27071
H	-4.14725	-2.85834	-3.36476
H	-2.93139	-1.94801	-4.29836
C	-6.50652	-2.02818	2.2229
H	-7.35487	-1.37788	2.17489
H	-6.82984	-3.04379	2.12853
H	-6.00982	-1.89776	3.16161
C	-5.13	-0.33552	1.27225
H	-5.99905	0.28859	1.26059
H	-4.64774	-0.25768	2.22423
O	-5.53506	-1.69012	1.07678

Table S3 Absorbance details of aggregate of 1b+2b+3

No.	Energy (cm^{-1})	Wavelength (nm)	Osc. Strength	Major contribution
1	35088.59	284.99	0.0061	HOMO→LUMO (99%)
2	35189.41	284.18	0.0008	HOMO→L+1 (98%)
3	35865.30	278.82	0.0024	HOMO→L+2 (99%)
4	36033.87	277.52	0.0063	HOMO→L+3 (98%)
5	36909.80	270.93	0.0007	H-1→LUMO (98%)
6	37099.34	269.55	0.0002	H-2→L+1 (23%) and H-1→L+1 (74%)
7	37296.95	268.12	0.0010	H-2→LUMO (90%)
8	37719.58	265.11	0.0007	H-1→L+2 (100%)
9	37941.39	263.56	0.0011	H-2→L+3 (21%), H-1→L+3 (76%)
10	38047.85	262.83	0.0003	H-4→LUMO (16%), H-3→LUMO (76%)
11	38097.06	262.49	0.0023	H-2→L+2 (88%)
12	38104.31	262.44	0.0002	H-3→L+1 (84%)
13	38214.81	261.68	0.0013	H-5→L+1 (20%), H-2→L+1 (44%), and H-1→L+1 (12%)
14	38293.05	261.14	0.0001	H-4→LUMO (15%), H-4→L+1 (81%)
15	38354.35	260.73	0.0003	H-5→LUMO (33%), H-4→LUMO (41%), H-4→L+1 (18%)
16	38819.73	257.60	0.0080	H-5→L+1 (50%), H-2→L+3 (26%)
17	38862.48	257.32	0.0005	H-4→L+2 (16%), H-3→L+2 (81%)
18	38949.59	256.74	0.0002	H-3→L+3 (95%)
19	39071.38	255.94	0.0158	H-6→L+1 (13%), H-5→L+1 (16%), H-5→L+3 (11%), H-2→L+3 (27%)
20	39135.90	255.52	0.0010	H-5→L+2 (14%), H-4→L+2 (35%), H-4→L+3 (47%)
21	39152.84	255.41	0.0017	H-5→L+2 (16%), H-4→L+2 (27%), H-4→L+3 (53%)
22	39182.68	255.21	0.0007	H-6→LUMO (94%)
23	39363.35	254.04	0.0018	H-6→L+1 (81%)
24	39685.98	251.98	0.0099	H-5→L+3 (77%)
25	39975.53	250.15	0.0018	H-6→L+2 (80%), H-5→L+2 (11%)
26	40152.17	249.05	0.0047	H-8→LUMO (10%), H-6→L+2 (17%), H-6→L+3 (12%), H-5→L+2 (26%)
27	40168.30	248.95	0.0001	H-6→L+3 (84%)
28	40355.42	247.80	0.0032	H-7→LUMO (89%)
29	40474.79	247.07	0.0039	HOMO→L+4 (100%)
30	**40582.87**	**246.41**	**0.0218**	**H-13→LUMO (13%), H-9→LUMO (24%) and H-5→LUMO (17%)**

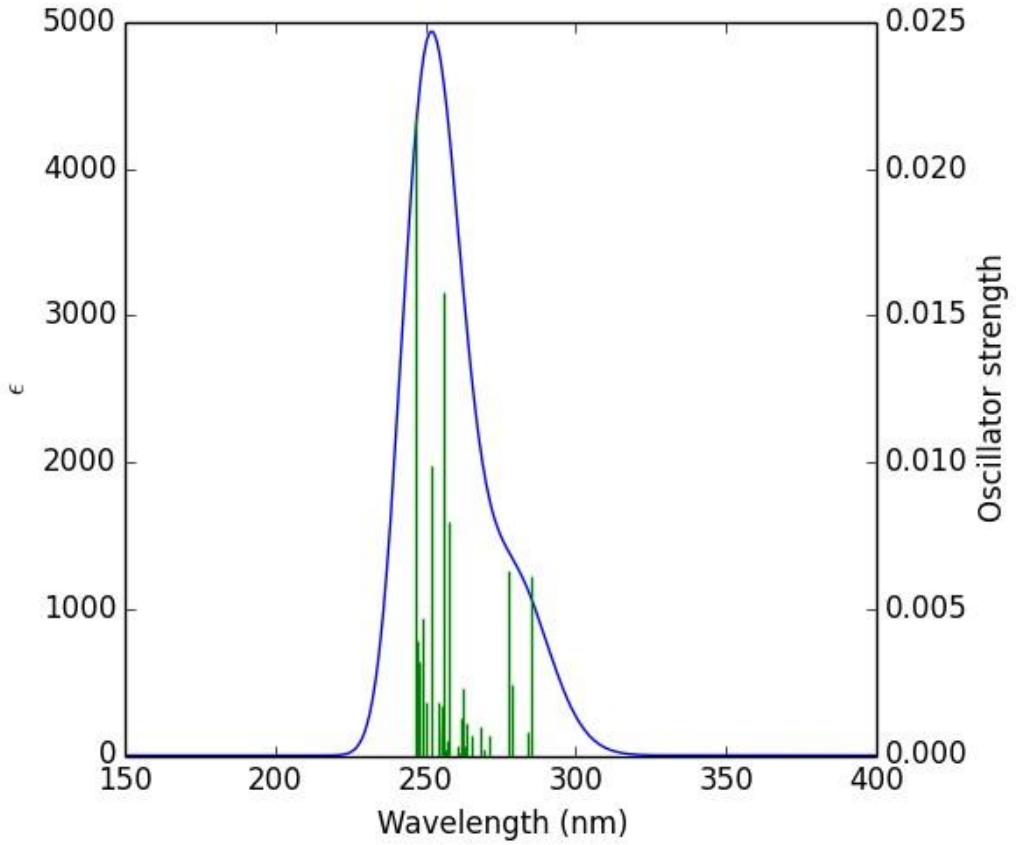

Figure S18. Absorbance spectrum of 1b+2b+3 (NIPUF1)

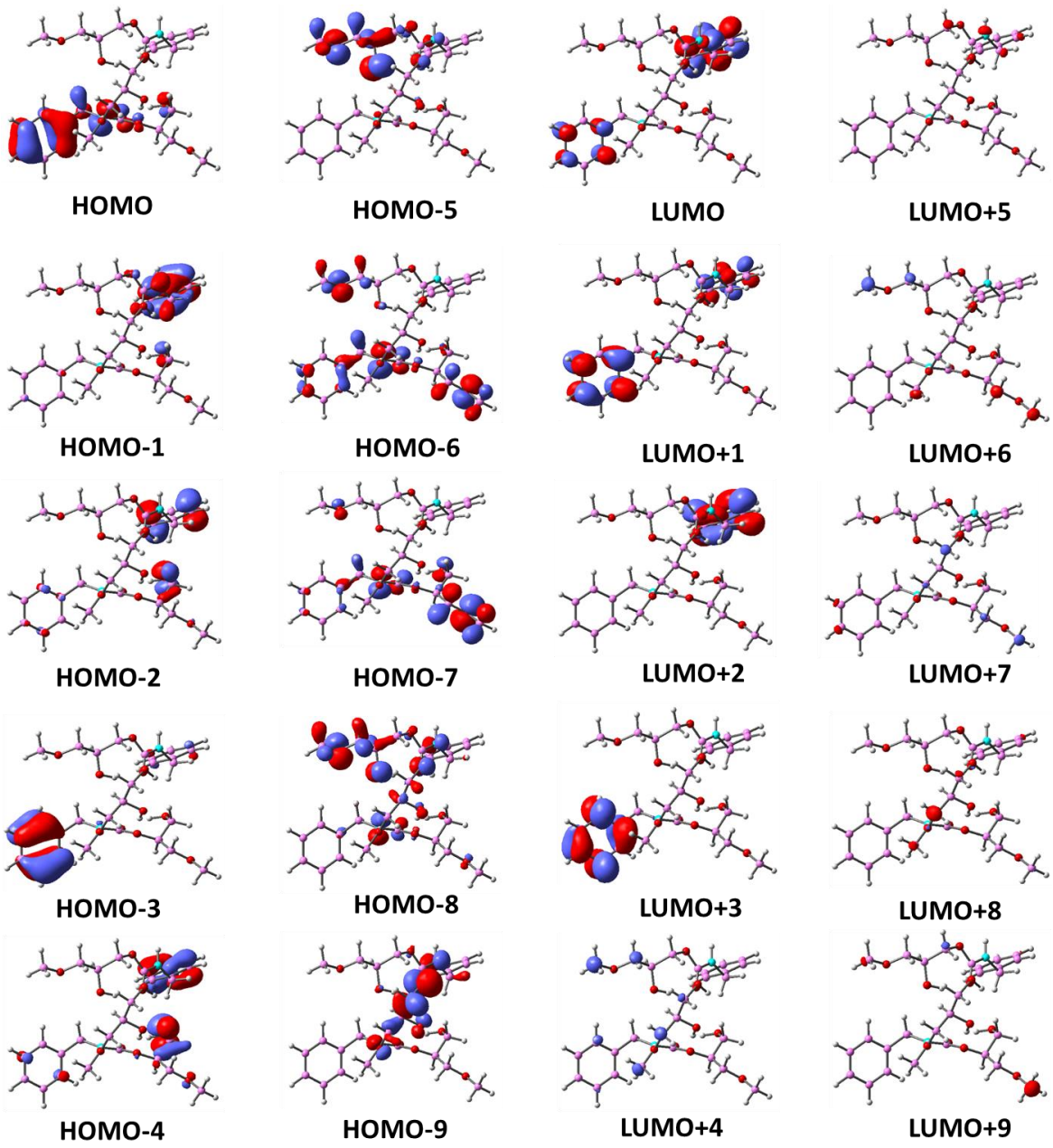

Figure S19. HOMOs and LUMOs of aggregate of 1b+2b+3 in ground state (S_0)

Coordinates of aggregate 1b+2b+3 in S_1

Optimized by B3LYP+6-311+G(d, p)

O	0.69642	5.56822	-0.59143
C	-0.67697	1.43739	1.26314
O	0.16969	1.3804	2.14254
O	-0.60003	2.30936	0.20795
C	0.41464	3.36213	0.2571
C	1.8053	2.84487	-0.10888
O	2.5328	2.30003	0.98115
C	-0.10083	4.40851	-0.72933
C	0.31906	6.60663	-1.4762
H	0.42666	3.78451	1.2642
H	1.69894	2.10868	-0.91802
H	2.38551	3.69215	-0.48126
H	1.89819	1.82967	1.54761
H	-0.05185	4.02281	-1.75879
H	-1.1529	4.62796	-0.50146
H	0.99199	7.44428	-1.29281
H	0.41154	6.29252	-2.52489
H	-0.71527	6.9306	-1.2956
C	-2.02159	-0.4675	2.04699
H	-1.27646	-0.41511	2.84302
H	-1.83938	-1.38386	1.47909
C	-3.41987	-0.47828	2.63125
C	-4.24303	-1.59446	2.46559
C	-3.90411	0.61262	3.36313
C	-5.52223	-1.62621	3.02306
H	-3.87731	-2.44277	1.89601
C	-5.18072	0.58537	3.91799
H	-3.27347	1.48502	3.49927
C	-5.99492	-0.53615	3.74955
H	-6.14846	-2.50121	2.88679
H	-5.53979	1.43569	4.4876
H	-6.98826	-0.55851	4.18379
N	-1.79007	0.68736	1.18022
H	-2.40956	0.82444	0.3847
C	-3.54165	0.69175	-2.4592
C	-2.07658	0.35268	-2.68595
C	-1.8186	-0.19281	-4.0876
O	-0.44123	-0.49585	-4.26562
O	-1.24623	1.5111	-2.56384
H	-3.83171	1.54328	-3.09014
H	-1.77011	-0.40703	-1.95767
H	-2.3728	-1.12083	-4.24603
H	-2.15055	0.54064	-4.83648
H	0.04378	0.2607	-3.9085
H	-1.09967	1.70953	-1.62701
H	-4.17685	-0.16939	-2.71639
O	-3.72215	1.02493	-1.08604
C	-5.04372	1.43979	-0.77265
H	-5.77101	0.6545	-1.015
H	-5.07655	1.63439	0.29914
H	-5.30859	2.35406	-1.31886
N	3.96924	-1.35182	-0.94265
C	2.6515	-1.49774	-1.18826

O	1.7982	-0.63333	-1.03039
H	4.56078	-2.14545	-1.138
O	2.38465	-2.75308	-1.62983
C	4.57009	-0.13949	-0.38125
H	5.07518	0.42229	-1.17395
H	3.76229	0.48804	0.00087
C	5.55744	-0.47031	0.7179
C	5.11285	-1.00079	1.93492
C	6.92537	-0.25485	0.53799
C	6.01762	-1.30971	2.94577
H	4.05149	-1.16229	2.09134
C	7.83573	-0.56191	1.55036
H	7.28213	0.16297	-0.39832
C	7.38334	-1.09157	2.75564
H	5.65828	-1.71279	3.88608
H	8.89447	-0.38572	1.39596
H	8.08746	-1.32929	3.54509
C	1.05214	-3.03236	-2.13134
H	1.19388	-3.95071	-2.70181
H	0.73276	-2.23346	-2.80484
C	0.01967	-3.24987	-1.01851
H	0.51301	-3.78475	-0.19351
O	-0.53358	-2.02749	-0.54761
H	0.17946	-1.36385	-0.57734
C	-3.06801	-5.25155	-0.82336
H	-2.75115	-6.19938	-1.2822
H	-3.642	-5.46984	0.07765
H	-3.70991	-4.71509	-1.53659
C	-1.11965	-4.12825	-1.52049
H	-0.70739	-5.04381	-1.9729
H	-1.68995	-3.58951	-2.29267
O	-1.95914	-4.46684	-0.43367

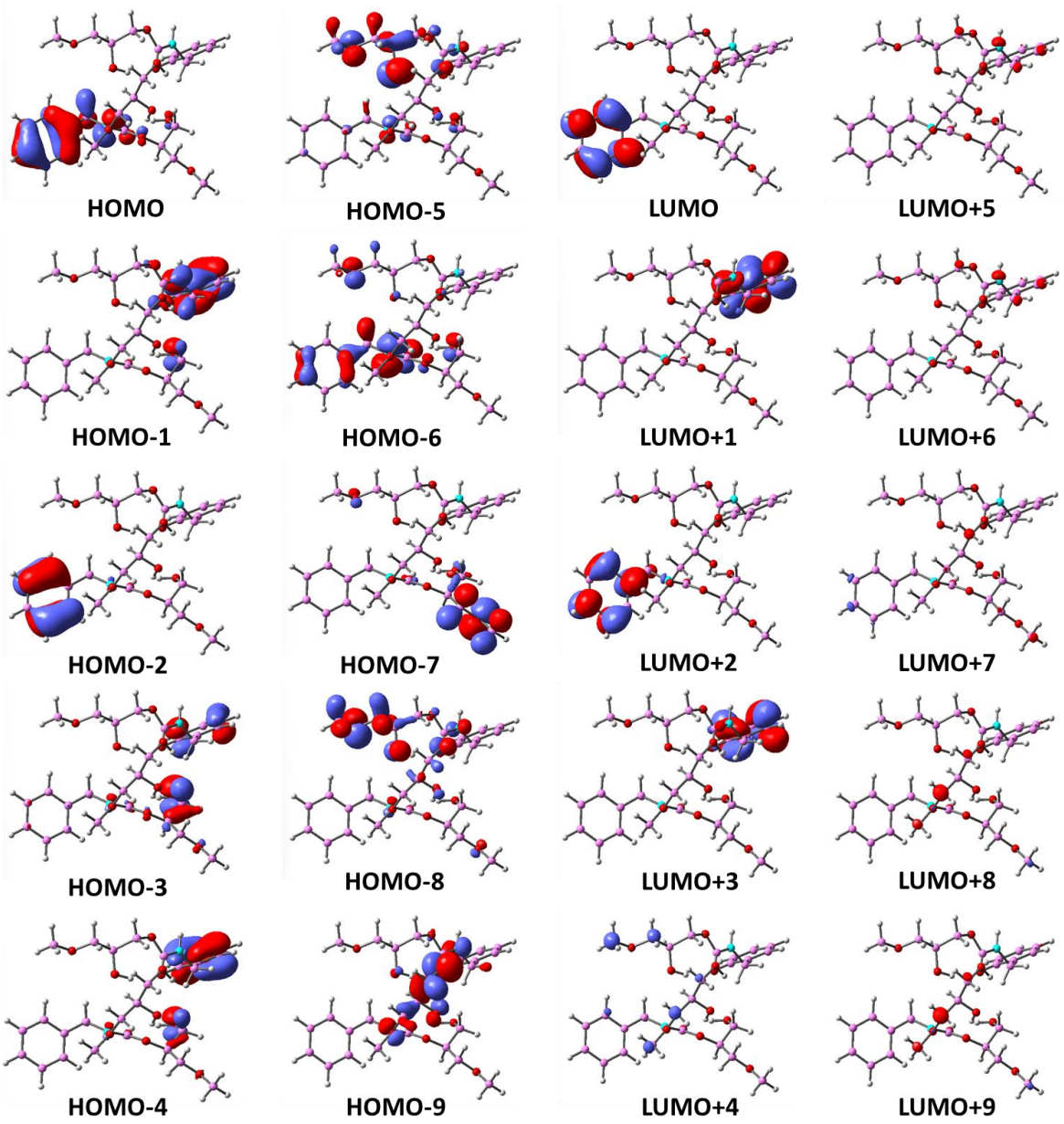

Figure S20. HOMOs and LUMOs of 1b+2b+3 aggregate in first excited state (S_1)

Aggregate of 1a+2a+3

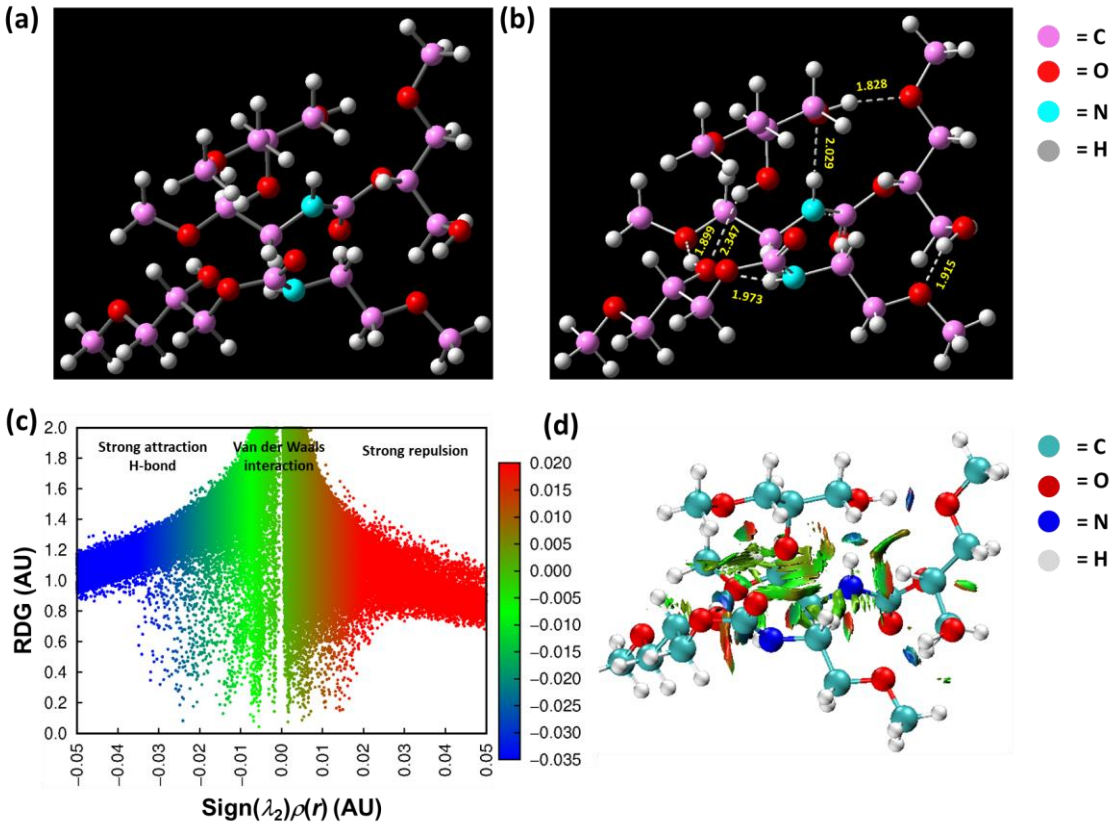

Figure S21. (a) Optimized structure of aggregate of 1a+2a+3; (b) structure of aggregate of 1a+2a+3 showing hydrogen bonding; (c) reduced density gradient (RDG) versus electron density × sign of second Hessian eigenvalue [sign(λ_2)ρ(r)] plot for aggregate of 1a+2a+3; (d) independent gradient model showing different interaction index for aggregate of 1a+2a+3.

Coordinates of aggregate of 1a+2a+3 in S_0

Optimized by B3LYP+6-311+G(d, p)

C	2.17924	4.90732	-0.77864
O	1.63654	3.62202	-1.06618
C	0.29976	3.46562	-0.58878
C	-0.31722	2.23518	-1.24828
N	-1.66892	1.99076	-0.74858
O	-3.96915	2.32902	-0.82251
C	-2.72188	2.68718	-1.26999
O	-2.62423	3.57413	-2.0857
H	3.20029	4.91812	-1.15887
H	1.59589	5.6925	-1.27321
H	2.1943	5.09774	0.30204
H	0.30221	3.35636	0.50448
H	-0.29129	4.35069	-0.84888
H	-0.3362	2.38145	-2.33095
H	0.27591	1.34609	-1.03026
H	-1.85764	1.08252	-0.34203
C	-4.2099	1.67573	0.43219
H	-5.19905	2.01434	0.73784
H	-3.47727	1.98443	1.18283
C	-4.24401	0.14628	0.29852
H	-4.58495	-0.11736	-0.70993
O	-2.95798	-0.44553	0.42939
H	-2.68848	-0.44856	1.37618
N	1.49973	-0.38369	1.70889
C	5.69902	-2.8928	-1.00442
O	4.64022	-2.04379	-0.58593
C	2.63994	-0.01138	2.34777
O	2.69546	0.541	3.42394
O	3.79696	-0.3294	1.66486
C	3.92362	0.08855	0.28862
C	4.19586	1.60053	0.22281
O	4.05477	2.08248	-1.10431
C	5.05945	-0.70306	-0.32427
H	5.27362	-3.88183	-1.17541
H	6.15372	-2.52862	-1.93434
H	6.47276	-2.96339	-0.23053
H	3.00412	-0.11787	-0.26379
H	3.51357	2.11131	0.90996
H	5.21588	1.81031	0.56022
H	3.1604	2.44939	-1.20296
H	5.36299	-0.21958	-1.26084
H	5.90966	-0.70979	0.36983
C	0.19186	0.01995	2.1847
H	-0.41238	0.29579	1.31997
H	0.3114	0.89594	2.82199
C	-0.54248	-1.08015	2.9486
H	-0.45286	-2.03956	2.42354
H	-0.13219	-1.19299	3.95848
O	-1.92211	-0.69564	3.02268
C	-2.68198	-1.47034	3.94376
H	-2.30066	-1.34086	4.96286
H	-3.70972	-1.11135	3.89253
H	-2.65349	-2.53595	3.68313

H	1.54373	-1.06147	0.948
C	-0.92211	-2.7614	-2.75685
C	-0.20747	-2.58344	-1.4221
C	1.30196	-2.57881	-1.59639
O	1.91319	-2.56392	-0.31214
O	-0.58054	-1.35765	-0.80379
H	-0.68297	-1.92053	-3.42477
H	-0.47621	-3.42662	-0.77034
H	1.60086	-3.47562	-2.15488
H	1.59626	-1.69566	-2.17953
H	2.88116	-2.50906	-0.41873
H	-1.53944	-1.35384	-0.65435
H	-0.60093	-3.6958	-3.24193
O	-2.31604	-2.79738	-2.49762
C	-3.10229	-2.83565	-3.67479
H	-2.88728	-3.7333	-4.27071
H	-4.14725	-2.85834	-3.36476
H	-2.93139	-1.94801	-4.29836
C	-6.50652	-2.02818	2.2229
H	-7.35487	-1.37788	2.17489
H	-6.82984	-3.04379	2.12853
H	-6.00982	-1.89776	3.16161
C	-5.13	-0.33552	1.27225
H	-5.99905	0.28859	1.26059
H	-4.64774	-0.25768	2.22423
O	-5.53506	-1.69012	1.07678

Table S4 Absorbance details of aggregate of 1a+2a+3

No.	Energy (cm^{-1})	Wavelength (nm)	Osc. strength	Major contribution
1	40820.81	244.97	0.0004	HOMO→LUMO (100%)
2	41582.20	240.49	0.0030	H-1→LUMO (100%)
3	42000.00	238.10	0.0008	HOMO→L+1 (100%)
4	42281.49	236.51	0.0006	H-2→LUMO (100%)
5	42637.18	234.54	0.0019	HOMO→L+2 (100%)
6	42766.23	233.83	0.0007	H-1→L+1 (100%)
7	43413.90	230.34	0.0018	H-1→L+2 (99%)
8	43462.29	230.08	0.0007	H-2→L+1 (100%)
9	43637.32	229.16	0.0009	HOMO→L+3 (100%)
10	43980.10	227.38	0.0003	HOMO→L+4 (100%)
11	44117.22	226.67	0.0025	H-2→L+2 (100%)
12	44201.91	226.23	0.0006	H-3→LUMO (100%)
13	44406.77	225.19	0.0026	H-1→L+3 (100%)
14	44523.73	224.60	0.0012	H-4→LUMO (100%)
15	44740.69	223.51	0.0007	H-1→L+4 (100%)
16	45027.02	222.09	0.0027	H-5→LUMO (100%)
17	45098.00	221.74	0.0030	H-2→L+3 (100%)
18	45195.59	221.26	0.0006	HOMO→L+5 (100%)
19	**45422.23**	**220.16**	**0.0080**	**H-3→L+1 (98%)**
20	45473.05	219.91	0.0012	H-2→L+4 (99%)
21	45619.84	219.20	0.0007	H-6→LUMO (100%)
22	45713.40	218.75	0.0005	H-4→L+1 (80%) and HOMO→L+6 (19%)
23	45740.82	218.62	0.0055	H-4→L+1 (19%) and HOMO→L+6 (78%)
24	45979.57	217.49	0.0006	H-1→L+5 (99%)
25	46018.28	217.30	0.0031	H-3→L+2 (98%)
26	46094.10	216.95	0.0002	H-7→LUMO (100%)
27	46204.60	216.43	0.0002	HOMO→L+7 (97%)
28	46219.11	216.36	0.0018	H-5→L+1 (97%)
29	46302.19	215.97	0.0006	HOMO→L+8 (98%)
30	46367.52	215.67	0.0032	H-4→L+2 (94%)

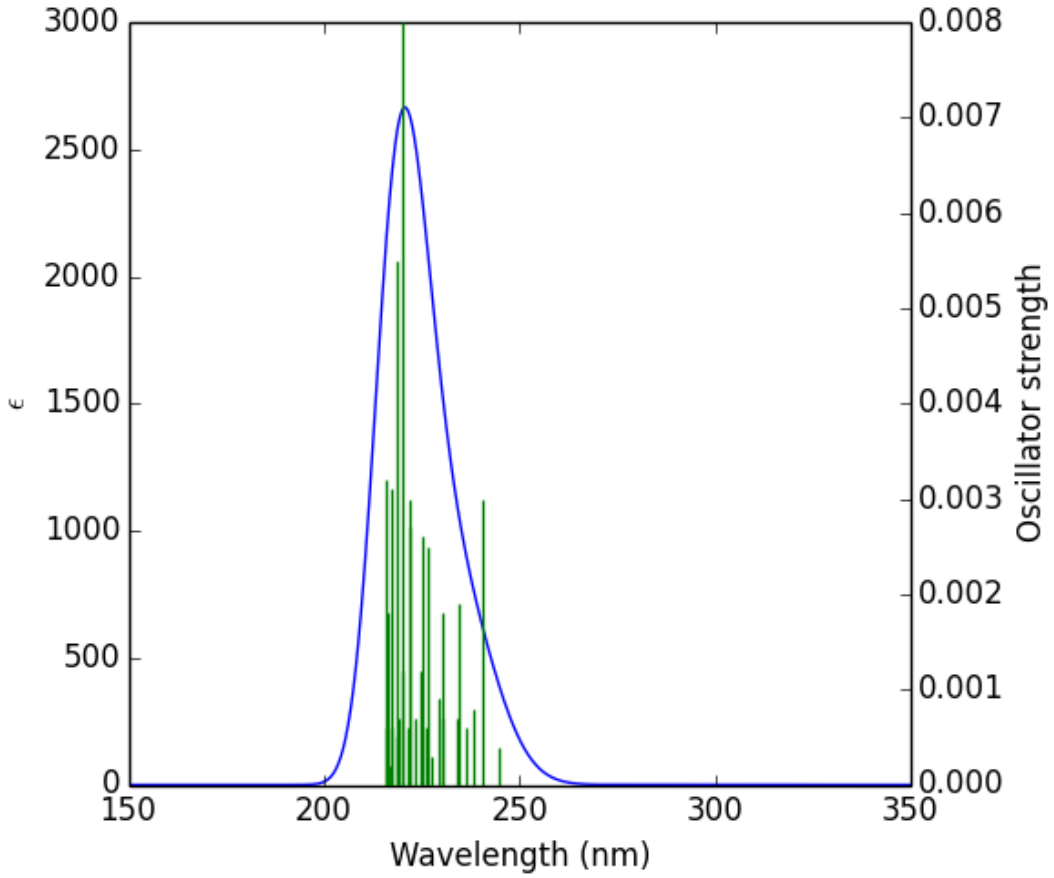

Figure S22. Absorbance spectrum of 1a+2a+3 (NIPUF2)

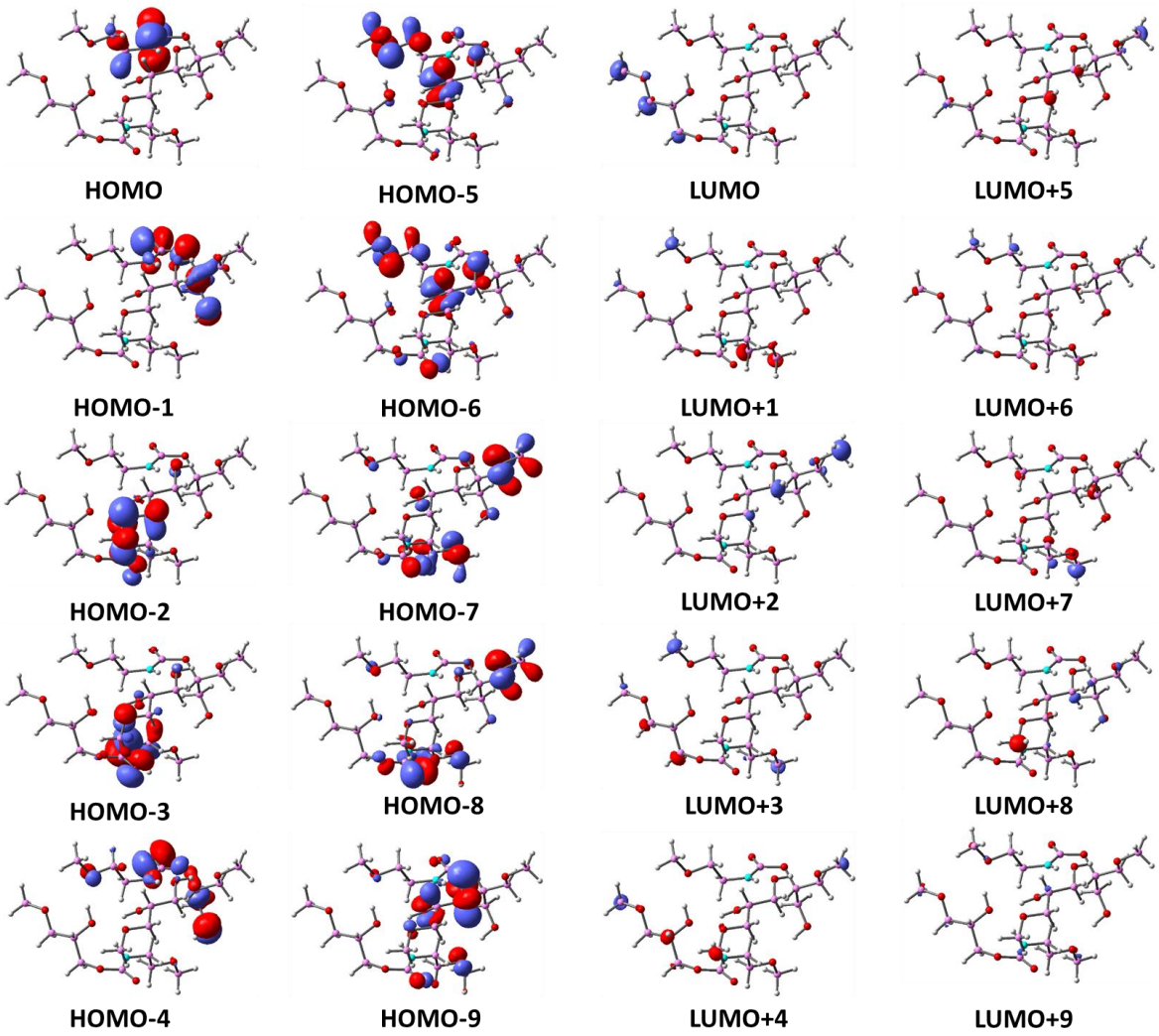

Figure S23. HOMOs and LUMOs of 1a+2a+3 aggregate in ground state (S_0)

Aggregate of 1a+2a+3+PEI

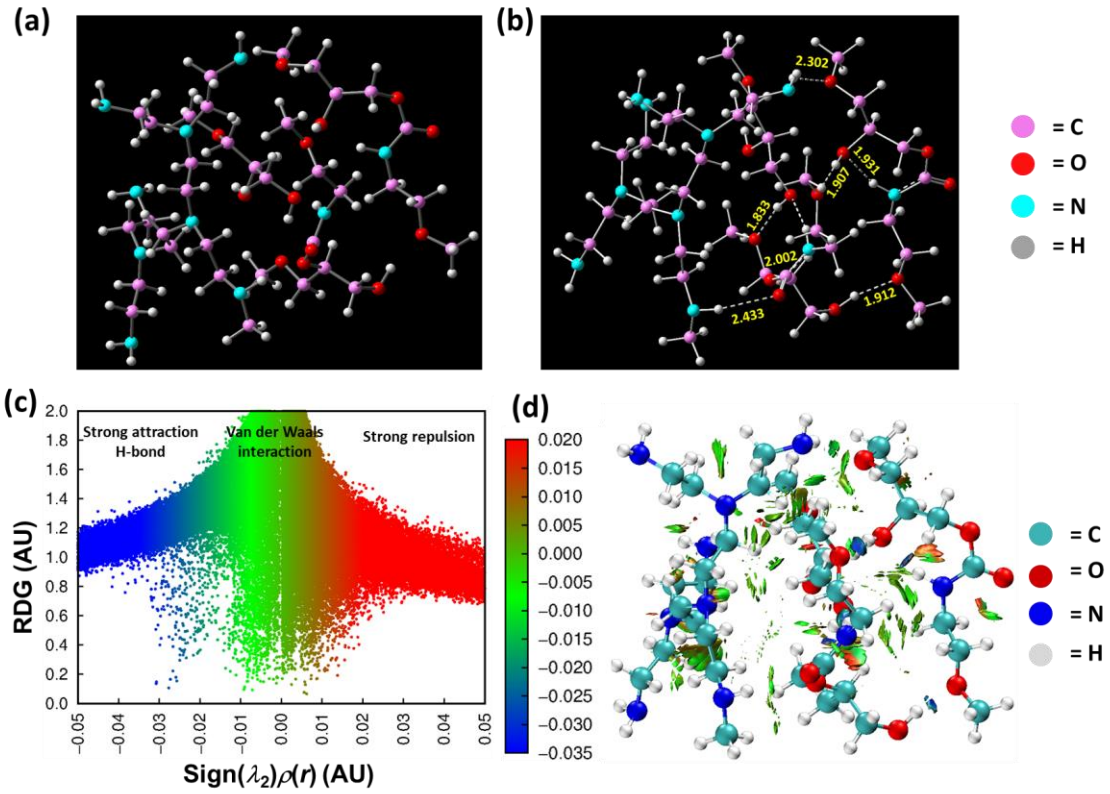

Figure S24. (a) Optimized structure of aggregate of 1a+2a+3+PEI; (b) reduced density gradient (RDG) versus electron density × sign of second Hessian eigenvalue [sign(λ_2)ρ(r)] plot for aggregate of 1a+2a+3; (c) independent gradient model showing different interaction index for aggregate of 1a+2a+3.

Coordinates of aggregate of 1a+2a+3+PEI in S_0

Optimized by B3LYP+6-311+G(d, p)

C	-6.87358	-3.87139	-0.37416
O	-5.77176	-3.10919	0.20357
C	-5.82625	-1.67324	-0.07678
C	-5.00343	-0.94037	0.98215
N	-4.92194	0.49966	0.69693
O	-5.87348	2.66432	0.6955
C	-6.01749	1.28423	0.90912
O	-7.11773	0.86805	1.29202
H	-6.68876	-4.91065	-0.12024
H	-7.82455	-3.54429	0.05055
H	-6.89735	-3.75945	-1.46133
H	-5.43027	-1.4846	-1.07882
H	-6.86245	-1.33585	-0.02792
H	-5.46441	-1.10255	1.95658
H	-3.98434	-1.31762	1.01592
H	-3.99825	0.91213	0.56005
C	-4.82704	3.26786	-0.13617
H	-5.22384	4.26272	-0.32828
H	-4.74092	2.73315	-1.08423
C	-3.45895	3.33181	0.56165
H	-3.63859	3.24573	1.63305
O	-2.65249	2.16597	0.22706
H	-2.34184	2.14886	-0.7171
N	-2.07974	-1.28927	-1.61171
C	0.29228	-3.58479	2.93844
O	-0.52978	-3.21443	1.79705
C	-1.39076	-2.34208	-2.12948
O	-1.11812	-2.49034	-3.33468
O	-0.96162	-3.29993	-1.20605
C	-1.87176	-3.75701	-0.12767
C	-2.85971	-4.78356	-0.69102
O	-3.86083	-5.08706	0.30825
C	-1.02015	-4.32053	0.98633
H	0.52766	-2.64949	3.43539
H	-0.26214	-4.24664	3.60962
H	1.2069	-4.08097	2.6043
H	-2.44213	-2.91247	0.25214
H	-3.30901	-4.38353	-1.6045
H	-2.35485	-5.71553	-0.93613
H	-4.47523	-4.31987	0.40632
H	-1.63997	-4.97564	1.60345
H	-0.17878	-4.8815	0.57143
C	-2.80282	-0.38505	-2.5065
H	-3.59497	0.09677	-1.93385
H	-3.27633	-0.99481	-3.27761
C	-1.975	0.67699	-3.21844
H	-1.00139	0.2762	-3.50424

H	-2.50103	0.99768	-4.12448
O	-1.78979	1.86065	-2.3687
C	-1.05357	2.91651	-3.06743
H	-1.59569	3.20964	-3.97121
H	-0.96332	3.76873	-2.39766
H	-0.05769	2.56136	-3.34057
H	-1.94691	-1.05434	-0.61892
C	0.72424	1.98703	2.58725
C	-0.19869	0.77951	2.53514
C	-0.3016	0.17998	1.14787
O	-1.36053	-0.81319	1.067
O	0.32528	-0.24882	3.44157
H	1.72498	1.71804	2.23554
H	-1.19844	1.0712	2.86562
H	-0.56434	0.96188	0.44224
H	0.65195	-0.27122	0.86168
H	-1.0621	-1.66429	1.48711
H	0.49819	0.1929	4.29476
H	0.32958	2.80811	1.98212
O	0.79132	2.38191	3.99297
C	1.886	3.29354	4.29717
H	1.80212	4.21442	3.71181
H	1.79569	3.53146	5.35411
H	2.84851	2.81437	4.10143
N	5.9324	4.86383	-2.90012
C	4.59489	4.26282	-2.95885
C	4.16834	3.78008	-1.56365
N	2.83632	3.14118	-1.53808
C	2.83771	1.72474	-1.12156
C	3.31106	0.7773	-2.23368
N	3.26264	-0.63082	-1.80174
C	2.90206	-1.58909	-2.86623
C	2.42957	-2.95094	-2.33945
N	1.83471	-3.72885	-3.43404
C	1.72586	-5.16909	-3.18465
C	1.76326	3.95064	-0.94343
C	1.39072	5.18651	-1.77363
N	0.05994	5.67194	-1.36785
C	4.38018	-1.03925	-0.9254
C	3.91577	-1.57871	0.44478
N	5.02315	-1.70982	1.40645
C	5.13276	-0.63402	2.39853
C	5.37441	-3.0652	1.8447
C	6.06628	-3.88467	0.74406
N	6.41492	-5.21973	1.24403
C	4.11952	-0.70391	3.55938
N	4.22997	0.49783	4.407
H	6.44488	4.85558	-3.76962
H	5.97188	5.76839	-2.45038
H	4.63499	3.39812	-3.62236
H	3.82415	4.93444	-3.36202

H	4.18839	4.63035	-0.86598
H	4.92833	3.07824	-1.21202
H	3.44998	1.57403	-0.21753
H	1.81836	1.43585	-0.86872
H	2.64177	0.90676	-3.08443
H	4.31976	1.06521	-2.57328
H	2.0808	-1.15096	-3.43677
H	3.73105	-1.75946	-3.57291
H	3.28263	-3.51629	-1.95217
H	1.73508	-2.79356	-1.50128
H	0.93155	-3.34143	-3.69707
H	1.23913	-5.64465	-4.03687
H	2.72294	-5.60623	-3.08682
H	1.15165	-5.42544	-2.27927
H	2.01341	4.27465	0.08433
H	0.87419	3.3254	-0.87046
H	1.36604	4.89106	-2.82477
H	2.17286	5.95231	-1.67139
H	-0.16233	5.56251	-0.38227
H	-0.16426	6.5986	-1.70447
H	5.02727	-0.17801	-0.73869
H	5.00968	-1.78939	-1.42185
H	3.41925	-2.54372	0.31822
H	3.15057	-0.89559	0.82694
H	5.00509	0.32563	1.89385
H	6.15015	-0.63834	2.80575
H	4.50769	-3.64371	2.19875
H	6.06203	-2.97576	2.69114
H	6.92147	-3.30398	0.37086
H	5.37845	-4.01164	-0.09461
H	6.5051	-5.932	0.53436
H	7.19313	-5.23608	1.8894
H	4.27477	-1.64019	4.11549
H	3.10458	-0.73262	3.16047
H	3.48542	0.58425	5.0873
H	5.13526	0.60509	4.84976
C	-1.6773	5.0421	2.47221
H	-1.98421	4.13312	2.99123
H	-0.70723	5.35184	2.84909
H	-2.4092	5.83606	2.65032
C	-2.73161	4.65083	0.2856
H	-3.40866	5.48347	0.51506
H	-2.42115	4.72689	-0.75492
O	-1.5005	4.81609	1.04307

Table S5 Absorbance details of aggregate of 1a+2a+3+PEI

No.	Energy (cm^{-1})	Wavelength (nm)	Osc. strength	Major contribution
1	28595.78	349.70	0.0007	HOMO→LUMO (100%)
2	29332.17	340.92	0.0002	H-1→LUMO (100%)
3	29812.88	335.43	0.0018	HOMO→L+1 (100%)
4	30138.73	331.80	0.0022	H-2→LUMO (99%)
5	30178.25	331.36	0.0017	HOMO→L+2 (99%)
6	30554.11	327.29	0.0026	H-1→L+1 (100%)
7	30917.86	323.44	0.0006	H-1→L+2 (100%)
8	31167.90	320.84	0.0003	HOMO→L+3 (99%)
9	31335.66	319.13	0.0017	H-2→L+1 (99%)
10	31699.42	315.46	0.0021	H-2→L+2 (100%)
11	31897.83	313.50	0.0002	H-1→L+3 (100%)
12	32040.60	312.10	0.0016	HOMO→L+4 (99%)
13	32187.39	310.68	0.0054	HOMO→L+5 (98%)
14	32535.82	307.35	0.0004	HOMO→L+6 (99%)
15	32610.03	306.65	0.0066	H-3→LUMO (92%)
16	32721.33	305.61	0.0039	H-2→L+3 (92%)
17	32778.60	305.08	0.0005	H-1→L+4 (98%)
18	32927.01	303.70	0.0058	H-1→L+5 (93%)
19	32975.40	303.26	0.0030	HOMO→L+7 (93%)
20	33277.05	300.51	0.0014	H-1→L+6 (100%)
21	33344.80	299.90	0.0028	HOMO→L+8 (100%)
22	33579.51	297.80	0.0063	H-2→L+4 (99%)
23	33677.11	296.94	0.0023	H-3→L+1 (96%)
24	33691.62	296.81	0.0013	H-1→L+7 (93%)
25	**33703.72**	**296.70**	**0.0099**	**H-2→L+5 (89%)**
26	34055.38	293.64	0.0014	H-3→L+2 (49%) and H-2→L+6 (50%)
27	34086.84	293.37	0.0061	H-3→L+2 (48%) and H-2→L+6 (46%)
28	34092.48	293.32	0.0018	H-1→L+8 (96%)
29	34189.27	292.49	0.0027	HOMO→L+9 (98%)
30	34444.14	290.33	0.0011	HOMO→L+10 (100%)

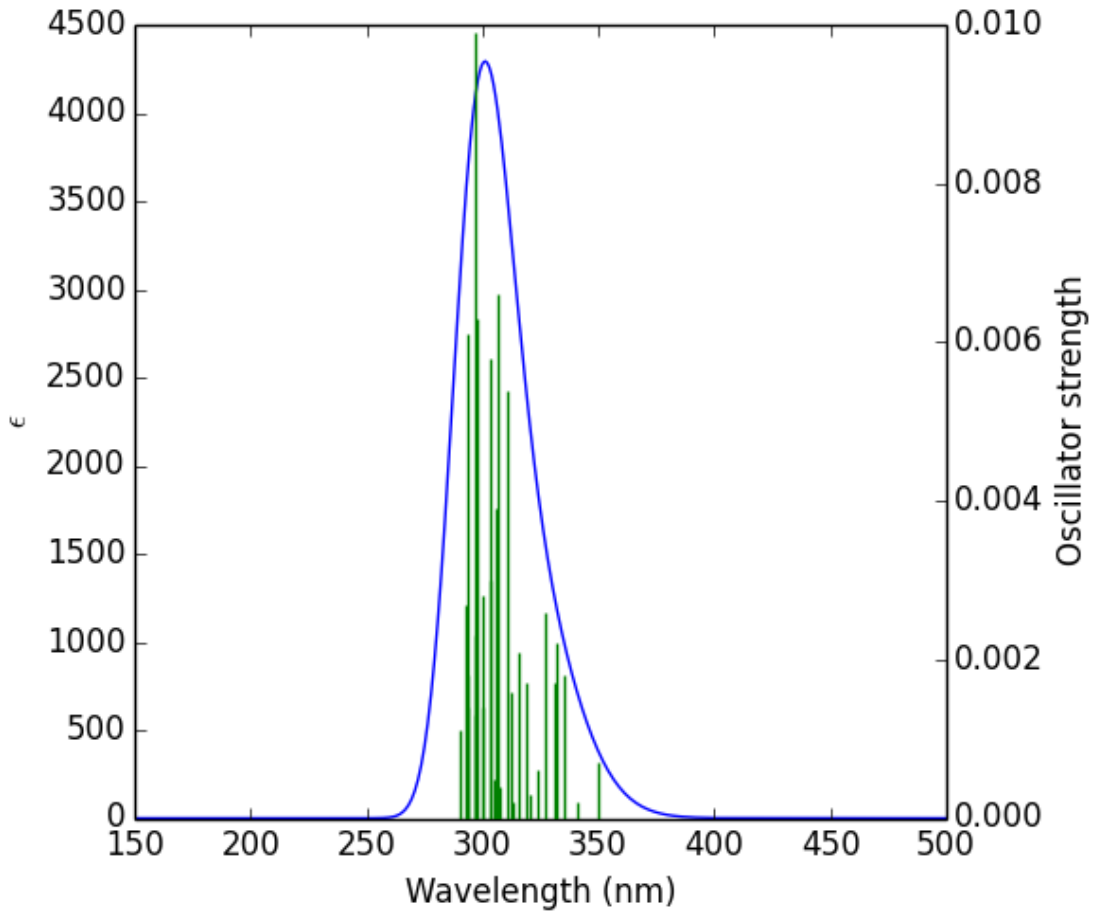

Figure S25. Absorbance spectrum of 1a+2a+3+PEI (**NIPUF3**)

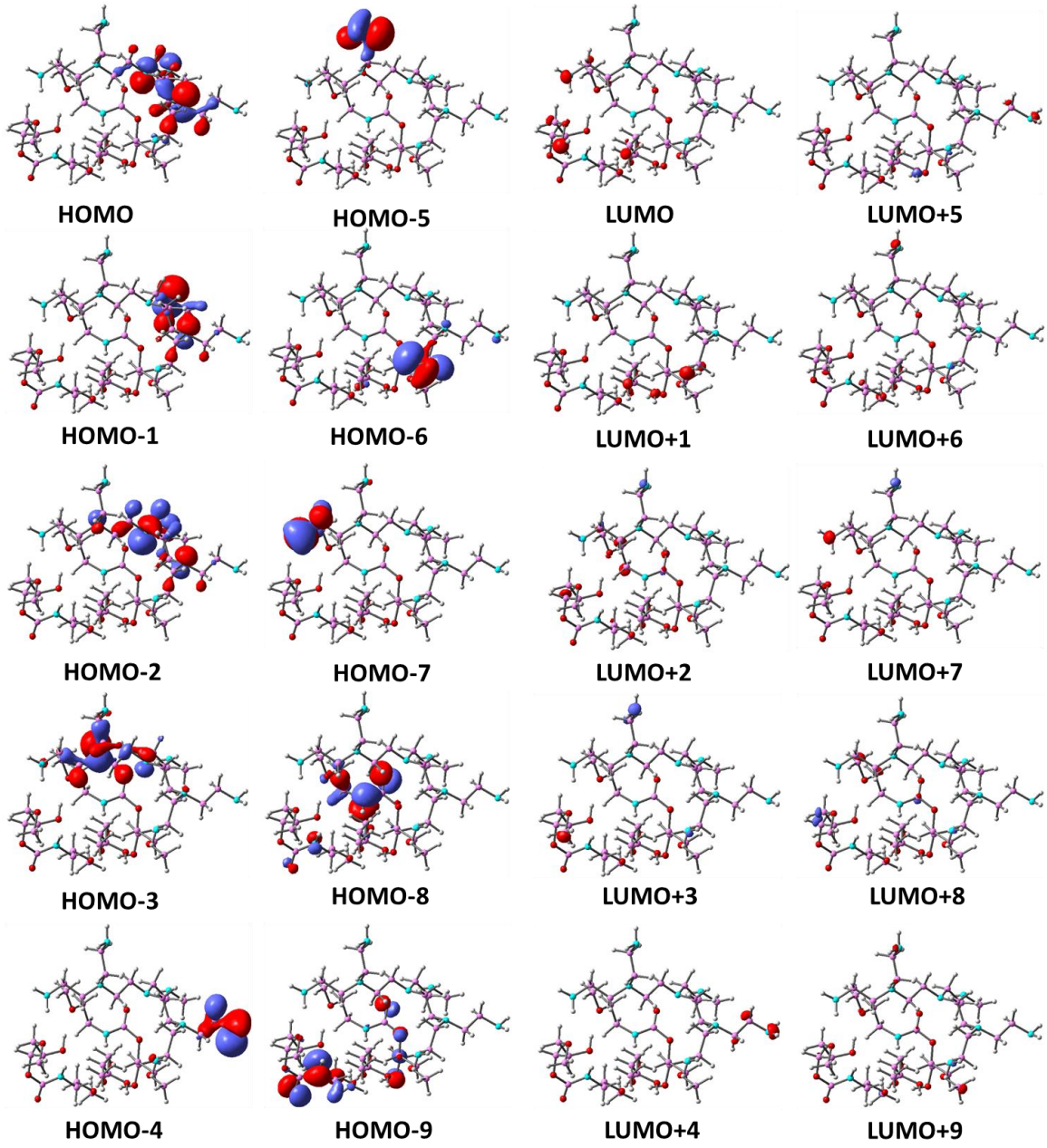

Figure S26. HOMOs and LUMOs of 1a+2a+3+PEI aggregate in ground state (S_0)

HOMOs and LUMOs of small, moderate and large aggregates in ground state by B3LYP+6-311+G

Aggregate	HOMO	LUMO	Gap (eV)
Three molecules (1a+2a+3) small	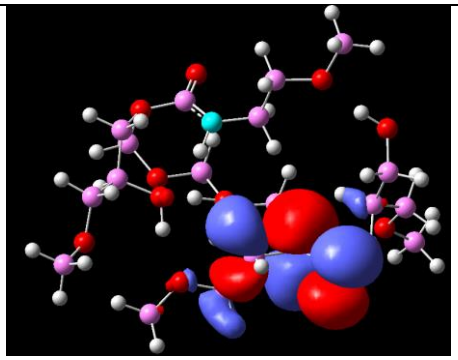	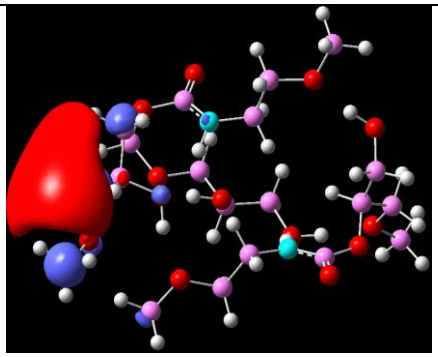	6.51
Six molecules 2 x (1a+2a+3) Modarate	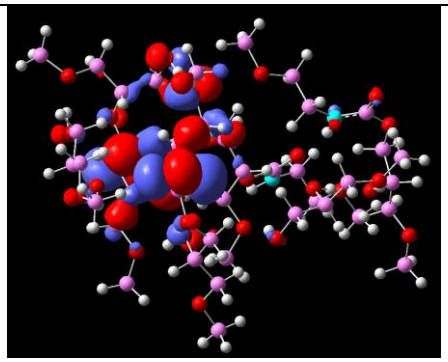	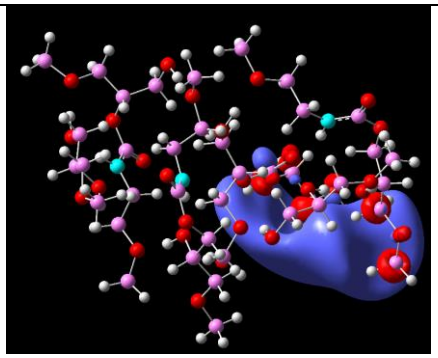	6.38
Nine molecules 3 x (1a+2a+3) Large	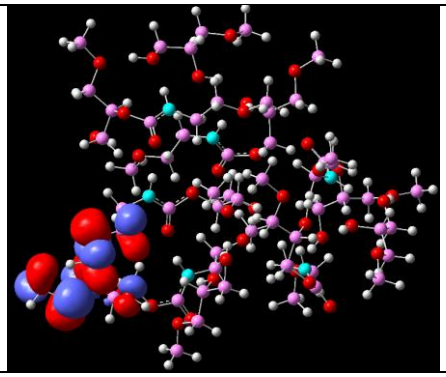	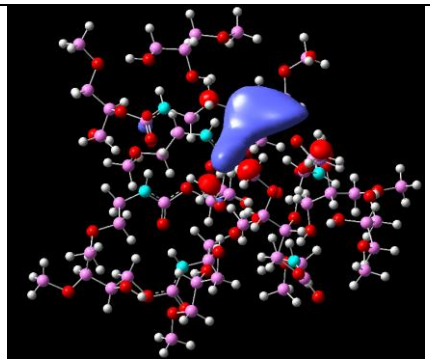	6.33

Coordinates of aggregate of 1a+2a+3 in S_0

Optimized by B3LYP+6-311+G

C	2.23904	4.9717	-0.47263
O	1.71183	3.64242	-0.76491
C	0.31182	3.46006	-0.37256
C	-0.24553	2.25739	-1.13024
N	-1.62623	1.96447	-0.7249
O	-3.94968	2.3162	-0.80983
C	-2.66091	2.71205	-1.19934
O	-2.5457	3.68229	-1.95805
H	3.27802	4.96437	-0.78951
H	1.68358	5.7285	-1.03079
H	2.17963	5.18341	0.59834
H	0.25754	3.30309	0.70924
H	-0.25295	4.35736	-0.63501
H	-0.20947	2.4638	-2.20039
H	0.34449	1.3653	-0.92993
H	-1.81807	1.06483	-0.29774
C	-4.25176	1.61513	0.44373
H	-5.27232	1.90708	0.67028
H	-3.58508	1.94676	1.24091
C	-4.19209	0.09878	0.27244
H	-4.46353	-0.17881	-0.7476
O	-2.85503	-0.42019	0.47236
H	-2.60758	-0.50237	1.44257
N	1.53159	-0.57571	1.70104
C	5.61315	-3.02158	-1.14005
O	4.56708	-2.07571	-0.78858
C	2.67568	-0.21592	2.33741
O	2.74679	0.29592	3.46447
O	3.85191	-0.47402	1.60694
C	3.94039	0.04155	0.22126
C	4.22171	1.54897	0.25432
O	3.98366	2.11589	-1.05978
C	5.04573	-0.73136	-0.45863
H	5.11881	-3.96893	-1.3382
H	6.1486	-2.69034	-2.03379
H	6.31461	-3.13952	-0.31063
H	2.99625	-0.1204	-0.29615
H	3.58151	2.01525	1.0065
H	5.26035	1.74175	0.5241
H	3.09769	2.55118	-1.08767
H	5.33682	-0.21788	-1.37837
H	5.90407	-0.81063	0.21414
C	0.22656	-0.14137	2.18288
H	-0.36144	0.15446	1.31819
H	0.3645	0.72133	2.83174
C	-0.53783	-1.23227	2.93101
H	-0.46295	-2.19203	2.4132
H	-0.17909	-1.34333	3.95641
O	-1.94801	-0.80856	2.95461
C	-2.77783	-1.46501	3.95607
H	-2.41784	-1.21898	4.95693
H	-3.78437	-1.08005	3.81775
H	-2.76876	-2.54946	3.81616

H	1.56286	-1.19938	0.88845
C	-1.00221	-2.4664	-2.85293
C	-0.23929	-2.4123	-1.53621
C	1.26091	-2.35887	-1.75632
O	1.92621	-2.45824	-0.46938
O	-0.6102	-1.22419	-0.79001
H	-0.82086	-1.55306	-3.43105
H	-0.47973	-3.30623	-0.95137
H	1.56653	-3.19153	-2.39829
H	1.5268	-1.41833	-2.25034
H	2.91287	-2.44177	-0.57564
H	-1.56928	-1.21238	-0.56412
H	-0.69849	-3.33657	-3.44811
O	-2.41524	-2.56723	-2.52109
C	-3.2969	-2.45951	-3.67001
H	-3.10806	-3.26373	-4.38852
H	-4.30999	-2.54846	-3.28729
H	-3.17531	-1.49171	-4.1663
C	-6.41644	-2.26153	2.11655
H	-7.28812	-1.64307	2.06567
H	-6.69991	-3.28728	2.0053
H	-5.9368	-2.12471	3.06319
C	-5.10415	-0.46911	1.22456
H	-6.00149	0.11298	1.19541
H	-4.65932	-0.39042	2.19453
O	-5.44422	-1.87226	0.98746

Coordinates of aggregate of 2 x (1a+2a+3) in S_0
Optimized by B3LYP+6-311+G

C	0.50303	-4.91949	-2.1711
O	1.10358	-3.59287	-2.05511
C	2.565	-3.57881	-2.13634
C	3.00188	-2.12437	-2.31476
N	4.40275	-1.93177	-1.94228
O	6.67039	-1.54377	-2.46556
C	5.36488	-1.79166	-2.88772
O	5.16956	-1.89947	-4.11156
H	-0.56159	-4.80261	-1.98608
H	0.67308	-5.31616	-3.17503
H	0.93636	-5.59898	-1.43073
H	2.97974	-3.99874	-1.21393
H	2.88801	-4.19545	-2.97963
H	2.87423	-1.81968	-3.35057
H	2.39124	-1.47187	-1.6943
H	4.57095	-1.75886	-0.96037
C	7.05345	-1.11765	-1.11581
H	8.01217	-1.60325	-0.93926
H	6.34268	-1.45006	-0.35981
C	7.20439	0.40248	-1.09814
H	7.91322	0.69537	-1.87604
O	5.91597	1.01592	-1.36071
H	5.77658	1.32436	-2.29157
N	4.33749	-1.71795	3.29434
C	0.96457	2.59272	2.7225
O	1.43646	1.63436	1.73004
C	3.70776	-1.46165	2.11739
O	4.22197	-1.60874	0.98509
O	2.42685	-1.03939	2.34972
C	1.52871	-0.72712	1.20152
C	0.72645	-2.00096	0.90769
O	-0.04985	-1.83922	-0.31413
C	0.64505	0.40831	1.66071
H	1.67306	3.41669	2.70092
H	-0.03517	2.95498	2.47716
H	0.96474	2.13358	3.715
H	2.14155	-0.41993	0.35662
H	1.41661	-2.84221	0.80978
H	0.03762	-2.20219	1.72848
H	0.32113	-2.41901	-1.02773
H	-0.17122	0.5405	0.94695
H	0.22527	0.17825	2.64283
C	5.7015	-2.23261	3.38559
H	5.99789	-2.58248	2.39965
H	5.72796	-3.08489	4.06573
C	6.68491	-1.16814	3.86746
H	6.68325	-0.30961	3.18653

H	6.41684	-0.81373	4.87138
O	7.99288	-1.79537	3.89381
C	9.05098	-0.94606	4.41047
H	8.84811	-0.6523	5.44557
H	9.96067	-1.53832	4.37205
H	9.1721	-0.0482	3.79554
H	3.79202	-1.58852	4.13173
C	3.40768	1.96388	-3.52281
C	3.08874	2.28381	-2.06568
C	1.65552	2.77159	-1.88344
O	1.41279	3.23814	-0.53624
O	3.2221	1.10501	-1.22129
H	2.90734	1.03974	-3.8263
H	3.77053	3.06647	-1.71814
H	1.46199	3.62433	-2.5345
H	0.96386	1.96167	-2.14206
H	1.56878	2.5272	0.13495
H	4.17353	0.93692	-1.01696
H	3.08564	2.78247	-4.17753
O	4.85494	1.8036	-3.67524
C	5.27004	1.37003	-5.0094
H	4.88716	2.06481	-5.76167
H	6.35618	1.39122	-5.01151
H	4.92672	0.3533	-5.20287
C	-3.42903	-2.22795	-4.04344
O	-2.81805	-2.07067	-2.72969
C	-2.4185	-0.69686	-2.38451
C	-3.60403	0.03965	-1.75257
N	-3.35155	1.47151	-1.58469
O	-3.83675	3.72712	-1.97665
C	-4.12437	2.38494	-2.23022
O	-5.06381	2.12402	-3.00374
H	-3.70533	-3.276	-4.12754
H	-4.31968	-1.60416	-4.14657
H	-2.71032	-1.97246	-4.82578
H	-1.58628	-0.80333	-1.69147
H	-2.08018	-0.18357	-3.28867
H	-4.48486	-0.06003	-2.3841
H	-3.8355	-0.40307	-0.78341
H	-2.83811	1.79416	-0.75983
C	-2.51613	4.18671	-1.51383
H	-2.40458	5.16018	-1.98649
H	-1.73823	3.51367	-1.87659
C	-2.44329	4.3194	0.00167
H	-3.35838	4.80102	0.36013
O	-2.35503	2.97295	0.54536
H	-2.6104	2.91587	1.50264
N	-4.03605	-0.98864	2.12134
C	-7.28366	-5.36346	1.36443
O	-6.2992	-4.33742	1.06288
C	-3.21053	-1.99634	2.47792

O	-2.07814	-1.8637	2.9759
O	-3.7438	-3.28397	2.24824
C	-3.96669	-3.68862	0.83859
C	-2.61905	-4.0698	0.21129
O	-2.77074	-4.33292	-1.20991
C	-4.93839	-4.84439	0.8636
H	-8.23209	-4.85094	1.502
H	-7.3642	-6.07457	0.53791
H	-7.01526	-5.89241	2.28221
H	-4.39578	-2.85117	0.28541
H	-1.89891	-3.26723	0.37559
H	-2.23835	-4.98264	0.66876
H	-2.75374	-3.48794	-1.72916
H	-4.89179	-5.37771	-0.08856
H	-4.68297	-5.51925	1.68526
C	-3.55983	0.39049	2.05042
H	-4.16258	0.89326	1.30112
H	-2.51581	0.38231	1.74014
C	-3.67166	1.15822	3.36462
H	-4.71464	1.24373	3.68328
H	-3.08181	0.68814	4.15593
O	-3.13554	2.49378	3.08424
C	-3.15528	3.426	4.19816
H	-2.5617	3.0384	5.03124
H	-2.71782	4.34675	3.8221
H	-4.18137	3.60303	4.53256
H	-5.00574	-1.18101	1.84709
C	-7.99416	0.99566	-1.11834
C	-7.46373	0.35221	0.16094
C	-7.1187	-1.11059	-0.03487
O	-6.68032	-1.6774	1.22985
O	-6.25012	1.06334	0.55692
H	-7.2859	0.85309	-1.93996
H	-8.20498	0.44567	0.95982
H	-8.00478	-1.64317	-0.39631
H	-6.32695	-1.20234	-0.78449
H	-6.62434	-2.66739	1.18947
H	-6.42942	2.01753	0.43083
H	-8.97306	0.58929	-1.39562
O	-8.10718	2.41847	-0.82222
C	-8.18903	3.27252	-2.00547
H	-9.0963	3.04996	-2.57522
H	-8.23616	4.2919	-1.63234
H	-7.30347	3.13983	-2.6295
C	-0.29969	6.24742	2.37528
H	-0.38915	7.25109	1.94639
H	-0.44549	6.30145	3.45151
H	0.69525	5.85017	2.15547
C	-1.24362	5.15834	0.41827
H	-1.27445	6.13248	-0.08763
H	-0.31018	4.64355	0.17107

O	-1.33826	5.37169	1.86152
C	8.64923	2.93346	1.22401
H	9.38897	2.38582	1.81969
H	9.072	3.88352	0.90936
H	7.75493	3.1144	1.82975
C	7.71719	0.91387	0.23723
H	8.46938	0.23285	0.65768
H	6.87884	0.99924	0.93684
O	8.31717	2.21651	0.00905

Coordinates of aggregate of 3 x (1a+2a+3) in S_0

Optimized by B3LYP+6-311+G

C	0.47904	-0.50405	-5.5197
O	0.16916	0.42658	-4.42429
C	0.96042	1.65122	-4.38516
C	0.1782	2.64143	-3.51885
N	1.01787	3.73988	-3.0314
O	1.92637	5.90165	-3.21244
C	1.07194	4.92673	-3.6989
O	0.34834	5.21401	-4.66678
H	-0.26529	-1.28962	-5.45585
H	0.38105	0.01686	-6.47444
H	1.47917	-0.92219	-5.40469
H	1.94759	1.44078	-3.96023
H	1.09462	2.03522	-5.4001
H	-0.64723	3.05808	-4.09108
H	-0.24418	2.11284	-2.66486
H	1.57226	3.5487	-2.20577
C	3.08528	5.67156	-2.3268
H	3.96447	5.60155	-2.97047
H	2.97338	4.76416	-1.7379
C	3.15721	6.891	-1.41302
H	3.01299	7.78305	-2.03008
O	2.11892	6.81856	-0.39367
H	1.21489	6.82117	-0.79647
N	3.24566	2.36994	1.40839
C	-0.46598	1.14626	3.14241
O	-1.04107	1.27262	1.80479
C	2.35558	2.14562	0.42826
O	2.19451	2.84802	-0.6042
O	1.63994	0.98304	0.6705
C	0.40113	0.73964	-0.11928
C	0.74938	-0.29664	-1.18273
O	-0.40563	-0.62906	-1.99154
C	-0.64927	0.24143	0.84802
H	-0.75744	2.04515	3.67856
H	-0.88153	0.26369	3.64125
H	0.62036	1.07077	3.09437
H	0.08843	1.6839	-0.56169
H	1.55851	0.09029	-1.80426
H	1.09709	-1.20559	-0.68915
H	-0.29146	-0.25294	-2.90136
H	-1.53517	-0.03092	0.27879
H	-0.2938	-0.64174	1.38261
C	4.07703	3.57333	1.46771
H	4.44806	3.81502	0.4723
H	4.93071	3.36086	2.10763
C	3.29354	4.75785	2.04105
H	2.50308	5.07402	1.35761
H	2.85788	4.48261	3.00572
O	4.24049	5.85742	2.22535
C	3.59093	7.08983	2.65449
H	3.05154	6.93557	3.5971
H	4.38836	7.80933	2.82036
H	2.90365	7.45062	1.88777

H	3.33611	1.67557	2.15183
C	-1.62997	6.47516	-0.52014
C	-1.35263	5.18252	0.22803
C	-2.50848	4.79809	1.13446
O	-2.19196	3.74053	2.05927
O	-1.18946	4.08702	-0.7258
H	-2.54312	6.37404	-1.11501
H	-0.44133	5.28423	0.82263
H	-2.79943	5.64657	1.75601
H	-3.3654	4.50509	0.52251
H	-1.82371	2.93528	1.6311
H	-0.46447	4.29779	-1.34666
H	-1.73749	7.3163	0.17395
O	-0.50181	6.71	-1.40799
C	-0.76067	7.67583	-2.47748
H	-0.93091	8.67119	-2.05816
H	0.11901	7.67198	-3.11122
H	-1.62677	7.36089	-3.06298
C	-3.9641	2.31164	-3.97005
O	-3.70392	1.26477	-2.98575
C	-3.76198	1.68227	-1.58756
C	-5.20321	1.65727	-1.07142
N	-5.30539	2.11694	0.31711
O	-6.47861	3.23788	2.02846
C	-6.36826	2.90097	0.68553
O	-7.23784	3.33114	-0.08949
H	-3.84553	1.84774	-4.94577
H	-4.97834	2.70285	-3.87313
H	-3.24024	3.12228	-3.85292
H	-3.1371	0.96431	-1.06439
H	-3.31845	2.67372	-1.4722
H	-5.83473	2.30563	-1.67781
H	-5.60106	0.64407	-1.13675
H	-4.89174	1.53402	1.04161
C	-5.3669	3.13487	2.99181
H	-5.50528	4.00317	3.63238
H	-4.41283	3.21263	2.48051
C	-5.44458	1.8646	3.82533
H	-6.44201	1.77161	4.26421
O	-5.21304	0.73337	2.92203
H	-5.03642	-0.13131	3.38364
N	-4.15277	-2.82826	0.28126
C	-6.85074	-5.30834	-3.9469
O	-6.20693	-4.32839	-3.08648
C	-3.23807	-3.61578	-0.32357
O	-2.18491	-4.04721	0.19506
O	-3.52719	-3.99279	-1.63668
C	-4.14384	-3.04392	-2.59523
C	-3.02137	-2.25211	-3.28078
O	-3.58837	-1.21921	-4.12227
C	-4.91994	-3.85042	-3.61132
H	-7.77554	-5.5925	-3.45196
H	-7.072	-4.87664	-4.92629
H	-6.21226	-6.18687	-4.06612
H	-4.8053	-2.36313	-2.06701
H	-2.34921	-1.82992	-2.5305

H	-2.43633	-2.9209	-3.92023
H	-3.58323	-0.34018	-3.66707
H	-5.10514	-3.21463	-4.48098
H	-4.33032	-4.72583	-3.89823
C	-3.9	-2.20848	1.58374
H	-4.0941	-1.14044	1.50315
H	-2.85342	-2.35793	1.83721
C	-4.8117	-2.78785	2.65983
H	-5.8273	-2.90085	2.27765
H	-4.44941	-3.75645	3.01557
O	-4.82279	-1.83662	3.77847
C	-5.58989	-2.29827	4.92896
H	-5.12542	-3.19066	5.3556
H	-5.57541	-1.48096	5.64213
H	-6.62073	-2.52119	4.6375
H	-5.10071	-2.74604	-0.10022
C	-9.51503	-0.70231	0.51411
C	-8.39604	-1.73825	0.51617
C	-8.13749	-2.31186	-0.8645
O	-7.10317	-3.33247	-0.75325
O	-7.15262	-1.14045	0.9652
H	-9.2515	0.14725	-0.12467
H	-8.67709	-2.55442	1.19247
H	-9.05809	-2.75751	-1.25264
H	-7.8104	-1.51948	-1.54309
H	-6.87756	-3.74369	-1.63303
H	-7.27087	-0.61295	1.78175
H	-10.45704	-1.13994	0.16134
O	-9.656	-0.26251	1.88986
C	-10.53162	0.89117	2.06299
H	-11.55264	0.65146	1.74691
H	-10.52541	1.11112	3.1268
H	-10.16497	1.75034	1.50035
C	6.71081	0.03174	-3.35334
O	6.18892	-0.30704	-2.03078
C	4.81684	-0.82465	-2.01124
C	4.80381	-2.34099	-2.23159
N	3.44347	-2.8774	-2.35683
O	1.59212	-3.54541	-3.64657
C	2.79964	-2.86406	-3.55217
O	3.22694	-2.29395	-4.57521
H	7.72396	0.39006	-3.19285
H	6.72497	-0.84182	-4.00652
H	6.10389	0.81914	-3.80555
H	4.4166	-0.57254	-1.03073
H	4.23166	-0.31523	-2.78029
H	5.35271	-2.58395	-3.14173
H	5.27688	-2.84164	-1.38808
H	3.07106	-3.41878	-1.57758
C	0.73565	-3.9524	-2.51526
H	-0.17149	-4.26285	-3.02582
H	0.5065	-3.0756	-1.91038
C	1.27335	-5.10292	-1.65135
H	1.97888	-5.70104	-2.23039
O	2.07015	-4.57214	-0.54111
H	1.54717	-4.23453	0.24075

N	4.41564	-1.83185	2.33819
C	9.5838	-2.48569	4.14215
O	8.47395	-2.22162	3.24152
C	4.70817	-0.64392	2.90809
O	3.88523	0.24634	3.21456
O	6.06504	-0.41832	3.18117
C	7.06091	-0.60871	2.09597
C	7.06814	0.64848	1.21609
O	7.84065	0.4001	0.01741
C	8.39947	-0.84187	2.75652
H	9.50766	-3.53111	4.42928
H	10.53896	-2.30967	3.64025
H	9.51186	-1.85454	5.03137
H	6.78579	-1.46611	1.48436
H	6.0376	0.92277	0.97524
H	7.52641	1.48302	1.74723
H	7.25498	0.10017	-0.7212
H	9.19359	-0.67317	2.02601
H	8.51595	-0.15721	3.60123
C	3.0949	-2.11714	1.77742
H	3.24152	-2.53876	0.78466
H	2.5459	-1.18391	1.6921
C	2.30401	-3.12192	2.61199
H	2.90244	-4.01108	2.83147
H	1.96846	-2.67749	3.55382
O	1.14041	-3.50667	1.8128
C	0.13273	-4.2627	2.56512
H	-0.16354	-3.69196	3.45036
H	-0.72543	-4.38844	1.90953
H	0.54932	-5.22681	2.86166
H	5.11652	-2.58359	2.31206
C	5.71299	-6.81885	0.32826
C	5.46248	-5.56132	1.15664
C	6.75265	-4.86454	1.54016
O	6.45177	-3.82499	2.5111
O	4.65644	-4.60297	0.41406
H	6.19985	-6.55878	-0.61975
H	4.93694	-5.84568	2.07436
H	7.44116	-5.59099	1.98412
H	7.21818	-4.42817	0.65058
H	7.26116	-3.3492	2.82747
H	3.79321	-4.9793	0.11541
H	6.34725	-7.52317	0.87862
O	4.42312	-7.4342	0.0728
C	4.41885	-8.43956	-0.98251
H	4.99175	-9.32089	-0.67679
H	3.37406	-8.67479	-1.16045
H	4.85515	-8.02666	-1.89994
C	0.12715	-5.98293	-1.17839
H	-0.43705	-6.32077	-2.05747
H	-0.55524	-5.43805	-0.528
C	-0.36554	-7.98241	0.10051
H	-0.98019	-8.42343	-0.69094
H	0.14698	-8.77557	0.64088
H	-1.00656	-7.42303	0.78761
O	0.66859	-7.13152	-0.46182

C	-4.40538	1.90946	4.93336
H	-4.49905	2.84708	5.49921
H	-3.39654	1.85073	4.51019
C	-3.65314	0.66361	6.87891
H	-3.655	1.55109	7.51972
H	-3.93359	-0.2076	7.46409
H	-2.65279	0.5178	6.4614
O	-4.64213	0.78628	5.8213
C	5.95647	8.62855	0.34987
H	6.79594	8.43277	-0.32654
H	5.96036	9.67794	0.63426
H	6.05915	8.00578	1.24184
C	4.50097	7.00089	-0.7187
H	5.30978	6.72563	-1.40881
H	4.53623	6.3482	0.15554
O	4.68533	8.39371	-0.31521

Coordinates of aggregate of 1b+2b+3 in S_1

Optimized by B3LYP+6-311+G(d,p)

C	2.12167	-4.69596	2.73341
O	1.86579	-3.37086	2.28429
C	0.51308	-2.96812	2.4539
C	0.39883	-1.50468	2.03948
N	-0.99714	-1.09252	1.98031
O	-2.69038	0.47005	2.25154
C	-1.38123	0.12388	2.46935
O	-0.67139	0.90084	3.06912
H	3.17	-4.90678	2.52527
H	1.9381	-4.78516	3.81115
H	1.49274	-5.42051	2.20055
H	-0.14433	-3.59746	1.83574
H	0.20871	-3.08963	3.5022
H	0.915	-0.86267	2.75159
H	0.87926	-1.37505	1.06301
H	-1.54996	-1.45034	1.20239
C	-3.71864	-0.4851	1.93561
H	-4.61413	-0.08832	2.41723
H	-3.48569	-1.45705	2.3799
C	-3.95921	-0.62724	0.43451
H	-3.96435	0.37488	-0.01051
O	-2.89832	-1.40172	-0.11929
H	-2.73297	-1.13485	-1.04494
N	1.32697	0.12607	-1.99007
C	5.73682	2.21306	0.37741
O	4.64839	1.38585	-0.00619
C	2.37648	-0.7239	-2.60811
O	2.23029	-0.60677	-3.85999
O	3.63483	-0.42544	-2.05459
C	3.85256	-0.79441	-0.69359
C	4.13316	-2.3019	-0.5678
O	4.24587	-2.71344	0.78772
C	5.02966	0.02083	-0.19384
H	5.35323	3.2282	0.48309
H	6.16072	1.88579	1.33523
H	6.52553	2.20512	-0.38501
H	2.97436	-0.54667	-0.082
H	3.344	-2.84345	-1.09995
H	5.08264	-2.53785	-1.05604
H	3.36267	-2.78977	1.1816
H	5.37909	-0.39733	0.75723
H	5.84003	-0.03722	-0.93268
C	0.00316	-0.37134	-1.7879
H	-0.44209	0.19586	-0.96415
H	0.06042	-1.43514	-1.5528
C	-0.88892	-0.16601	-3.02777
H	-0.89491	0.89241	-3.31289
H	-0.49621	-0.75809	-3.85991
O	-2.20405	-0.58821	-2.67544
C	-3.12054	-0.55812	-3.76701
H	-2.80976	-1.25562	-4.55333
H	-4.08956	-0.85298	-3.3674
H	-3.18825	0.45195	-4.18822

H	1.42425	1.14609	-2.07278
C	-0.44479	4.00776	1.28429
C	0.24348	3.52638	0.01004
C	1.61194	2.94612	0.31413
O	2.2784	2.63712	-0.90522
O	-0.56036	2.52059	-0.61632
H	-0.4851	3.19825	2.02423
H	0.36337	4.37169	-0.68118
H	2.18504	3.6849	0.89123
H	1.49062	2.05143	0.93695
H	3.12933	2.21216	-0.68876
H	-1.47034	2.84111	-0.55204
H	0.09727	4.86273	1.71287
O	-1.76506	4.39587	0.91511
C	-2.60885	4.64243	2.02965
H	-2.2258	5.47161	2.63909
H	-3.58802	4.91647	1.63539
H	-2.70221	3.74905	2.65853
C	-6.73001	-1.92922	-1.61574
H	-7.61451	-1.47434	-1.14935
H	-6.81974	-1.84728	-2.6992
H	-6.68983	-2.99098	-1.33845
C	-5.3091	-1.28382	0.15706
H	-6.10948	-0.7421	0.68438
H	-5.29591	-2.32288	0.51867
O	-5.54269	-1.25372	-1.23951

Coordinates of aggregate of 1a+2a+3 in S_1

Optimized by B3LYP+6-311+G(d,p)

O	0.80131	5.5695	-0.32312
C	-0.71491	1.39403	1.3038
O	0.12032	1.2453	2.18128
O	-0.60959	2.32328	0.30984
C	0.44157	3.33887	0.4182
C	1.81946	2.79614	0.03951
O	2.53122	2.20284	1.11404
C	-0.03355	4.44649	-0.52051
C	0.46089	6.66497	-1.15347
H	0.45608	3.70953	1.44547
H	1.69926	2.08878	-0.79273
H	2.42173	3.64021	-0.30316
H	1.89397	1.69289	1.63973
H	0.0099	4.10728	-1.56662
H	-1.07928	4.68979	-0.28794
H	1.16139	7.46838	-0.92616
H	0.54545	6.40233	-2.21675
H	-0.56217	7.01352	-0.95641
C	-2.12843	-0.50326	1.97211
H	-1.43078	-0.4811	2.82182
H	-1.88054	-1.40043	1.38944
C	-3.54822	-0.54681	2.43518
C	-4.2474	-1.78946	2.42427
C	-4.1819	0.63023	2.93708
C	-5.56246	-1.87102	2.96906
H	-3.76939	-2.662	1.99636
C	-5.50674	0.54821	3.46302
H	-3.62763	1.55872	2.98118
C	-6.18057	-0.69964	3.47346
H	-6.08716	-2.81713	2.99432
H	-5.97885	1.42248	3.89233
H	-7.18095	-0.7605	3.88664
N	-1.85237	0.6779	1.16873
H	-2.47684	0.8868	0.38983
C	-3.52083	0.80196	-2.45501
C	-2.05363	0.45764	-2.65915
C	-1.77477	-0.07902	-4.06001
O	-0.39833	-0.39925	-4.21452
O	-1.21827	1.61076	-2.51452
H	-3.79927	1.65385	-3.09058
H	-1.76278	-0.30879	-1.93128
H	-2.33743	-0.99831	-4.23754
H	-2.08282	0.66533	-4.80813
H	0.09151	0.35056	-3.85038
H	-1.09432	1.80414	-1.57433
H	-4.15312	-0.05803	-2.72191
O	-3.72473	1.13586	-1.08506
C	-5.06211	1.51883	-0.78856
H	-5.76596	0.72091	-1.05552
H	-5.11679	1.69397	0.28586
H	-5.33502	2.43475	-1.32762
N	3.98593	-1.35771	-0.96213

C	2.66378	-1.48531	-1.19282
O	1.82427	-0.61095	-1.01259
H	4.56751	-2.15324	-1.17862
O	2.37479	-2.7308	-1.64518
C	4.60526	-0.15786	-0.39409
H	5.08041	0.42501	-1.19012
H	3.80964	0.45666	0.03229
C	5.63223	-0.51276	0.66021
C	5.23564	-1.09543	1.86994
C	6.9898	-0.26578	0.44589
C	6.17715	-1.42388	2.84028
H	4.18287	-1.28329	2.05283
C	7.9368	-0.59198	1.41782
H	7.3096	0.19119	-0.48543
C	7.53207	-1.17318	2.61625
H	5.85489	-1.868	3.7755
H	8.98689	-0.39099	1.23714
H	8.26483	-1.42629	3.37418
C	1.02959	-2.99012	-2.1255
H	1.14992	-3.90811	-2.70129
H	0.71103	-2.184	-2.79076
C	0.01369	-3.19777	-0.99605
H	0.51466	-3.73743	-0.17899
O	-0.51743	-1.96809	-0.51602
H	0.20627	-1.316	-0.55288
C	-3.10304	-5.14463	-0.73948
H	-2.81754	-6.09751	-1.20823
H	-3.66154	-5.35284	0.17338
H	-3.74848	-4.59053	-1.43544
C	-1.14512	-4.06252	-1.4759
H	-0.75283	-4.98437	-1.93334
H	-1.72259	-3.51879	-2.23919
O	-1.9678	-4.38625	-0.37243

5. Capture of gaseous formaldehyde by the foams

Capture of formaldehyde by the foams (non-contact)

In a plastic container, an emission vial containing 10 mL of about 1 mM formaldehyde solution in water and 0.04 g of foams **NIPUF1**, **NIPUF2** and **NIPUF3** were placed. The container was then hermetically closed and the system was allowed to equilibrate for various periods of time (1 day, 3 days, 5 days and 7 days). Then, 160 µL of the formaldehyde solution was picked out from the emission vial and mixed with 160 µL of the NASH reagent (prepared by maxing 10 µL of acetyl acetone, 750 mg of ammonium acetate and 15 µL of acetic acid in 5 mL of millipore water). The solution was reacted at 60 °C for 10 min before analyzing at 412 nm by UV-Vis spectroscopy. The concentration of formaldehyde in the emission vial was calculated using a calibration curve as shown in Figure S27. The content of captured formaldehyde by the foam was then obtained by the following equation:

$$C_{\mathrm{Foam}} = C_0 - C_{\mathrm{Emi}} - C_{\mathrm{Atm}}$$

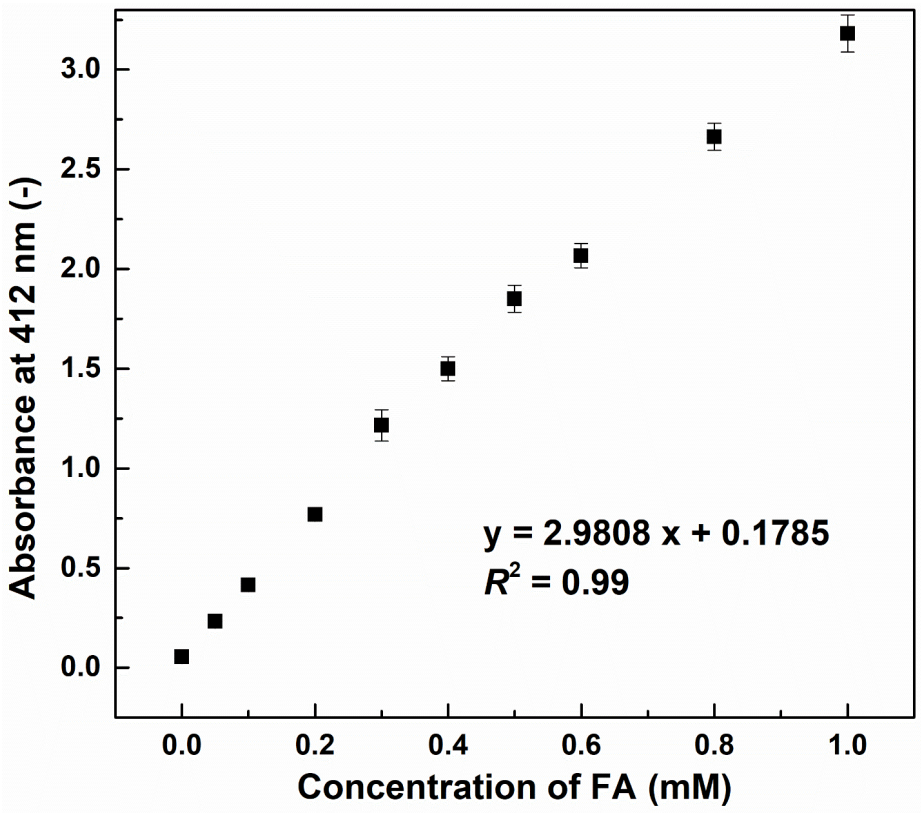

Figure S27. Formaldehyde calibration curve used to determine unknown formaldehyde concentration by the NASH test

where C_{foam}, C_0, C_{Emi} and C_{Atm} are the concentrations of formaldehyde in the foam, the initial concentration of formaldehyde, the concentration of formaldehyde in emission vial and the formaldehyde in the closed atmosphere, respectively. The C_{Atm} was obtained by carrying out the same experiment without the foam. The emission vials were removed after the capturing experiment. The emission vials were replaced by the reception vials containing 5 ml water between release measurements. The same NASH test was performed taking 160 µL solution from reception vials. All experiments were carried out in triplicate.

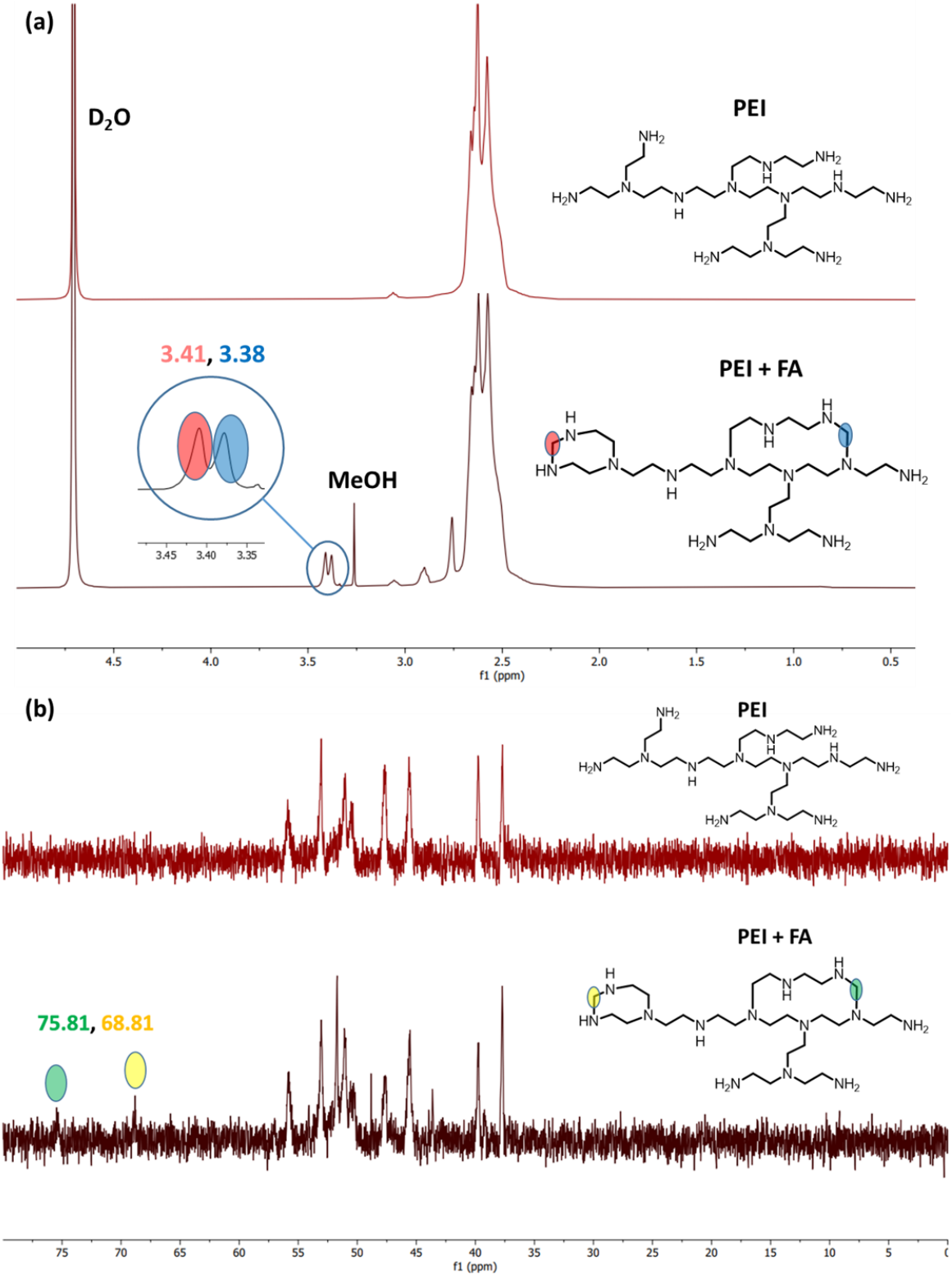

Figure S28. (a) ^{1}H and (b) ^{13}C NMR spectra of PEI and PEI + FA

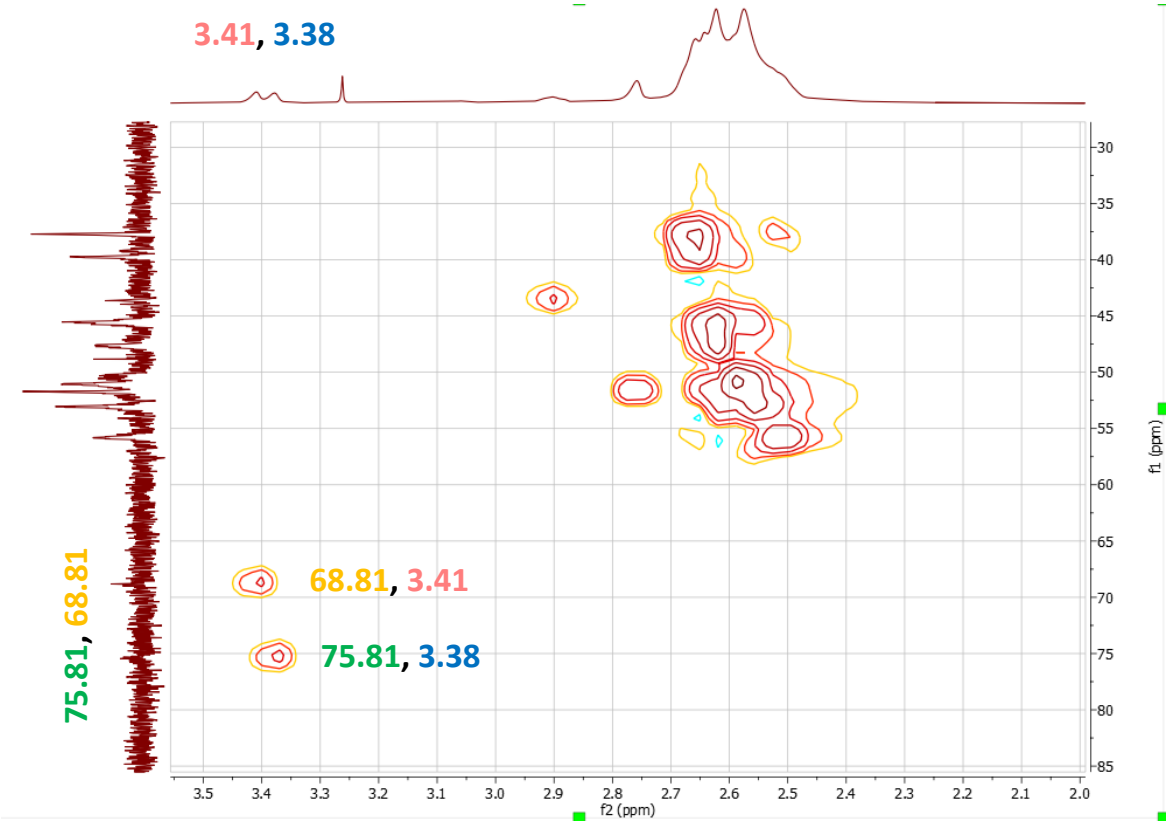

Figure S29. HSQC spectrum of PEI + FA

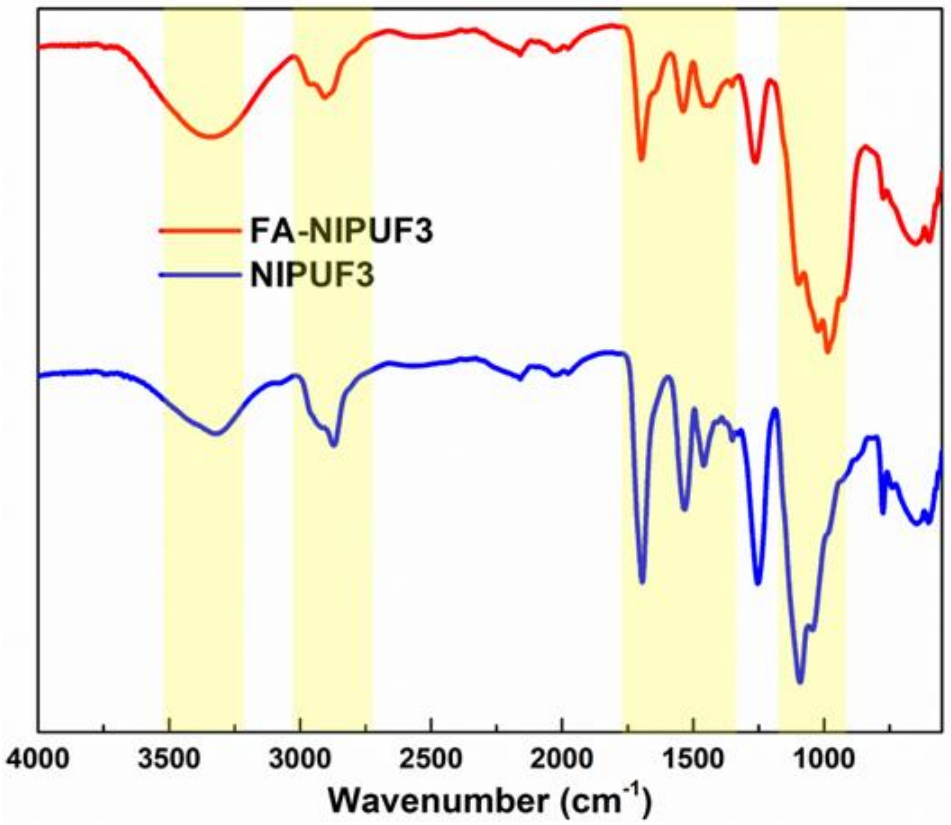

Figure S30. ATR-infrared spectra of **NIPUF3** and FA-**NIPUF3**

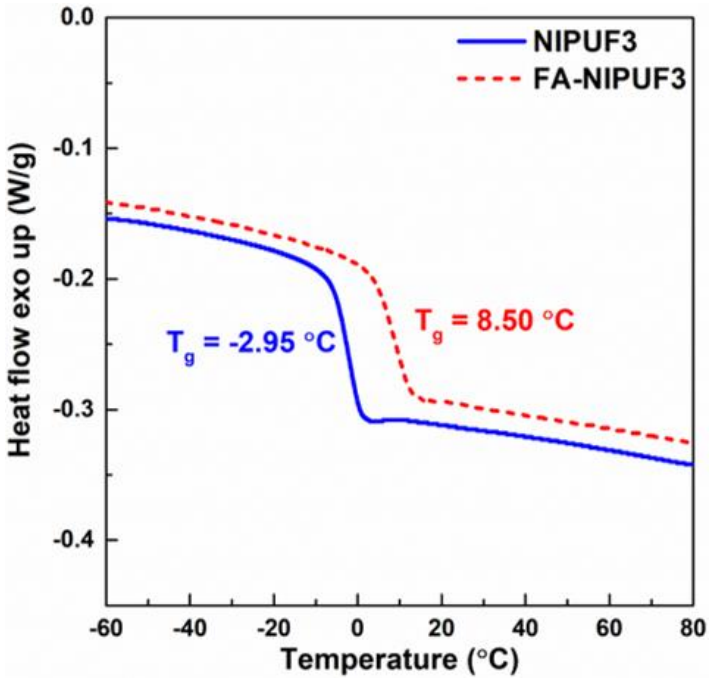

Figure S31. DSC thermogram of dried **NIPUF3** and FA-**NIPUF3**

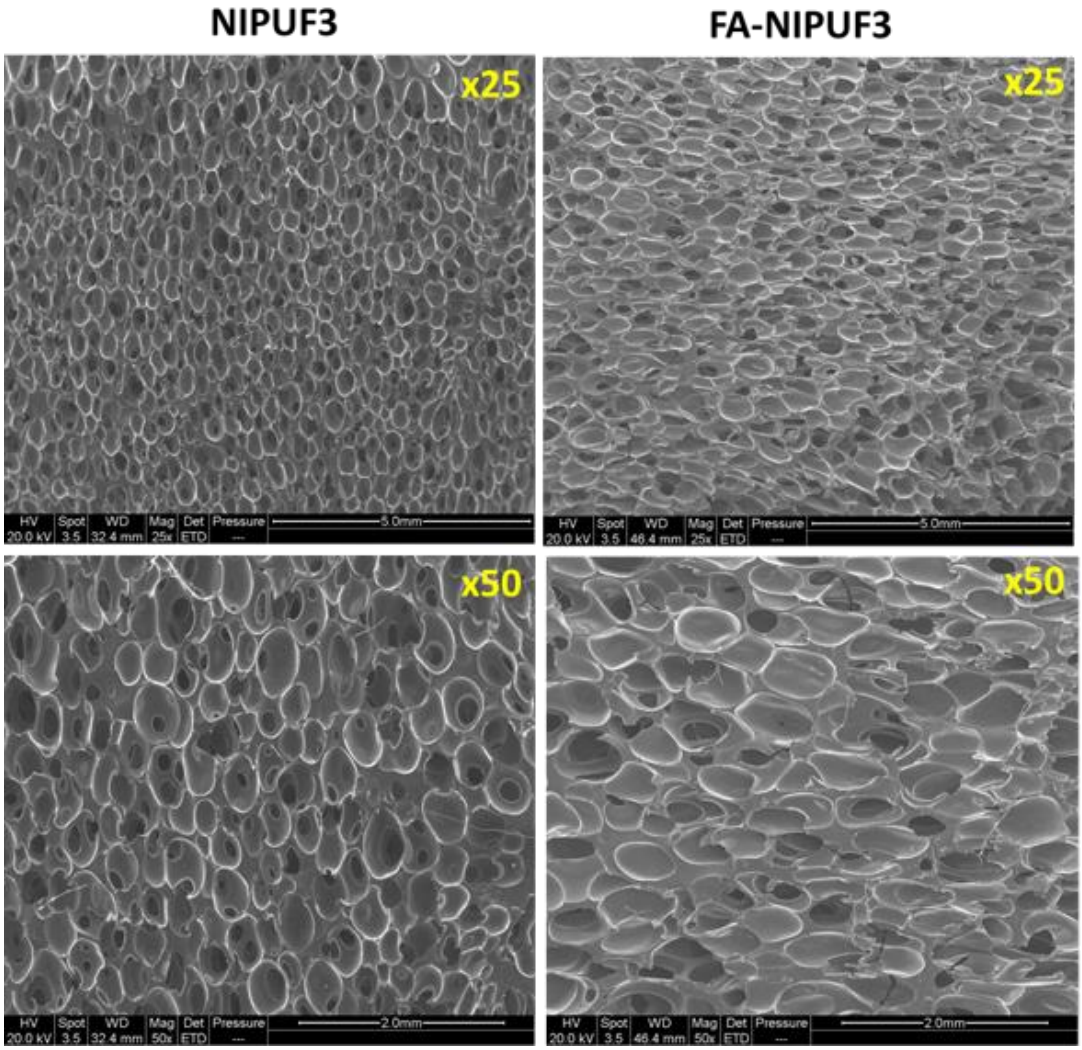

Figure S32. SEM photomicrographs of **NIPUF3** and FA-**NIPUF3** at 25x and 50x magnifications

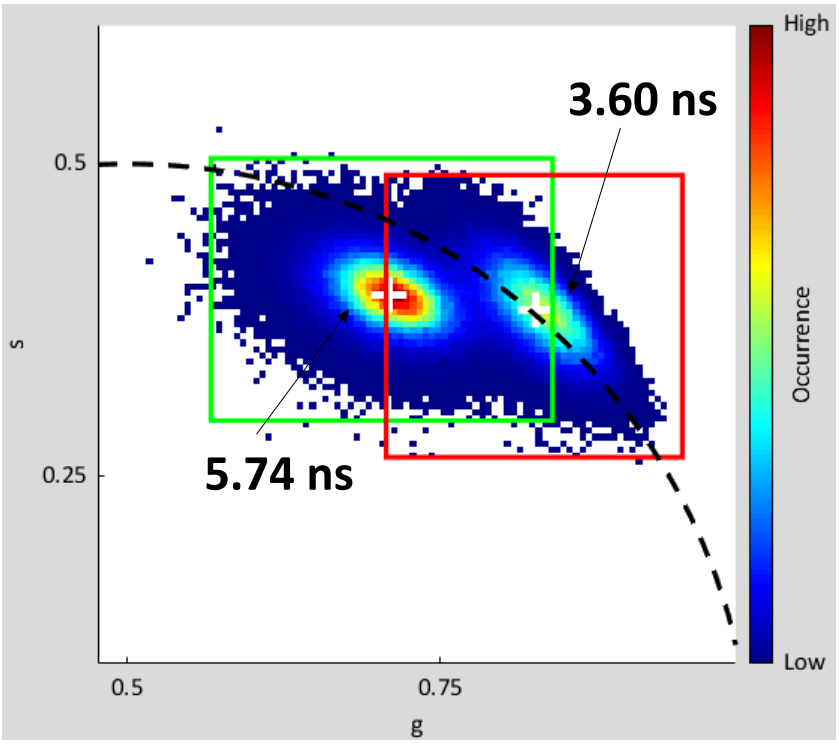

Figure S33. Phasor histogram plots of FA-**NIPUF3** showing lifetime; the atto-425 having 3.60 ns lifetime is used as the reference; the black dotted line corresponds to the universal circle highlighting all possible phasors for monoexponential decays; JET colormaps are used for generating the p**hasor colormap; the threshold minimum/maximum = 100/ 5000 is used**

6. On-Off sensing of metal ions

Preparation of metal ions solutions of exact concentration

Fe^{2+} (0.84, 2.6, 7.1, 12.4, 17.1, 22.5, 27.8, 38.2, 49.5, 60.2, 71.7 and 82.8 ppm), Cu^{2+} (2.1, 7.7, 12.5, 17.3, 24.1, 29.2, 40.1, 51.3, 60.0, 70.4, 80.6, 93.2, 103.8, 116.3 and 126.2 ppm) and Fe^{3+} (2.3, 6.8, 11.8, 20.1, 25.2, 34.3, 45.3, 52.5, 61.2, 78.8, 84.3, 87.9, 100.3) solutions of varying concentrations were prepared by exact dilution of 300 ppm stock solutions and estimated by inductively coupled plasma optical emission spectrometer (ICP-OES: Varian 720-ES) at the characteristic wavelengths. For Cu and Fe, working concentrations were measured at 212.604/ 213.598/ 217.941/ 221.458/ 327.395 nm and 234.350/ 238.204/ 239.563/ 240.489/ 259.837 nm, respectively.

Inductively coupled plasma (ICP) optical emission spectrometer

The concentrations of used metal ions were determined using an inductively coupled plasma optical emission spectrometer (ICP-OES: Varian 720-ES) at the characteristic wavelengths. For Cu and Fe, working concentrations were measured at 212.604/ 213.598/ 217.941/ 221.458/ 327.395 nm and 234.350/ 238.204/ 239.563/ 240.489/ 259.837 nm of wavelengths, respectively.

Fluorescence measurement for selectivity study

The fluorescence of metal ions loaded **NIPUF3** which was prepared by the additions of 0.05 g of **NIPUF3** to the fixed concentration (2 mM (10–70 ppm)) of metal ions were recorded within 350–800 nm using the spectrofluorometer (Tecan Infinite 200Pro) using 350–430 nm of excitation wavelengths (λ_{ex}s). **NIPUF3** foams were allowed to bind for 2 h for selectivity study. The UV-star® microplate, 96 well, half area, μclear®, transparent, 10 ST/BTL of Greiner Bio-One GmbH, Germany (REF: 675801) was used as sample holder. The fluorescence spectra were recorded from the bottom of the well with manual gain of 60, number of flashes of 10, integration time of 20 μs, 0 μs of lag time. The excitation and emission slit widths were 10 and 20 nm for source and detector, respectively. It is important to mention that while performing metal ions sensing and capturing, we paid attention to the sponge effect of the foams. The sponge effect means that, as NIPU foams are hydrophilic, they absorb water when dipped into the metal cation solutions. Therefore, besides being captured by the foams by multiple interactions, part of the metal cations remained dissolved in water trapped within the foam (i.e. unbounded metal cations). To avoid overestimating the content of metal cations effectively captured (i.e. bounded to the foams), we quantified the content of unbonded cations by squeezing the foam and quantifying the metal cation that was released. The content of metal cations captured by the foam (i.e. bound to the foam) was thus obtained by the equation 1.

$$C_{\mathrm{bm}} = C_{\mathrm{tm}} - C_{\mathrm{um}} \quad (1)$$

where C_{bm}, C_{tm} and C_{um} are the concentrations of metal ion bound to the foam, the total concentration of metal ions in foam and the concentration of unbound metal ions obtained from sponge effect, respectively. All the results were done twice with three replicates.

Calculation of fluorescence quenching

Fluorescence quenching was calculated using equation 2:

$$\text{Quenching } (\eta) = \frac{F_f - F_0}{F_0} \times 100 \quad (2)$$

Here, F_0 and F_f are the initial and final (after treatment of metal) fluorescence, respectively

Fluorescence spectroscopy for quantification metal ions

The calibration plots were prepared by recording the fluorescence spectra of Fe^{2+} (0.84, 2.6, 7.1, 12.4, 17.1, 22.5, 27.8, 38.2, 49.5, 60.2, 71.7 and 82.8 ppm), Cu^{2+} (2.1, 7.7, 12.5, 17.3, 24.1, 29.2, 40.1, 51.3, 60.0, 70.4, 80.6, 93.2, 103.8, 116.3 and 126.2 ppm) and Fe^{3+} (2.3, 6.8, 11.8, 20.1, 25.2, 34.3, 45.3, 52.5, 61.2, 78.8, 84.3, 87.9, 100.3) loaded **NIPUF3** foams (0.05 g) within 350–800 nm using the spectrofluorometer (Tecan Infinite 200Pro) using 350–430 nm of excitation wavelengths (λ_{ex}s). The contact time depended on the concentration of the metal cation. To evaluate the optimal contact time of the foam with the solution, we followed the evolution of the fluorescence spectra with time. When no more evolution of the fluorescence spectra was noted, the equilibrium was reached, and the optimal contact time was known. A contact time of 3h was here used, where the equilibrium was reached for all the concentrations. The UV-star® microplate, 96 well, half area, μclear®, transparent, 10 ST/BTL of Greiner Bio-One GmbH, Germany (REF: 675801) was used as sample holder. The fluorescence spectra were recorded from the bottom of the well with manual gain of 60, number of flashes of 10, integration time of 20 μs, 0 μs of lag time. The excitation and emission slit widths were 10 and 20 nm for source and detector, respectively. All the results were done thrice with three replicates. The error bars were included in the relative fluorescence vs concentration plots, however, the fluorescence intensity vs concentration plots the average value of spectrum were shown.

Calculation of exclusion performance

Here, 0.05 g of dry **NIPUF3** foams was added to solutions of metal ions having concentrations within 0-600 ppm (Fe^{2+}), 0-450 ppm (Cu^{2+}) and 0-700 ppm (Fe^{3+}) with constant shaking of 300 rpm. The progress of exclusion and remaining concentration of metal ions were monitored by fluorescence spectrophotometer and ICP-OES, respectively. The performance of sensing q_t (mg g^{-1}) values were determined at concentrations (C_t) using Equation 3.

$$q_t = \frac{(C_0 - C_t)V}{m_s} \quad (3)$$

Here, C_0/ C_t (ppm), V (mL), and m_s (g) are concentrations at t = 0/ t, volume of metal ion solution, and mass of **NIPUF3** foam, respectively. The equilibrium adsorption capacity (q_e, mg g^{-1}) was obtained via replacement of C_t by C_e in Equation 3.

Exclusion isotherm study

The equilibrium adsorption data were fitted to three different isotherm models, i.e., Langmuir, Freundlich and BET (Equation 4–6), for estimation of various model parameters to enlighten the various aspects of adsorption mechanism.

$$q_e = q_{max}\frac{k_L C_e}{1 + k_L C_e} \quad (4)$$

$$q_e = k_F C_e^{1/n} \quad (5)$$

$$q_e = q_{BET}\frac{k_1 C_e}{(1 - k_2 C_e)(1 - k_2 C_e + k_1 C_e)} \quad (6)$$

Here, q_{max}, n and q_{BET} and k_L, k_F, k_1, and k_2 are isotherm parameters and isotherm constants, respectively.

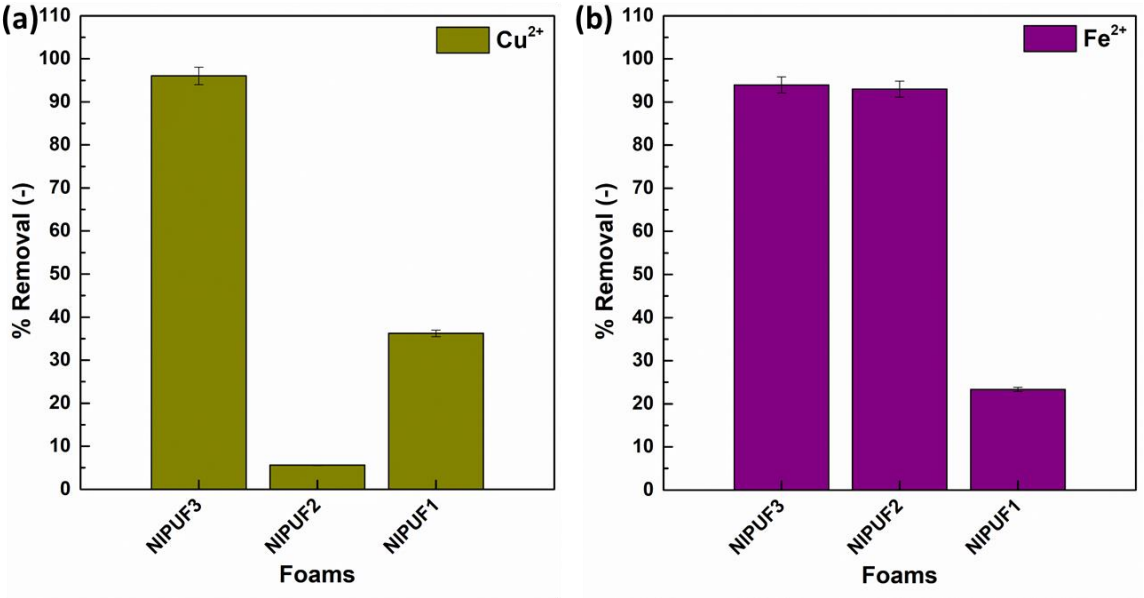

Figure S34. %Removal of (a) Cu^{2+} and (b) Fe^{2+} ions using **NIPUF3**, **NIPUF2** and **NIPUF1** foams; concentration of Cu^{2+} = 22.50 ppm and concentration of Fe^{2+} = 20.98 ppm; experiment was performed with taking only relatively hydrophilic foams; Cu^{2+} and Fe^{2+} were estimated by an inductively coupled plasma optical emission spectrometer (ICP-OES: Varian 720-ES) at 212.604/ 213.598/ 217.941/ 221.458/ 327.395 nm and 234.350/ 238.204/ 239.563/ 240.489/ 259.837 nm wavelength; experiment was performed twice with three replicates.

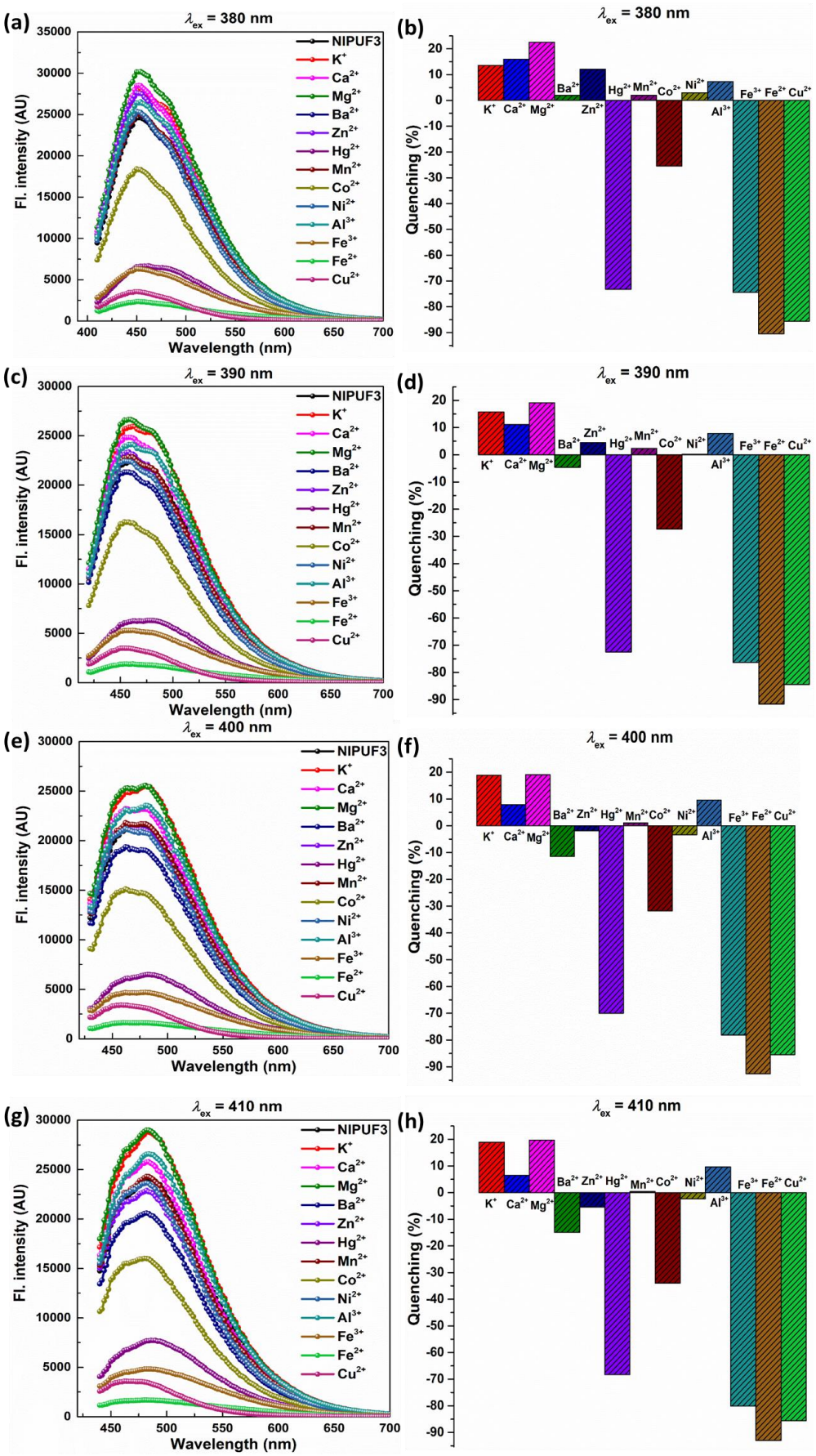

Figure S35. Continued

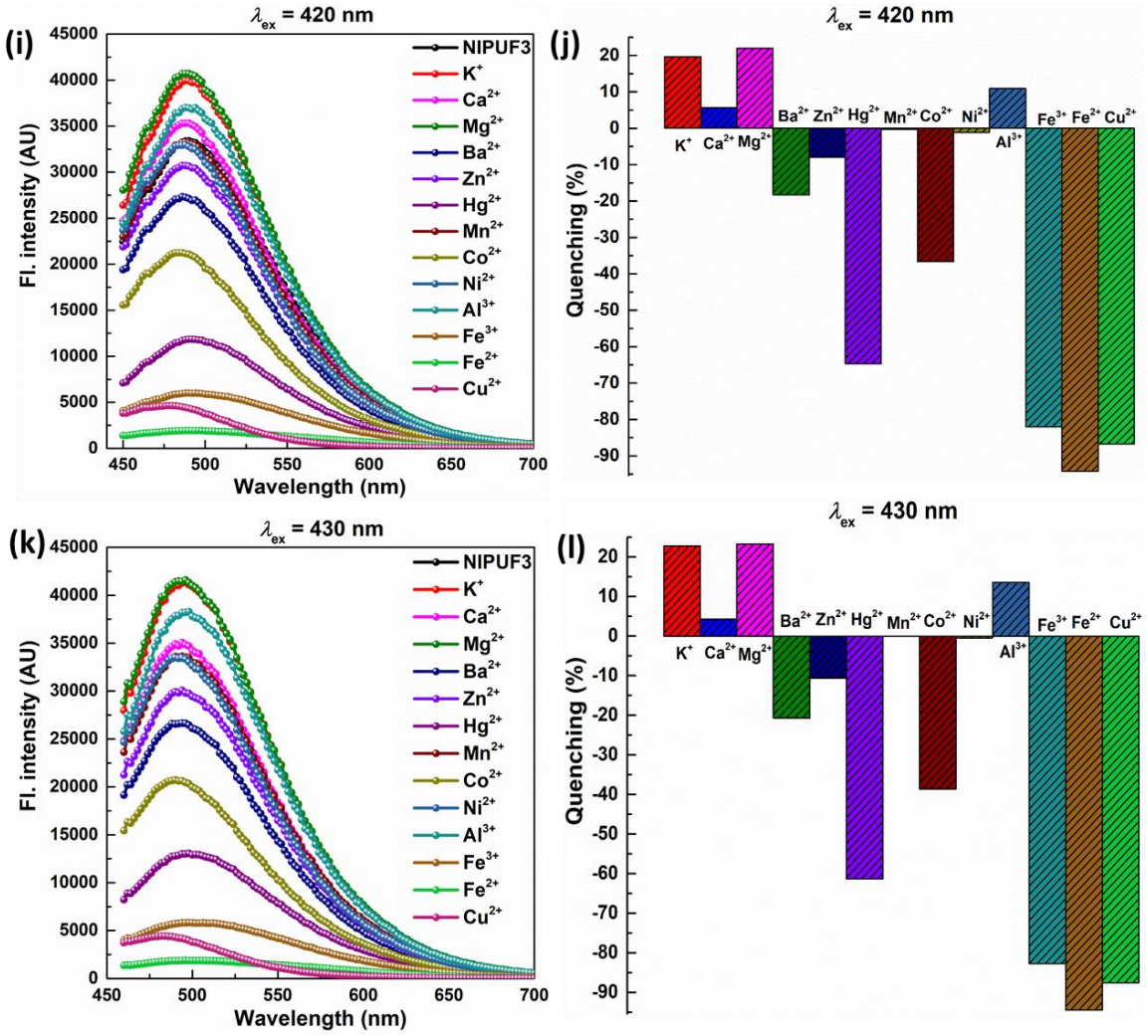

Figure S35. Full spectral mode binding of **NIPUF3** with metal ions, e.g. K^+, Ca^{2+}, Mg^{2+}, Ba^{2+}, Zn^{2+}, Hg^{2+}, Mn^{2+}, Co^{2+}, Ni^{2+}, Al^{3+}, Fe^{3+}, Fe^{2+} and Cu^{2+} at room temperature (~20 °C) in aqueous solution (pH about 7.0–7.6) using (a) λ_{ex} = 380 nm, (c) λ_{ex} = 390 nm, (e) λ_{ex} = 400 nm, (g) λ_{ex} = 410 nm, (i) λ_{ex} = 420 nm, and (k) λ_{ex} = 430 nm; fluorescence quenching of **NIPUF3** at (b) λ_{ex} = 380 nm, (d) λ_{ex} = 390 nm, (f) λ_{ex} = 400 nm, (h) λ_{ex} = 410 nm, (j) λ_{ex} = 420 nm, and (l) λ_{ex} = 430 nm using K^+, Ca^{2+}, Mg^{2+}, Ba^{2+}, Zn^{2+}, Hg^{2+}, Mn^{2+}, Co^{2+}, Ni^{2+}, Al^{3+}, Fe^{3+}, Fe^{2+} and Cu^{2+} metal ions; for each measurement, **NIPUF3** was excited within 380–430 nm, and the full emission spectra were recorded within 410–850 nm using 10 nm and 20 nm bandwidths for excitation (source) and emission (detector), respectively; The fluorescence measurements were carried out using the metal loaded **NIPUF3** which was prepared by the additions of 0.05 g of **NIPUF3** to the fixed concentration (2 mM (10–70 ppm)) of metal ions.

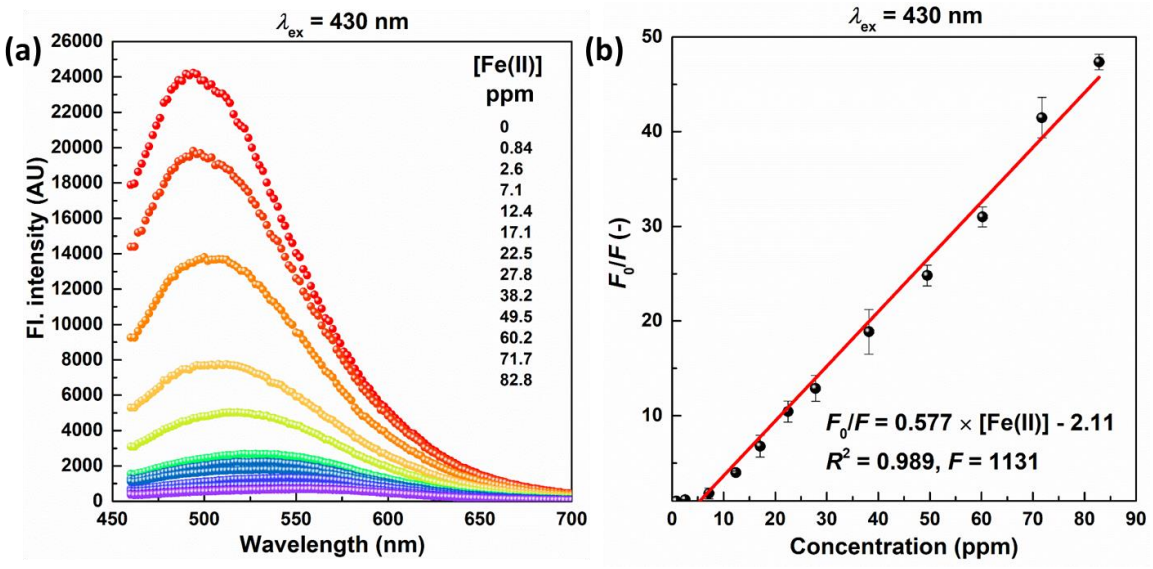

Figure S36. (a) Fluorescence intensities of **NIPUF3** loaded with different concentration (0-82.8 ppm) of Fe^{2+} ion measured at λ_{ex} = 430 nm; (b) relative fluorescence versus concentration plots of Fe^{2+}-**NIPUF3** at λ_{ex} = 430 nm; the mass of **NIPUF3** used for each measurement was 0.05 g; all loaded **NIPUF3** were excited at 380 and 430 nm and the full emission spectra were recorded within 410/ 460–850 nm using 10 nm and 20 nm bandwidths for excitation (source) and emission (detector), respectively; The exact concentration of Fe^{2+} was determined by an inductively coupled plasma optical emission spectrometer (ICP-OES: Varian 720-ES) at 234.350/ 238.204/ 239.563/ 240.489/ 259.837 nm wavelength; experiment was performed twice with three replicates.

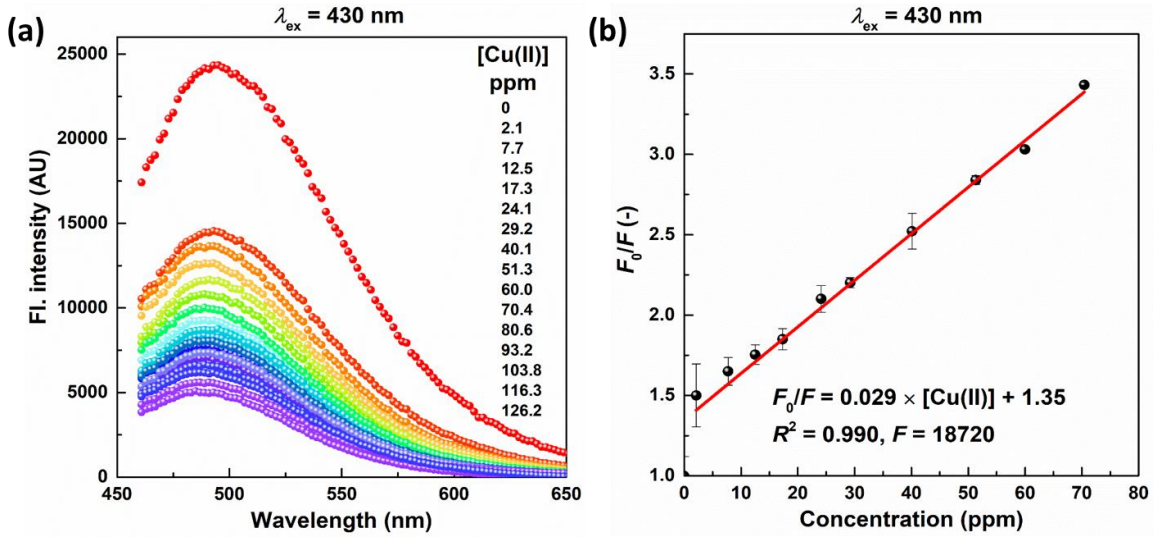

Figure S37. (a) Fluorescence intensities of **NIPUF3** loaded with different concentration (0-126.2 ppm) of Cu^{2+} ion measured at λ_{ex} = 430 nm; (b) relative fluorescence versus concentration plots of Cu^{2+}-**NIPUF3** at λ_{ex} = 430 nm; the mass of **NIPUF3** used for each measurement was 0.05 g; all loaded **NIPUF3** were excited at 380 and 430 nm and the full emission spectra were recorded within 410/ 460–850 nm using 10 nm and 20 nm bandwidths for excitation (source) and emission (detector), respectively; The exact concentration of Cu^{2+} was determined by an inductively coupled plasma optical emission spectrometer (ICP-OES: Varian 720-ES) at 212.604/ 213.598/ 217.941/ 221.458/ 327.395 nm wavelengths; experiment was performed twice with three replicates.

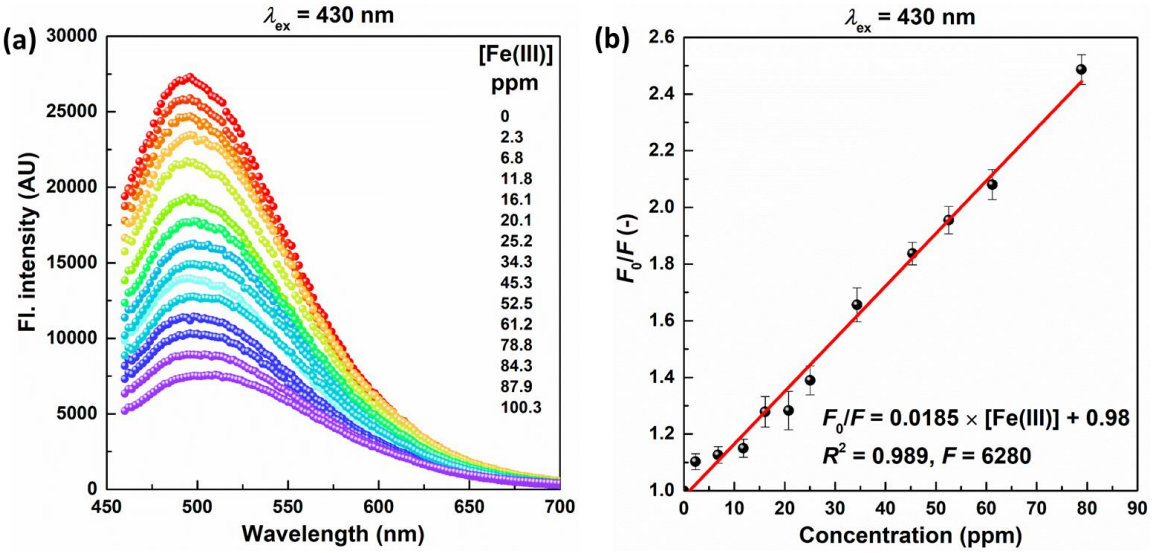

Figure S38. (a) Fluorescence intensities of **NIPUF3** loaded with different concentration (0-100.3 ppm) of Fe^{3+} ion measured at λ_{ex} = 430 nm; (b) relative fluorescence versus concentration plots of Fe^{3+}-**NIPUF3** at λ_{ex} = 430 nm; the mass of **NIPUF3** used for each measurement was 0.05 g; all loaded **NIPUF3** were excited at 380 and 430 nm and the full emission spectra were recorded within 410/ 460–850 nm using 10 nm and 20 nm bandwidths for excitation (source) and emission (detector), respectively; The exact concentration of Fe^{3+} was determined by an inductively coupled plasma optical emission spectrometer (ICP-OES: Varian 720-ES) at 234.350/ 238.204/ 239.563/ 240.489/ 259.837 nm wavelength; experiment was performed twice with three replicates.

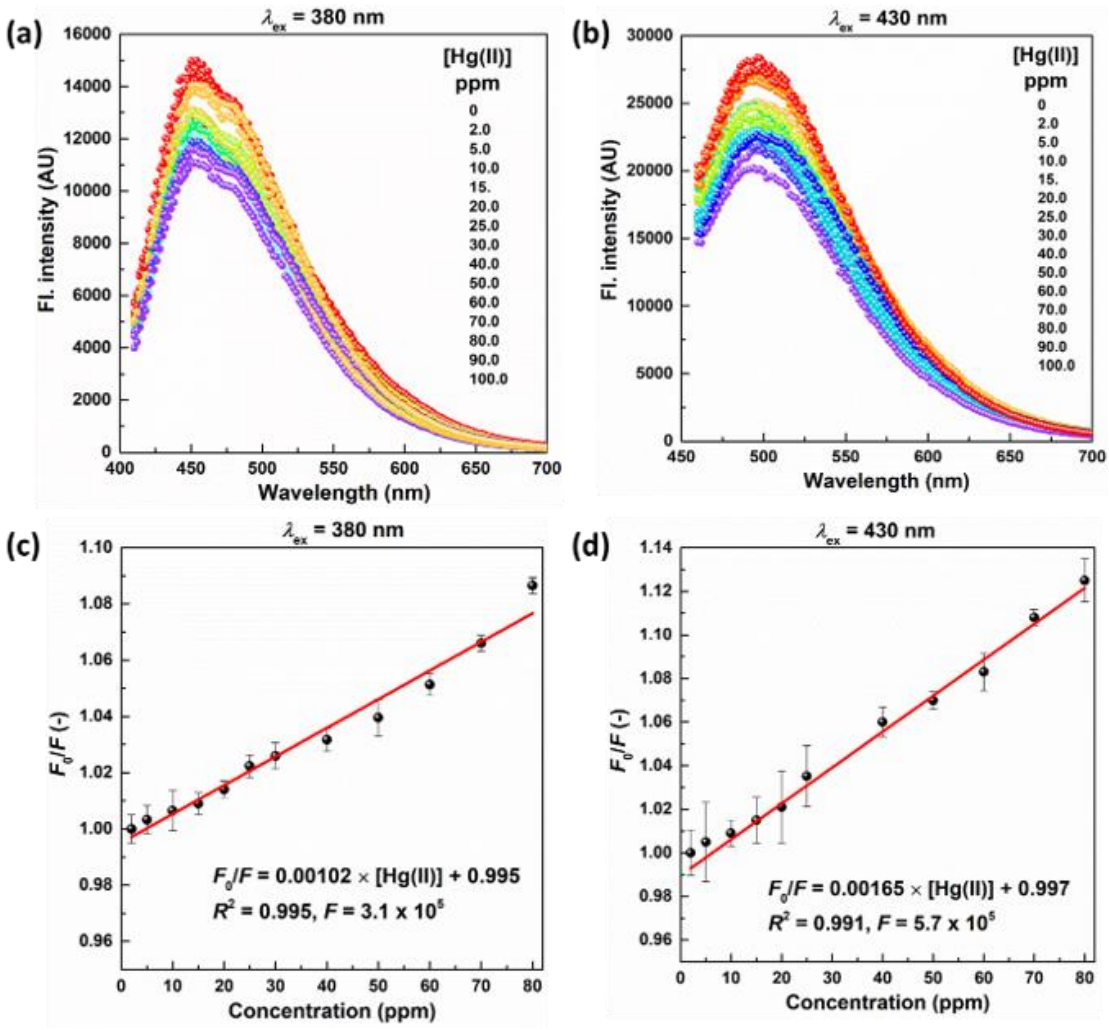

Figure S39. Fluorescence intensities of **NIPUF3** loaded with different concentration (0-100 ppm) of Hg^{2+} ion measured at (a) λ_{ex} = 380 nm and (c) λ_{ex} = 430 nm; relative fluorescence versus concentration plots of Hg^{2+}-**NIPUF3** at (b) λ_{ex} = 380 nm and (d) λ_{ex} = 430 nm; the mass of **NIPUF3** used for each measurement was 0.05 g; all loaded **NIPUF3** were excited at 380 and 430 nm and the full emission spectra were recorded within 410/ 460–850 nm using 10 nm and 20 nm bandwidths for excitation (source) and emission (detector), respectively; The exact concentration of Hg^{2+} was prepared by exact dilution from the known stock solution; experiment was performed twice with three replicates.

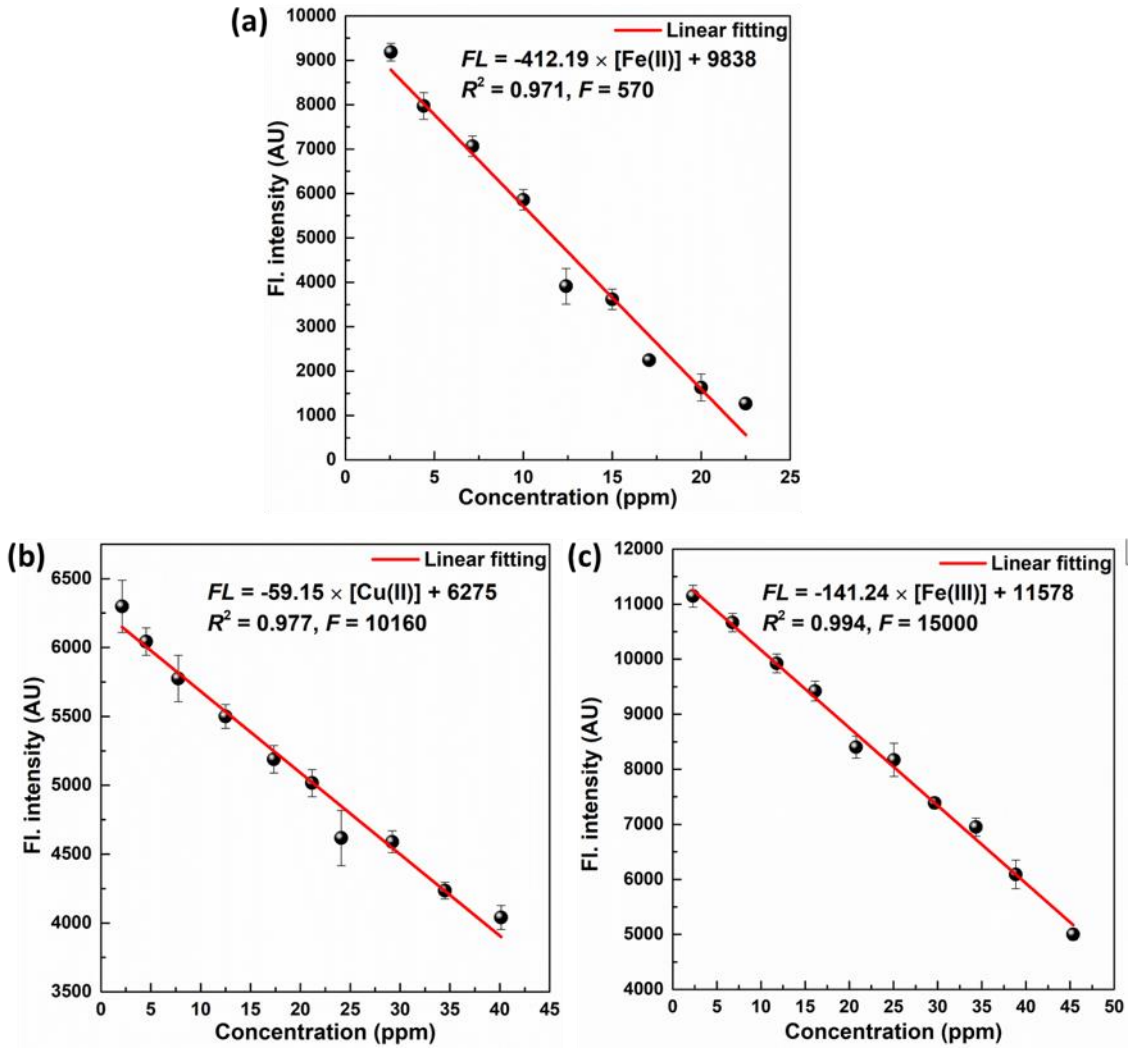

Figure S40. Limit of detection (LOD) plots of (a) Fe(II)-**NIPUF3**, (b) Fe(III)-**NIPUF3** and (c) Fe(III)-**NIPUF3**; fluorescence intensities of **NIPUF3** loaded with different concentration of Fe(II), Fe(III) and Cu(II) ion measured at λ_{ex} = 380 nM; the exact concentration of metal ions were measured using an inductively coupled plasma optical emission spectrometer (ICP-OES: Varian 720-ES).

$$LOD = \frac{3 \times standard\ error}{slope}$$

$$\text{LOD for Fe(II)} = \frac{3 \times 25}{412.19}\ ppm = 0.18195\ ppm \times 3.597\ (\mu M/ppm) = 0.65\ \mu M$$

$$\text{LOD for Cu(II)} = \frac{3 \times 2.98}{59.15}\ ppm = 0.15114\ ppm \times 5.009\ (\mu M/ppm) = 0.76\ \mu M$$

$$\text{LOD for Fe(III)} = \frac{3 \times 3.57}{141.24}\ ppm = 0.07582\ ppm \times 2.475\ (\mu M/ppm) = 0.19\ \mu M$$

Table S6 Comparison of results from the literature

Name of materials	Origin of fluorescence	Synthesis process	Sensor	Estimation process	Limit of detection (M)	Binding constant (M^{-1})	References
Luminescent Eu(III) complex containing polyurethane foam	Ex situ added Eu(III) complex	Introduced during synthesis	Cu^{2+}	Turn-off at 615 nm	3.40×10^{-6}	36000	Anal. Methods, **2013**, *5*, 6045–6050.
Fluorescent aminoquinoline containing polyurethane foam	Ex situ added aminoquinoline derivative	Introduced during synthesis	Cu^{2+}	Turn-On at 515 nm	5.00×10^{-5} [a]	ND [b]	RSC Adv., **2014**, *4*, 18222–18228.
Luminescent Eu(III)-complex containing polyurethane foam	Ex situ added Eu(III) complex	co-polycondensation reaction	Cu^{2+}	Turn-off at 617 nm	0.28×10^{-6}	9511	Eur. Polym. J., **2019**, *112*, 461–465.
Fluorescent polyurethane foam containing rhodamine derivative	Ex situ added rhodamine derivative	Introduced during synthesis	Fe^{3+}	Turn-On at 561 nm	1.64×10^{-6}	ND [a]	Polym. Int., **2022**, *71*, 169–174.
Waterborne polyurethane-nitrogen-carbon-dots fluorescent film	Intrinsically fluorescent	electrochemical-hydrothermal method	Fe^{3+}	Turn-off at nm 420 nm	2.19×10^{-6}	ND [a]	Macromol. Mater. Eng., **2020**, *305*, 1900810.
Nonconventional fluorescent non-isocyanate polyurethane foam	**Intrinsically fluorescent foam without any fluorescent dye/ probe/ metal complex**	**Simple synthesis from low cost reagents in one step by water based foaming technology; could be synthesized in kg scale in few hours**	**Fe^{2+}**	**Turn-off sensing within 452-498 nm range with similar selectivity; for instance, we showed only two 452 (λ_{ex} = 380 nm) nm and 498 nm (λ_{ex} = 430 nm)**	**0.66×10^{-6}** [c]	**139838** [c]	**This study** [d]
			Cu^{2+}		**0.76×10^{-6}** [c]	**5599** [c]	**This study**
			Fe^{3+}		**0.18×10^{-6}** [c]	**6061** [c]	**This study**

[a]The color change was visualized by the naked eye even at Cu^{2+} ion concentrations as low as 5.00×10^{-5} mol L^{-1}; [b]Not determined; [c]Determined at λ_{ex} = 380 nm; [d]**NIPUF3** can remove Fe^{2+}, Cu^{2+} and Fe^{3+} ions from solution with adsorption capacity of 175.27, 54.37 and 45.37 mg/g, respectively.

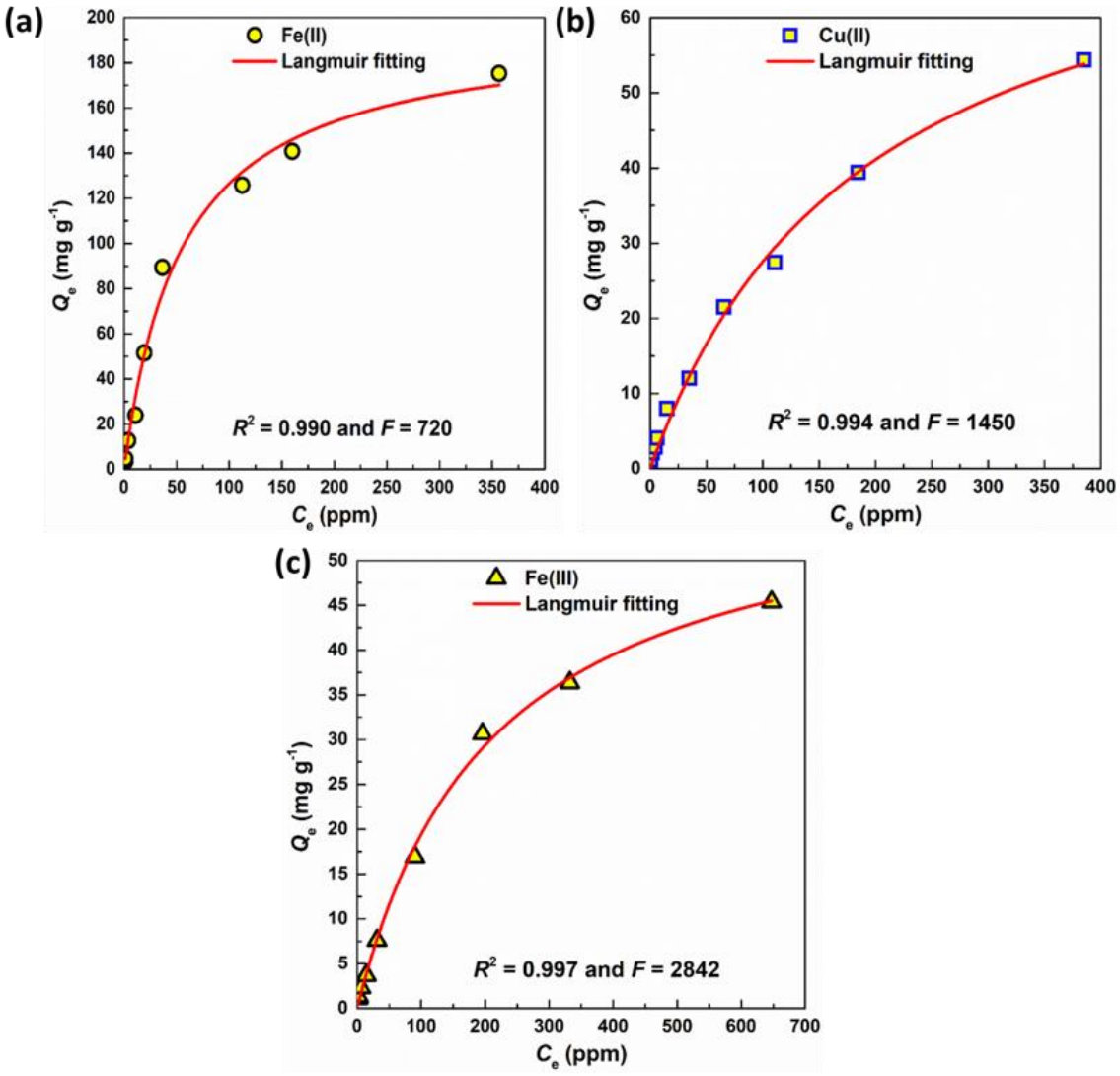

Figure S41. Langmuir fitting for Fe^{2+}, Cu^{2+} and Fe^{3+} ions from concentrated solution; experiment was performed twice with three replicates; the errors are too small to see.

Table S7 Langmuir isotherm details

Parameters	Metal ions		
	Fe^{2+}	Cu^{2+}	Fe^{3+}
C_0 (ppm)	0–600	0–450	0–700
pH_i	7.00	7.00	7.00
Q_{max} (mg g^{-1})	196.63	81.03	60.27
Q_{expt} (mg g^{-1})	175.27	54.37	45.37
k_L (L mg^{-1})	0.0180	0.0052	0.0048
R^2	0.990	0.994	0.997
F	720	1450	2842

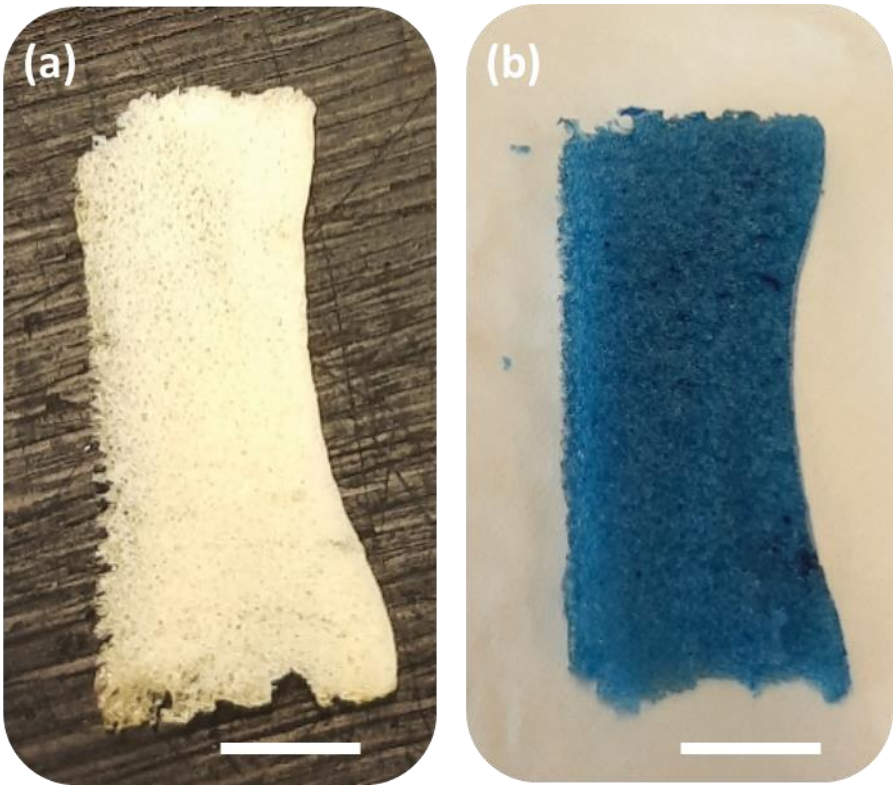

Figure S42. Photographic picture of (a) **NIPUF3** and (b) Cu(II)-**NIPUF3** showing color changes under visible light; scale bar = 1 cm

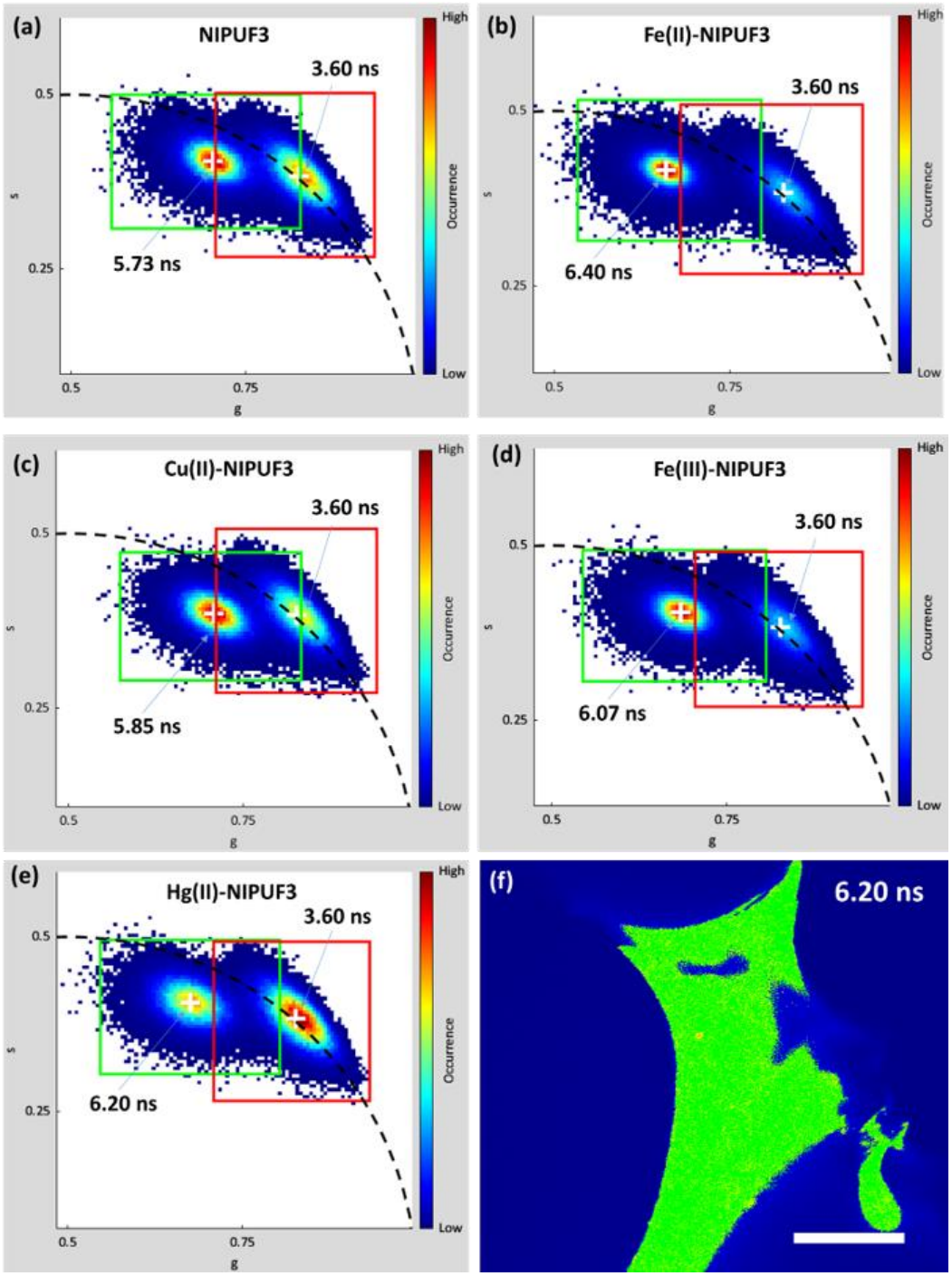

Figure S43. Phasor histogram plots of (a) **NIPUF3**, (b) Fe(II)-**NIPUF3**, (c) Cu(II)-**NIPUF3**, (d) Fe(III)-**NIPUF3** and (e) Hg(II)-**NIPUF3** showing lifetimes; the atto-425 having 3.60 ns lifetime is used as the reference; the black dotted line corresponds to the universal circle highlighting all possible phasors for monoexponential decays; jet colormaps are used for generating the p**hasor colormaps; the threshold minimum/maximum = 100/ 5000 is used; (f)** phasor image colormap showing lifetime of Hg(II)-**NIPUF3;** jet colormap is used for generating the p**hasor image colormap, scale bar = 100 μm**

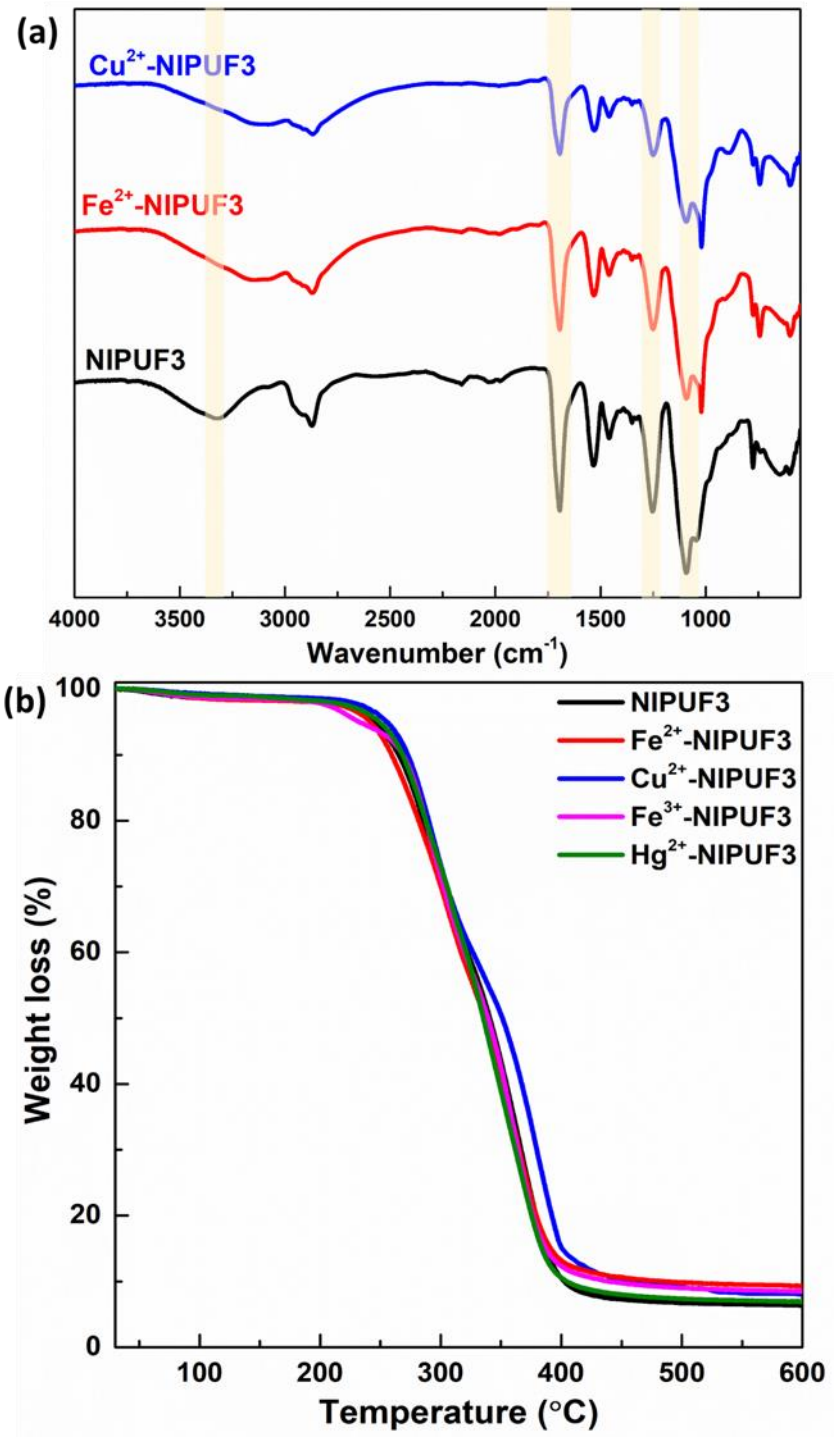

Figure S44. (a) ATR-FTIR of **NIPUF3**, Fe^{2+}-**NIPUF3** and Cu^{2+}-**NIPUF3** and (b) TGA of **NIPUF3**, Fe^{2+}-**NIPUF3**, Cu^{2+}-**NIPUF3**, Fe^{3+}-**NIPUF3** and Hg^{2+}-**NIPUF3**

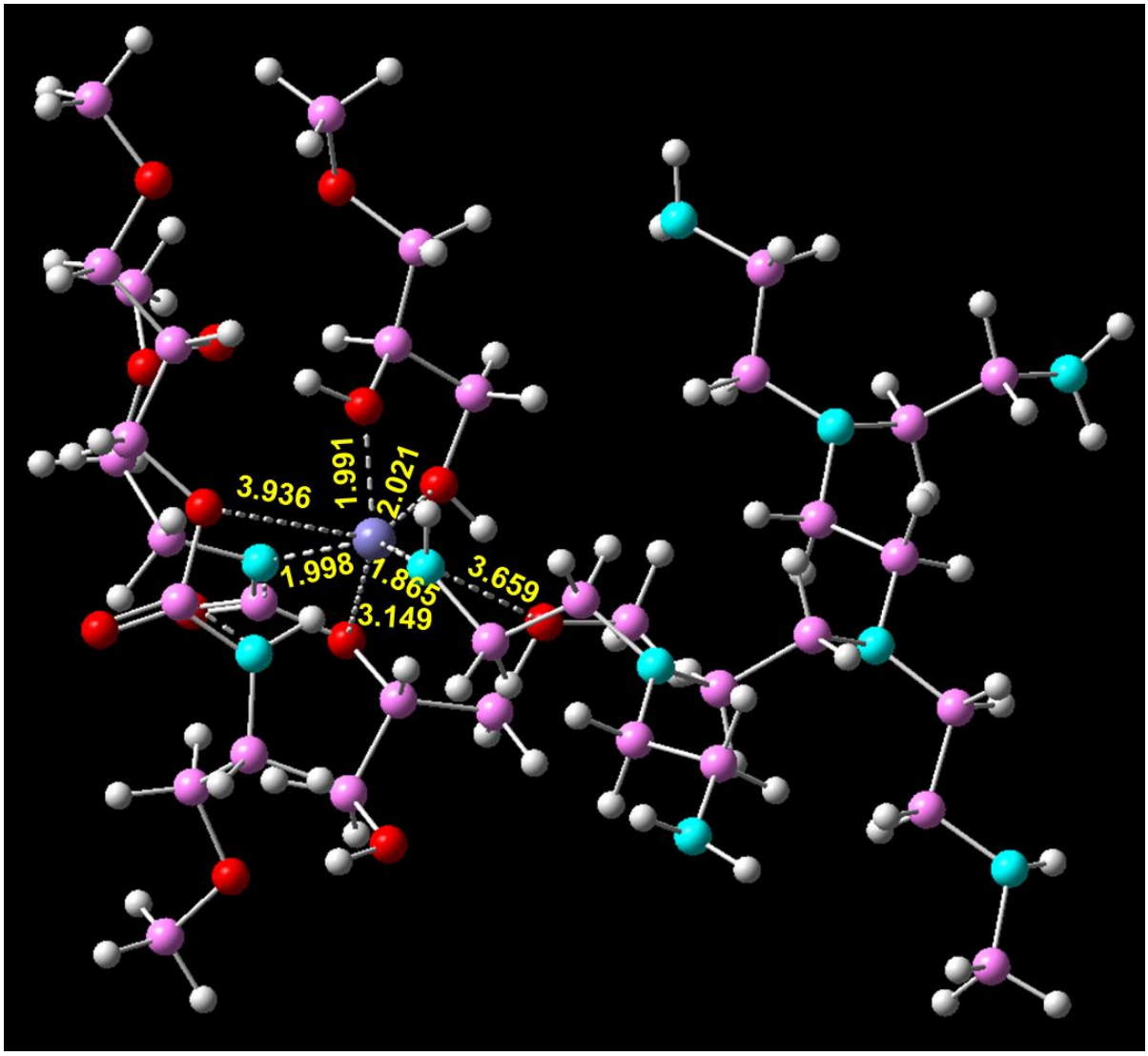

Figure S45. Optimized structures of Fe^{2+}-**NIPUF3** showing strong interactions with metal

Entry	Interactions	Bond length
1	Fe^{2+}···**N**HCH_2–	1.865 Å
2	Fe^{2+}···**N**(COO–)CH_2–	1.998 Å
3	Fe^{2+}···**O**H–CH<	1.991 Å
4	Fe^{2+}···**O**H–CH_2–	2.021 Å
5	Fe^{2+}···**O**(CON)CH<	3.149 Å
6	Fe^{2+}···**O**<	3.659 Å
7	Fe^{2+}···**O**(CON)CH_2–	3.936 Å

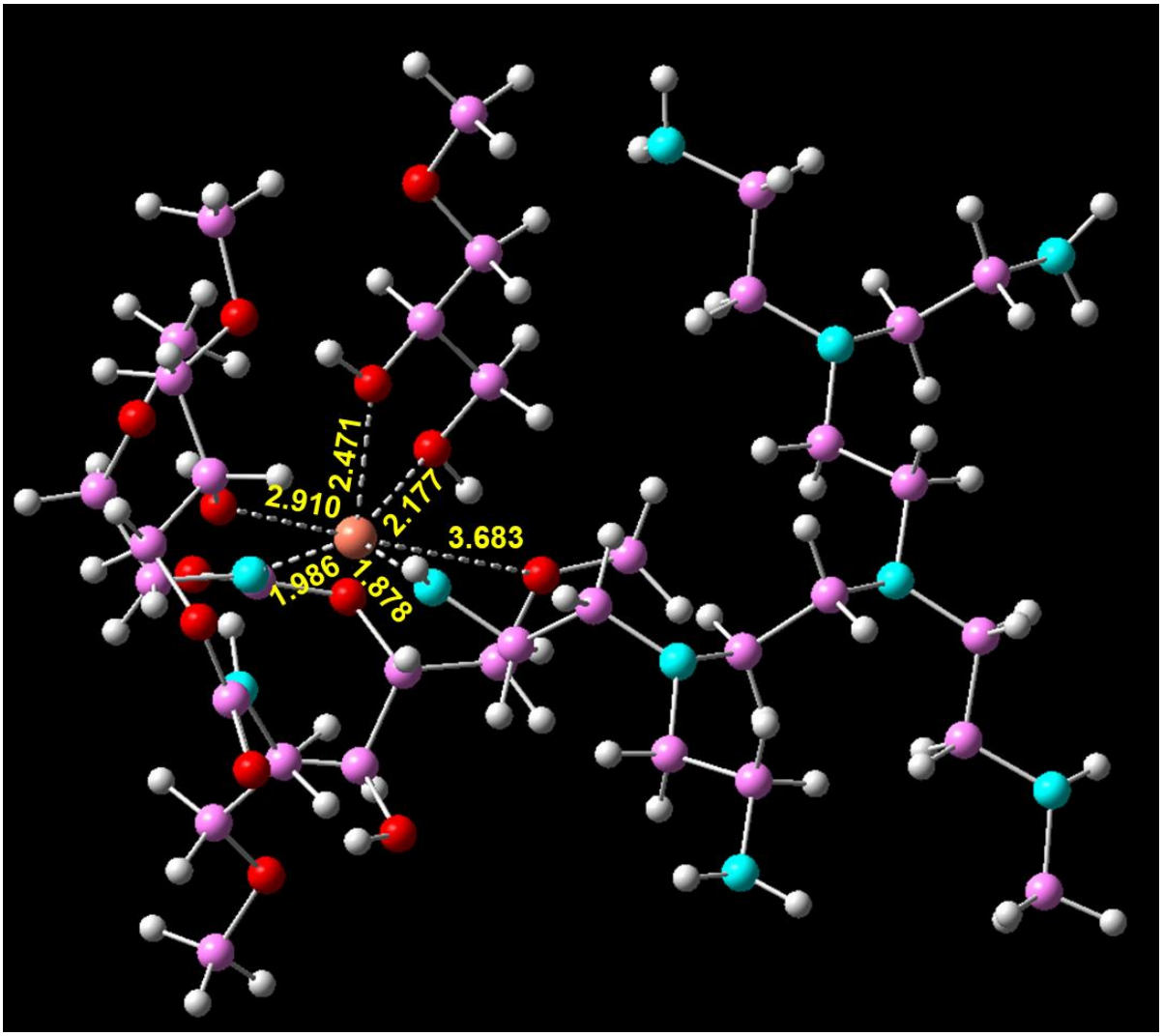

Figure S46. Optimized structures of Cu^{2+}-**NIPUF3** showing strong interactions with metal

Entry	Interactions	Bond length
1	Cu^{2+}···**N**HCH_2–	1.878 Å
2	Cu^{2+}···**N**(COO–)CH_2–	1.986 Å
3	Cu^{2+}···**O**H–CH_2–	2.177 Å
4	Cu^{2+}···**O**H–CH<	2.471 Å
5	Cu^{2+}···**O**HCH(O)–	2.910 Å
6	Cu^{2+}···**O**<	3.683 Å

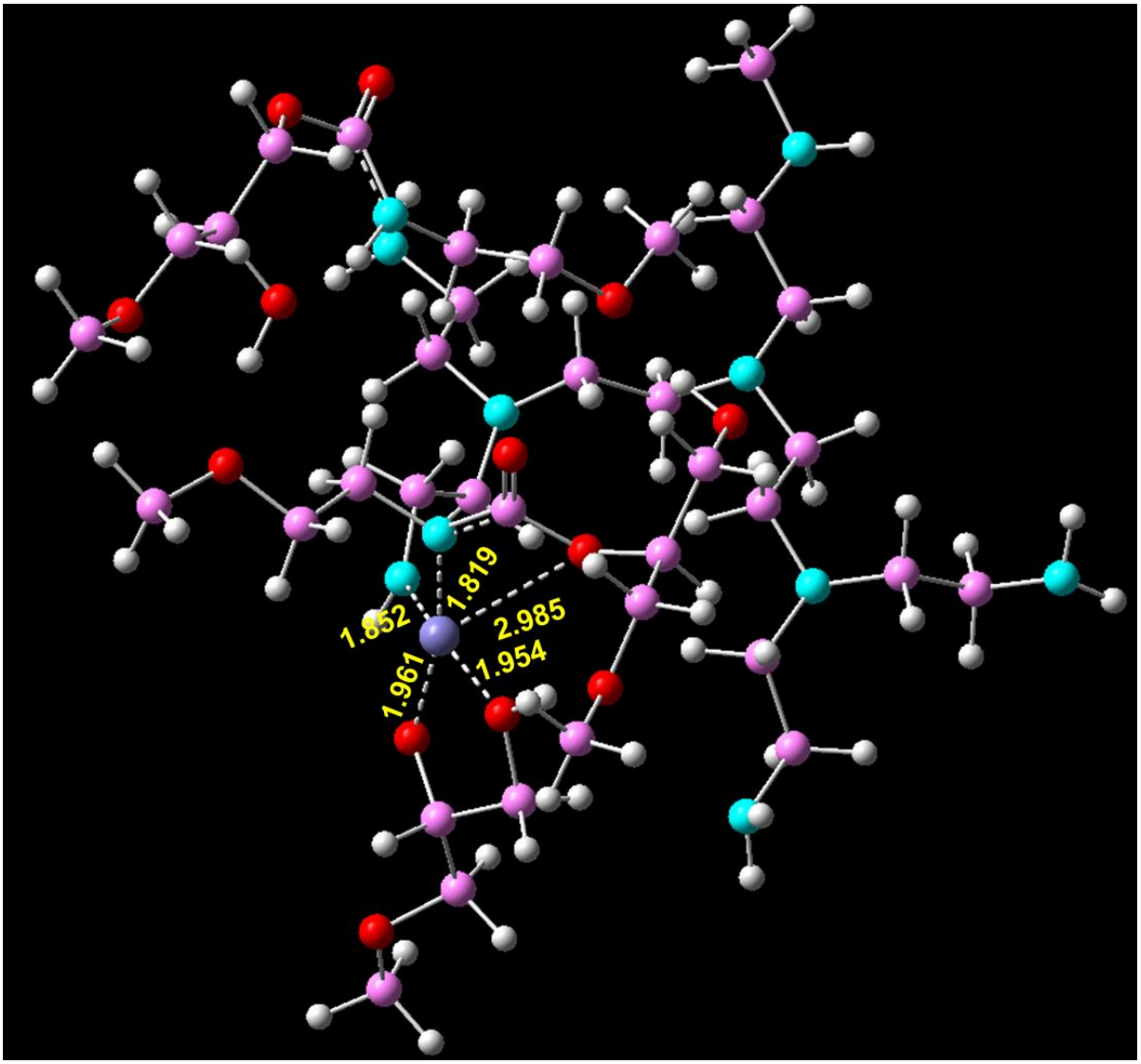

Figure S47. Optimized structures of Fe^{3+}-**NIPUF3** showing strong interactions with metal

Entry	Interactions	Bond length
1	Fe^{3+}···**N**HCH_2–	1.852 Å
2	Fe^{3+}···**N**(COO–)CH_2–	1.819 Å
3	Fe^{3+}···**O**CH<	1.961 Å
4	Fe^{3+}···**O**H–CH_2–	1.954 Å
5	Fe^{3+}···**O**(CON)CH<	2.985 Å

Table S8 Frequency obtained from optimized structure of metal complexes

Complex with Fe^{3+}

mode	Frequency	Infrared
1	10.1	0.8707
2	11.35	1.1781
3	11.93	0.6132
4	12.57	1.2206
5	14.35	0.7654
6	18.21	0.3851
7	20.68	0.1766
8	24.08	0.222
9	26.75	0.4449
10	28.03	0.3643
11	29.69	0.1941
12	32.59	1.4269
13	36.86	0.3664
14	37.44	0.2591
15	40.35	1.1593
16	41.97	0.8567
17	44.18	0.9209
18	45.59	1.1428
19	49.38	1.3195
20	51.56	1.9588
21	51.98	1.0818
22	56.4	1.1782
23	62.65	0.639
24	64.26	3.5256
25	67.43	0.438
26	70.58	0.8748
27	75.35	1.3327
28	76.85	7.3099
29	78.7	4.9822
30	83.36	0.505
31	85.87	4.4235
32	86.22	0.3988
33	88.95	2.7481
34	91.42	0.493
35	94.81	2.9933
36	96	4.9112
37	98.93	5.8826
38	102.19	3.8298
39	105	1.6424
40	107.57	1.6877
41	108.09	1.7214
42	113.41	5.0856
43	115.01	1.2534
44	122.64	3.0598
45	125.17	16.9995

Complex with Fe^{2+}

mode	Frequency	Infrared
1	7.84	0.0965
2	9.51	0.318
3	12.02	0.0347
4	13.73	0.0984
5	16.74	0.2075
6	21.25	0.1215
7	24.91	2.8461
8	26.27	0.1505
9	27.31	0.2683
10	31.15	0.1095
11	33.42	0.7122
12	38.77	1.3922
13	39.52	1.9358
14	41.43	0.3789
15	44.25	1.5041
16	47.41	0.6637
17	48.89	0.3525
18	50.36	0.6466
19	51.29	0.1113
20	51.98	0.6323
21	55.21	0.4176
22	59.1	1.5541
23	60.37	4.0012
24	61.44	3.2705
25	67.33	2.7729
26	69.48	1.4164
27	70.95	8.4162
28	73.67	2.1929
29	76.72	5.8789
30	79.2	5.349
31	82.81	6.9382
32	84.57	6.0157
33	87.18	3.9834
34	91.68	1.7975
35	94	5.663
36	97.59	1.0897
37	98.29	0.4195
38	102.38	5.4674
39	103.98	1.77
40	105.5	1.2201
41	108.24	6.8543
42	108.78	1.5577
43	113.97	1.9517
44	116.99	2.4713
45	118.54	3.2417

Complex with Cu^{2+}

mode	Frequency	Infrared
1	6.59	0.025
2	8.9	1.0163
3	11.34	0.8265
4	13.24	0.5501
5	15.65	0.2525
6	20	0.2379
7	21.05	0.9178
8	24.48	0.5716
9	26.56	3.297
10	30.19	0.1673
11	32.6	0.581
12	34.58	1.7005
13	40	0.8019
14	41.41	0.6336
15	42.05	0.2882
16	44.8	1.875
17	47.72	0.6822
18	52.03	2.7065
19	54.69	0.7362
20	55.82	4.2013
21	57.77	2.8068
22	60.86	1.6496
23	62.97	1.1608
24	66.52	1.6424
25	70	2.8201
26	72.38	1.3292
27	74.17	0.5416
28	76.68	1.2058
29	79.83	3.7481
30	83.48	3.2375
31	87.75	0.5476
32	88.76	0.227
33	91.57	2.1914
34	92.85	0.9417
35	93.8	2.5442
36	96.31	1.3523
37	99.57	1.5617
38	100.7	0.5363
39	103.77	3.6012
40	105.97	5.2424
41	108.7	3.3682
42	111.02	3.8758
43	115.17	0.9644
44	117.78	3.324
45	118.34	2.7729

46	127.87	0.7874
47	130.63	2.637
48	133.62	8.1003
49	139.39	1.9372
50	142.56	3.1327
51	147.66	0.9219
52	151.65	7.1672
53	154.2	1.4557
54	156.3	1.2707
55	163.71	0.9827
56	167.06	8.0597
57	171.41	31.6823
58	176.63	3.398
59	185.05	4.0773
60	187.86	6.1845
61	188.79	1.767
62	190.72	0.8759
63	198.84	1.9895
64	202.28	3.3852
65	212.89	24.0766
66	214.82	5.2585
67	215.66	7.6932
68	219.17	1.5359
69	222.02	17.0572
70	223.25	13.8884
71	226.03	10.8551
72	236.09	7.0804
73	236.69	2.8749
74	240.89	49.174
75	249.61	9.5434
76	253.04	2.3856
77	258.6	13.8564
78	268.5	1.2715
79	273.59	11.6471
80	280.95	2.3153
81	293.79	3.4338
82	299.55	10.5768
83	300.87	2.8913
84	305.57	9.6133
85	308.7	9.3962
86	322.57	5.2238
87	328.9	2.1009
88	330.93	15.3912
89	335.08	17.4126
90	340.47	13.2369
91	344.17	4.4817
92	352.7	6.7694

46	121.62	2.9424
47	122.92	3.9933
48	127.3	8.4641
49	134.22	1.865
50	136.46	0.6122
51	150.41	5.4122
52	156.93	2.6086
53	159.69	1.7245
54	161.69	0.8753
55	165.8	3.9929
56	169.8	3.1023
57	178.52	2.1381
58	179.6	7.108
59	187.94	0.5991
60	188.14	1.2554
61	188.85	3.2542
62	194.45	0.2698
63	196.37	16.2884
64	201.22	7.1454
65	205.09	3.2579
66	208.32	24.3157
67	210.32	46.255
68	217.26	5.9646
69	220.18	16.8044
70	224.08	0.5442
71	226.65	0.2548
72	229.26	5.7369
73	234.15	35.0323
74	236.62	1.2279
75	237.66	8.5835
76	239.84	5.3788
77	250.54	22.7278
78	254.63	11.7056
79	257.47	2.1829
80	265.6	8.2009
81	269.74	8.1979
82	283.38	11.316
83	287.42	9.0942
84	297.11	2.6487
85	301.25	1.1202
86	304.21	2.1019
87	310.61	3.4565
88	319.47	8.1628
89	326.04	9.8286
90	333.69	9.1777
91	344.97	3.992
92	347.98	19.5471

46	120.14	1.5385
47	121.93	2.0047
48	128.6	11.5598
49	129.28	4.5435
50	132.71	3.0828
51	138.73	7.2197
52	142.28	1.2966
53	147.64	2.3933
54	149.56	2.0988
55	155.31	0.1431
56	157.94	2.6364
57	163.82	4.9732
58	173.44	2.468
59	176.47	0.6821
60	177.11	0.8361
61	181.52	3.3436
62	186.34	4.5827
63	188.03	2.1699
64	194.11	4.3502
65	199.56	21.8256
66	208.66	7.1603
67	210.51	13.8952
68	215.11	34.5804
69	216.35	19.6579
70	220.32	5.1905
71	222.27	1.5609
72	225.49	6.6798
73	231.99	10.7948
74	237.55	12.5635
75	239.76	23.9499
76	242.57	19.5741
77	251.33	16.554
78	252.26	3.1799
79	254	9.1218
80	255.56	8.9544
81	265.72	6.424
82	272.29	29.8063
83	283.83	3.6545
84	287.21	6.025
85	290.3	6.7357
86	296.18	5.3987
87	306.14	3.1791
88	308.11	1.5625
89	320.32	0.8384
90	335.22	14.3466
91	338.36	9.6957
92	349.93	0.368

93	355.2	5.9329
94	359.62	7.5891
95	365.69	9.2208
96	367.07	3.5555
97	370.35	11.9001
98	376.39	4.734
99	377.44	7.7471
100	396.41	36.6308
101	414.08	5.1666
102	418.68	8.1054
103	432	28.7438
104	448.47	1.2611
105	457.59	11.579
106	462.74	11.7571
107	465.64	12.1633
108	468.16	6.3311
109	488.24	7.3184
110	493.9	13.8087
111	500.48	16.2208
112	511.66	41.7024
113	539.5	203.8848
114	545.15	19.9437
115	549.07	13.5879
116	557.43	18.795
117	580.82	36.1245
118	589.96	9.9018
119	591.22	6.6553
120	599.51	34.935
121	614.24	20.0477
122	618.26	25.1578
123	623.33	43.4823
124	627.57	216.0075
125	664.92	90.2726
126	676.87	139.9963
127	698.59	171.5591
128	702.62	140.5684
129	709.1	23.9966
130	738.81	10.544
131	745.42	97.9579
132	764.12	112.1345
133	783.57	8.4016
134	803.21	73.2468
135	804.68	0.4563
136	806.9	9.2472
137	811.22	39.1625
138	813.63	1.4056
139	816.74	23.429

93	350.88	10.9913
94	355.23	5.2465
95	359.48	4.7911
96	364.96	7.5776
97	375.1	4.3991
98	381.56	1.5693
99	399	5.0007
100	402.33	1.7367
101	402.55	17.1293
102	420.49	11.4517
103	426.82	19.0578
104	442.35	10.0748
105	451.53	7.6938
106	456.2	19.1544
107	457.56	2.0859
108	481.19	6.227
109	491.93	14.1129
110	492.19	8.2665
111	513.11	19.3285
112	516.36	1.3231
113	530.41	20.2358
114	533.98	33.4434
115	541.67	0.5078
116	550.17	22.4778
117	552.15	14.4864
118	561.43	24.3007
119	574.49	3.218
120	591.4	13.5282
121	599.77	215.3951
122	618.54	224.2152
123	619.64	20.489
124	640.53	32.884
125	663.05	6.3256
126	678.95	146.0801
127	690.01	312.9214
128	694.8	12.3248
129	706.33	66.7656
130	738.05	25.8459
131	757.99	4.8973
132	767.9	88.7327
133	784.44	13.685
134	794.57	34.5617
135	799.01	1.6578
136	801.26	2.6698
137	814.43	3.9083
138	815.52	5.4819
139	822.08	31.6815

93	352.22	9.6648
94	354.09	4.3709
95	356.17	5.3778
96	362.35	1.5515
97	377.39	3.0802
98	381.23	33.7098
99	389.39	9.0103
100	397.19	7.8133
101	402.93	5.7394
102	408.42	8.6339
103	420.2	6.5684
104	427.18	18.9613
105	439.49	8.7608
106	441.59	2.6534
107	451.34	14.7667
108	455.42	6.0823
109	466.83	20.9392
110	483.17	6.5039
111	489.36	21.409
112	493.81	6.0223
113	506.68	21.7151
114	514.46	14.0686
115	521.23	102.9787
116	543.94	20.9561
117	547.05	34.2771
118	551.04	18.0551
119	556.78	15.753
120	585.95	11.0182
121	591.39	13.2949
122	597.92	208.243
123	611.88	17.5935
124	616.05	236.5343
125	621.36	20.0582
126	625.92	6.0859
127	665.63	8.567
128	678.3	131.8321
129	707.98	219.8672
130	725.91	260.4514
131	734.24	17.9488
132	765.01	11.5752
133	776.38	161.5977
134	783.07	7.5153
135	794.13	31.5794
136	795.78	20.7449
137	801.75	2.8996
138	804.77	15.0498
139	813.83	1.4308

140	823.64	3.9138
141	834.58	3.4969
142	837.28	59.8451
143	847.33	12.2965
144	847.95	3.9648
145	854.73	41.9029
146	869.39	4.9956
147	876.35	33.0194
148	893.31	2.4294
149	895.03	53.093
150	897.02	28.5687
151	898.92	89.5063
152	900.81	53.3558
153	914.21	57.7223
154	919.68	151.1972
155	922.14	136.1231
156	924.57	120.5723
157	936.45	117.2044
158	943.06	14.0934
159	945.1	8.1213
160	955.27	13.2722
161	960.88	84.1017
162	964.02	7.9397
163	973	0.3186
164	975.94	10.2893
165	980.83	16.2176
166	988.78	96.3557
167	1025.41	1.3861
168	1030.83	81.6362
169	1039.13	8.9059
170	1042.44	67.0184
171	1049.51	167.4796
172	1051.46	15.6728
173	1053.59	98.4787
174	1062.31	6.7212
175	1065.59	112.1188
176	1068.8	10.5049
177	1070.52	58.5015
178	1073.59	28.375
179	1075.61	13.8847
180	1081.31	14.152
181	1086.96	49.8658
182	1087.01	87.1583
183	1091.94	164.694
184	1093.87	112.7976
185	1093.95	3.0484
186	1102.04	34.465

140	825.88	3.3445
141	834.92	4.9915
142	842.91	111.5878
143	846.47	13.9328
144	864.18	21.2417
145	870.53	3.69
146	876.97	3.9535
147	881.65	17.2268
148	885.38	16.7468
149	890.91	44.622
150	891.07	3.4476
151	891.44	14.219
152	907.77	70.7507
153	915.5	34.1017
154	920.62	34.4079
155	927.07	33.0198
156	932.01	32.5884
157	944.31	4.247
158	959.37	5.5645
159	965.2	2.5434
160	966.84	106.4525
161	971.23	0.8719
162	973.67	22.3293
163	979.8	18.9945
164	980.14	26.3355
165	1006.05	28.4111
166	1016.51	33.6659
167	1017.41	52.8144
168	1026.32	82.3763
169	1027.64	29.9733
170	1030.98	11.0707
171	1037.97	2.4455
172	1054.78	47.0767
173	1055.75	109.2302
174	1059.45	131.0069
175	1062.69	21.3351
176	1065.78	17.5274
177	1066.58	29.9582
178	1076.36	29.9616
179	1077.79	70.1462
180	1078.93	122.1112
181	1079.8	200.6818
182	1080.27	46.2613
183	1081.36	90.0406
184	1087.03	79.5717
185	1087.16	26.7645
186	1092.97	36.2509

140	816.15	8.4177
141	829.61	0.5405
142	833.42	4.1691
143	842.88	8.2764
144	851.49	95.5726
145	855.38	37.7083
146	868.77	5.8437
147	871.46	28.6267
148	874.56	33.5055
149	877.38	5.1636
150	889.48	1.0286
151	891.64	41.7733
152	893.86	24.1173
153	899.55	22.7434
154	905.24	46.9756
155	913.12	25.3641
156	917.28	33.1628
157	930.33	80.4948
158	934.56	43.0729
159	958.21	0.1916
160	962.4	2.2189
161	966.16	3.799
162	970.75	29.9388
163	970.93	9.3125
164	971.62	42.9947
165	979.7	18.4733
166	980.33	15.2104
167	987.38	104.5583
168	1020.97	70.8114
169	1023.33	56.454
170	1030.06	64.9199
171	1031.59	5.6585
172	1037.76	3.1989
173	1054.46	27.2955
174	1054.57	217.3488
175	1062.32	42.5483
176	1063.72	64.3256
177	1065.12	22.7259
178	1067.86	43.1006
179	1068.95	48.0825
180	1070.42	84.7403
181	1074.35	61.0078
182	1082.44	13.9756
183	1082.71	160.3595
184	1086.56	3.1106
185	1089.52	20.2105
186	1092.01	4.0391

187	1104.99	7.7793
188	1105.61	1.5712
189	1108.86	31.6021
190	1111.54	131.0904
191	1112.45	7.38
192	1113.62	116.9445
193	1113.75	73.6349
194	1116.75	80.9145
195	1118.69	41.4652
196	1126.71	30.1413
197	1128.25	50.7485
198	1133.04	90.7844
199	1133.6	16.6617
200	1137.71	32.0741
201	1142.56	22.6222
202	1143.31	52.0452
203	1144.27	101.4214
204	1145.85	9.434
205	1150.42	12.628
206	1150.87	14.9687
207	1154.89	1.1595
208	1155.15	7.2582
209	1155.87	7.4758
210	1162.09	7.7701
211	1167.41	13.343
212	1167.61	22.0452
213	1175.58	40.1477
214	1179.19	3.2759
215	1184.52	61.6206
216	1195.8	11.9375
217	1197.33	6.7607
218	1198.2	21.6712
219	1202.5	15.6649
220	1210.8	2.9452
221	1220.8	66.2398
222	1239.07	3.1743
223	1244.64	0.3744
224	1245.82	40.993
225	1250.34	20.4541
226	1251.52	171.5823
227	1251.79	169.7398
228	1254.93	31.0768
229	1257.56	8.1531
230	1260.38	8.5807
231	1271.57	14.8796
232	1277.92	13.7468
233	1278.43	8.7257

187	1093.82	65.8912
188	1094.28	6.8632
189	1101.4	26.7076
190	1103.68	11.2686
191	1107.85	2.4203
192	1110	63.3892
193	1110.99	51.4955
194	1116.18	66.1202
195	1117.36	6.2868
196	1120.75	12.8912
197	1128.02	96.8748
198	1129.86	8.7026
199	1135.76	71.0937
200	1140.36	70.3325
201	1143.2	7.6455
202	1143.61	14.2412
203	1144.94	39.6073
204	1146.71	15.6655
205	1147.99	4.7895
206	1149.88	58.4567
207	1152.48	31.5824
208	1157.91	35.9186
209	1158.4	4.4007
210	1161.57	29.1138
211	1163.16	3.0656
212	1165.88	131.9537
213	1170.18	18.6099
214	1171.46	29.6412
215	1181.67	20.1604
216	1184.95	51.3728
217	1194.39	13.8003
218	1196.56	6.2821
219	1197.88	14.8183
220	1198.72	1.5156
221	1203.66	3.7897
222	1212.98	25.591
223	1226.85	1.0198
224	1240.64	8.4021
225	1241.46	5.7744
226	1244.36	74.7816
227	1245.69	6.2986
228	1256.25	21.7472
229	1258.88	2.8603
230	1260.61	1.2093
231	1265.37	5.1865
232	1265.52	11.4371
233	1269.13	60.5815

187	1093.62	12.4304
188	1099.83	20.5652
189	1102.24	28.4451
190	1102.97	23.1486
191	1103.9	85.7641
192	1106.18	2.5214
193	1106.76	26.3976
194	1111.21	71.0252
195	1116.19	75.3577
196	1116.81	11.656
197	1121.59	93.9638
198	1127.34	26.7281
199	1128.28	91.6584
200	1132.39	60.8781
201	1139.63	56.3942
202	1142.3	29.4903
203	1145.72	5.1496
204	1146.86	21.9152
205	1148.39	7.4305
206	1149.67	11.8774
207	1150.03	15.3312
208	1155.23	38.4568
209	1156.95	0.3335
210	1160.48	0.5361
211	1163.27	10.0488
212	1164.49	1.7197
213	1167.03	20.0793
214	1173.78	11.297
215	1180.31	6.9845
216	1184.44	51.0697
217	1194.54	3.2715
218	1195.45	8.827
219	1198.09	18.3657
220	1202.42	14.1245
221	1204.96	16.0296
222	1214.39	1.1668
223	1236.88	0.5742
224	1237.3	11.4554
225	1243.18	16.6674
226	1246.06	15.4666
227	1249.7	111.4525
228	1255.44	70.5992
229	1255.72	44.9658
230	1257.62	313.3313
231	1262.3	2.9008
232	1276.36	5.8266
233	1276.49	19.4029

234	1282.4	12.1443
235	1291.86	106.3471
236	1293.06	64.1659
237	1294.26	4.2421
238	1299.92	2.7691
239	1301.94	138.279
240	1308.74	25.2869
241	1314.18	8.2709
242	1314.53	11.5409
243	1316.66	1.1005
244	1317.2	11.9441
245	1318.8	5.5134
246	1321.34	1.9414
247	1325.44	4.7705
248	1340.78	5.5692
249	1342.15	5.068
250	1343.79	3.4292
251	1348.87	52.8289
252	1349.47	4.7121
253	1355.68	1.3945
254	1363.31	22.2907
255	1366.48	51.81
256	1367.52	23.4546
257	1369.8	35.7842
258	1372.33	25.1318
259	1376.24	48.1614
260	1377.43	23.1161
261	1378.93	83.1304
262	1383.63	4.1829
263	1387.03	19.8021
264	1391.06	15.4247
265	1394.58	4.2831
266	1394.87	34.1767
267	1397.9	2.6112
268	1415.2	12.4359
269	1416.07	0.84
270	1418.09	1.7134
271	1423	1.5461
272	1424.12	2.8883
273	1424.5	5.223
274	1426.04	12.0012
275	1426.46	1.291
276	1426.48	8.5197
277	1427.31	18.254
278	1427.79	26.2114
279	1437.15	3.4364
280	1439.01	0.3065

234	1274.3	5.3584
235	1276.27	21.6642
236	1280.27	153.4446
237	1281.53	28.9334
238	1289.51	10.9406
239	1292.39	278.2128
240	1298.14	14.6268
241	1309.64	38.3525
242	1313.19	11.9778
243	1313.66	8.4834
244	1319.93	1.2763
245	1323.32	4.3305
246	1327.92	6.425
247	1329.18	9.3995
248	1332.42	12.0255
249	1335.41	5.5805
250	1337.75	13.4382
251	1340.69	1.9494
252	1341.14	3.6317
253	1349.39	8.646
254	1352.49	3.6779
255	1356.1	11.8918
256	1361.74	13.2736
257	1364.91	29.2694
258	1369.23	8.2216
259	1370.91	8.2829
260	1372.9	6.2239
261	1376.71	19.3653
262	1378.77	125.9771
263	1382.61	4.4573
264	1388.8	45.933
265	1393.01	35.2278
266	1393.66	9.7909
267	1397.12	2.7623
268	1399.03	10.4759
269	1400.2	10.1111
270	1402.84	3.9642
271	1407.25	1.8098
272	1414.57	2.987
273	1416.52	0.8908
274	1418.2	8.3068
275	1421.52	46.827
276	1425	3.3975
277	1426.59	4.774
278	1429.74	40.2356
279	1430.17	1.0801
280	1430.39	2.5226

234	1277.88	5.7486
235	1279.77	1.9534
236	1281.41	24.7677
237	1285.13	17.7017
238	1288.72	70.2311
239	1290.03	17.4168
240	1297.33	3.2334
241	1298.41	19.3832
242	1307.46	1.435
243	1315.29	13.1056
244	1320.5	12.19
245	1320.61	6.0066
246	1321.24	2.0985
247	1326.93	3.5593
248	1328.11	32.6636
249	1340.08	0.6057
250	1342.39	7.287
251	1343.68	74.5681
252	1349.85	11.9514
253	1350.23	13.0521
254	1352.27	0.5111
255	1353.96	12.736
256	1362.85	6.9013
257	1364.3	7.8273
258	1368.74	12.2879
259	1372.32	8.2429
260	1376.03	14.1872
261	1379.14	6.9288
262	1381.61	17.5871
263	1384.2	10.2715
264	1387.7	42.3554
265	1390.88	31.9343
266	1394.94	4.296
267	1395.47	3.9773
268	1395.85	19.8677
269	1400.52	4.9056
270	1408.18	5.5359
271	1409.07	6.5709
272	1413.98	0.6931
273	1414.69	3.933
274	1416.69	1.1381
275	1418.37	2.8456
276	1426.14	2.2857
277	1426.66	10.2235
278	1429.94	2.7725
279	1431.62	1.5037
280	1435.99	9.0073

281	1456.46	0.3379
282	1459.04	25.0095
283	1481.34	0.9787
284	1481.49	1.5667
285	1483.05	2.6066
286	1484.54	4.8269
287	1487.19	23.5537
288	1487.62	10.5578
289	1489.59	10.1477
290	1496.59	19.1501
291	1499.72	26.907
292	1500.45	16.2089
293	1502.35	10.4877
294	1504.27	24.5338
295	1504.44	12.7535
296	1505.11	8.7554
297	1505.98	11.9526
298	1506.1	14.2305
299	1507.51	20.4663
300	1509.68	2.3373
301	1510.93	17.9939
302	1511.65	14.7547
303	1513.08	20.9063
304	1513.82	15.3549
305	1514.49	1.895
306	1514.58	12.8503
307	1516.27	2.4869
308	1517.6	16.5703
309	1519.51	2.8834
310	1519.87	13.8767
311	1521.22	15.3901
312	1522.21	4.031
313	1523.77	15.9944
314	1524.43	9.4044
315	1525.43	10.7461
316	1529.78	48.0776
317	1530.52	3.0342
318	1531.28	24.0884
319	1532.7	32.151
320	1532.97	14.0535
321	1534.56	13.6701
322	1535.07	10.9259
323	1535.3	3.2243
324	1536.4	6.2936
325	1540.5	3.0031
326	1541.75	0.3141
327	1545.23	5.375

281	1434.19	5.1755
282	1437.74	0.2308
283	1452.18	0.0447
284	1456.42	20.4931
285	1478.35	23.8612
286	1481.41	1.6463
287	1484.93	2.8851
288	1484.97	0.1518
289	1486.79	0.729
290	1488.54	2.1557
291	1491.63	11.8841
292	1493.06	19.5049
293	1496.02	18.4753
294	1501.28	10.3888
295	1502.2	7.6578
296	1505.86	4.2788
297	1506.05	15.764
298	1506.22	11.5553
299	1507.91	6.3539
300	1508	13.1083
301	1509.02	6.0973
302	1509.04	23.8051
303	1510.26	7.3477
304	1511.39	6.967
305	1511.53	7.9537
306	1514.01	9.9841
307	1514.83	2.8117
308	1516.98	6.073
309	1517.19	0.0118
310	1517.39	14.831
311	1521.06	6.7655
312	1521.25	26.9129
313	1521.43	7.307
314	1522.9	0.8479
315	1525.34	3.3493
316	1525.55	20.2446
317	1525.82	1.4964
318	1528.9	14.0272
319	1529.05	2.4448
320	1530.91	8.3833
321	1532.35	20.0251
322	1533.21	4.8512
323	1535.11	16.3686
324	1536.2	1.7169
325	1537.25	1.9908
326	1539.26	2.8699
327	1539.94	52.8248

281	1437.58	20.749
282	1438.9	0.2564
283	1451.38	3.6894
284	1452.43	0.1407
285	1471.98	79.1211
286	1481.56	2.8557
287	1481.83	1.5538
288	1483.92	0.4131
289	1484.44	1.0711
290	1488.21	27.8292
291	1489.52	10.7505
292	1494.57	18.2166
293	1496	19.7168
294	1497.86	9.3909
295	1498.69	0.1922
296	1503.94	11.0643
297	1504.59	8.8855
298	1505.43	13.8169
299	1507.51	6.5056
300	1508.69	4.0451
301	1510.59	7.0482
302	1510.94	13.0564
303	1511.23	2.235
304	1512.66	11.2596
305	1513.01	10.1423
306	1514.08	3.7197
307	1515.4	20.3065
308	1515.65	11.1099
309	1515.73	13.5488
310	1516.16	4.2717
311	1518.35	8.1381
312	1518.82	8.0384
313	1520.72	11.8222
314	1521.31	21.9046
315	1522.99	16.5397
316	1524.79	4.769
317	1525.13	7.5113
318	1527.98	0.9877
319	1529.76	6.7669
320	1531.86	16.1595
321	1531.9	13.5195
322	1532.62	10.9118
323	1535.28	16.1121
324	1535.69	8.479
325	1537.43	1.8656
326	1537.57	9.7448
327	1537.84	1.6487

328	1616.38	522.182
329	1646	316.919
330	1680.5	41.7296
331	1682.74	46.4047
332	1685.26	46.7422
333	1715.88	368.7997
334	2920.23	121.7831
335	2945.31	11.4167
336	2947.71	121.11
337	2952.66	20.738
338	2963.36	272.0273
339	2969.14	67.66
340	2978.11	29.1575
341	2985.01	96.831
342	2987.47	88.04
343	2989.99	119.1183
344	2993.62	86.2037
345	2994.49	37.3309
346	2996.22	40.2164
347	3004.5	62.0933
348	3005.77	101.8378
349	3009.25	56.1707
350	3016.22	75.4214
351	3019.61	53.0372
352	3021.09	14.2122
353	3024.28	54.6588
354	3026.21	94.4765
355	3030.62	107.7009
356	3030.84	77.0591
357	3035.46	21.9813
358	3037.98	47.856
359	3040.81	43.891
360	3045.57	37.7108
361	3049.92	13.4731
362	3054.6	140.6907
363	3055.5	0.055
364	3056.87	104.0665
365	3059.67	54.4218
366	3066.72	8.5384
367	3068.3	50.5021
368	3069.03	19.438
369	3071.65	75.4161
370	3073.18	28.5043
371	3074.47	48.7799
372	3077.42	54.071
373	3077.7	40.024
374	3078.09	58.8715

328	1540.03	10.8462
329	1545.01	4.2934
330	1627.96	254.2813
331	1630.89	508.08
332	1684.24	46.464
333	1684.99	49.978
334	1685.12	40.8781
335	1696.46	369.2727
336	2824.03	1651.777
337	2883.82	126.4844
338	2926.66	133.4716
339	2942.64	48.2226
340	2945.83	18.8332
341	2949.97	110.0774
342	2958.21	40.8392
343	2958.38	76.6577
344	2965.47	256.868
345	2971.64	5.5018
346	2984.41	149.2829
347	2986.25	114.8267
348	2986.92	37.5343
349	2987.22	74.5667
350	2989.95	70.7852
351	3000.44	99.8454
352	3007.08	30.5208
353	3007.16	74.6517
354	3010.31	63.9537
355	3012.48	12.9023
356	3019.45	195.3789
357	3022.38	68.2442
358	3022.75	26.2678
359	3024.26	75.2946
360	3025.01	68.5443
361	3035.7	135.742
362	3037.83	60.0981
363	3044.69	21.231
364	3048.56	50.6969
365	3050.75	69.8852
366	3054.73	4.3732
367	3056.81	125.4468
368	3057.46	88.9511
369	3061.59	1.8591
370	3063.08	10.6729
371	3069.16	3.5457
372	3069.84	488.227
373	3071.78	204.9431
374	3072.65	46.5828

328	1542.59	1.7613
329	1544.91	3.8461
330	1625.43	667.9506
331	1640.34	202.341
332	1685.08	52.1779
333	1685.54	46.8435
334	1686.41	47.5444
335	1717.65	379.325
336	2881.3	120.9346
337	2941.61	41.5925
338	2946.61	28.6757
339	2952.28	131.0256
340	2958.13	46.2187
341	2967.16	247.8888
342	2972.8	31.6662
343	2981.69	21.2367
344	2986.05	82.575
345	2990.6	127.1226
346	2991.66	102.5977
347	2997.03	948.4124
348	2997.19	70.7007
349	2999.58	35.6826
350	3006.92	61.415
351	3011.16	30.9028
352	3016.4	7.6123
353	3017.93	143.9657
354	3018.24	70.2793
355	3020.04	46.35
356	3021.59	92.8454
357	3026.64	84.464
358	3027.23	17.4735
359	3029.72	32.8342
360	3032	64.6665
361	3041.05	53.883
362	3045.43	46.5145
363	3045.97	18.0983
364	3056.8	1.5589
365	3060.93	31.7222
366	3064.2	10.7652
367	3064.39	0.7131
368	3064.56	85.2885
369	3067.23	1.1555
370	3069.07	53.6174
371	3069.89	48.1825
372	3071.14	35.8063
373	3075.79	48.9394
374	3078.32	16.8088

375	3080.27	17.6297
376	3084.83	48.5277
377	3092.25	21.0192
378	3092.48	68.7682
379	3098.03	67.2852
380	3101.03	26.3669
381	3102.94	92.5264
382	3103.26	14.3105
383	3106.12	14.2528
384	3108.14	44.2639
385	3111.71	48.3058
386	3112.71	63.5638
387	3112.82	45.2009
388	3113.05	56.5387
389	3120.13	1.1947
390	3126.03	78.7725
391	3130.04	55.5748
392	3139.83	25.0398
393	3140.28	42.1232
394	3141.3	15.7133
395	3147.64	24.017
396	3150.22	44.8451
397	3158.83	44.2234
398	3160.16	13.7504
399	3161.59	25.7418
400	3170.87	8.3008
401	3172.06	14.2846
402	3193.38	17.5398
403	3202.45	1217.0715
404	3226.34	1040.9263
405	3293.35	396.3794
406	3324.81	711.09
407	3442.73	34.5434
408	3516.79	0.4691
409	3533.11	0.8361
410	3536.32	0.6195
411	3569.22	0.4067
412	3637.75	0.3998
413	3659.77	0.4051
414	3696.51	2.2314

375	3074.62	49.8521
376	3078.46	40.5717
377	3082.84	47.8201
378	3083.68	2.6453
379	3085.49	70.392
380	3086.81	117.6251
381	3091.04	183.827
382	3096.68	107.8143
383	3102.06	20.0686
384	3102.78	26.5784
385	3102.91	12.7857
386	3106.21	30.364
387	3107.25	53.6906
388	3108.13	26.0945
389	3108.77	45.6244
390	3108.8	15.9241
391	3110.62	1051.952
392	3111.39	297.9507
393	3115.65	45.0779
394	3115.8	103.0017
395	3116.53	117.58
396	3125.67	67.0605
397	3128.83	16.7246
398	3129.32	51.7519
399	3135.4	47.279
400	3137.75	7.7953
401	3144.28	23.213
402	3155.84	45.2828
403	3158.16	3.5854
404	3165.51	31.6669
405	3172.62	22.2448
406	3172.93	30.5893
407	3177.34	5.3585
408	3203.37	827.4677
409	3399.17	555.4348
410	3432.41	4.4178
411	3527.68	0.2805
412	3531.34	1.3197
413	3544.12	0.5172
414	3547.77	0.3775
415	3648.38	1.0897
416	3667.68	1.0517
417	3672.61	0.6501

375	3079.49	33.7142
376	3080.53	9.7921
377	3081.36	59.3371
378	3083.65	17.5343
379	3087.2	37.3551
380	3088.18	103.0513
381	3088.9	55.3298
382	3093.52	58.784
383	3095.24	79.1501
384	3096.81	84.2261
385	3097.02	13.2391
386	3099.79	37.6056
387	3100.83	49.1337
388	3102.43	78.5086
389	3104.24	86.6517
390	3105.79	12.5004
391	3109.63	97.9477
392	3111.08	22.7627
393	3121.2	94.9956
394	3125.5	57.8439
395	3130.42	53.6632
396	3132.04	14.5837
397	3136.46	38.4515
398	3145.87	30.0364
399	3153.7	27.7046
400	3156.68	41.4427
401	3165.91	8.0367
402	3166.57	31.4017
403	3174.97	17.6816
404	3185.72	0.1869
405	3191.04	21.8616
406	3264.76	729.4376
407	3324.53	416.1137
408	3429.24	358.9994
409	3432.11	666.582
410	3446.98	9.5897
411	3516.51	0.1696
412	3531.53	1.3006
413	3545.68	0.479
414	3550.17	0.1827
415	3635.01	0.8314
416	3669.25	1.2199
417	3675.24	1.0196

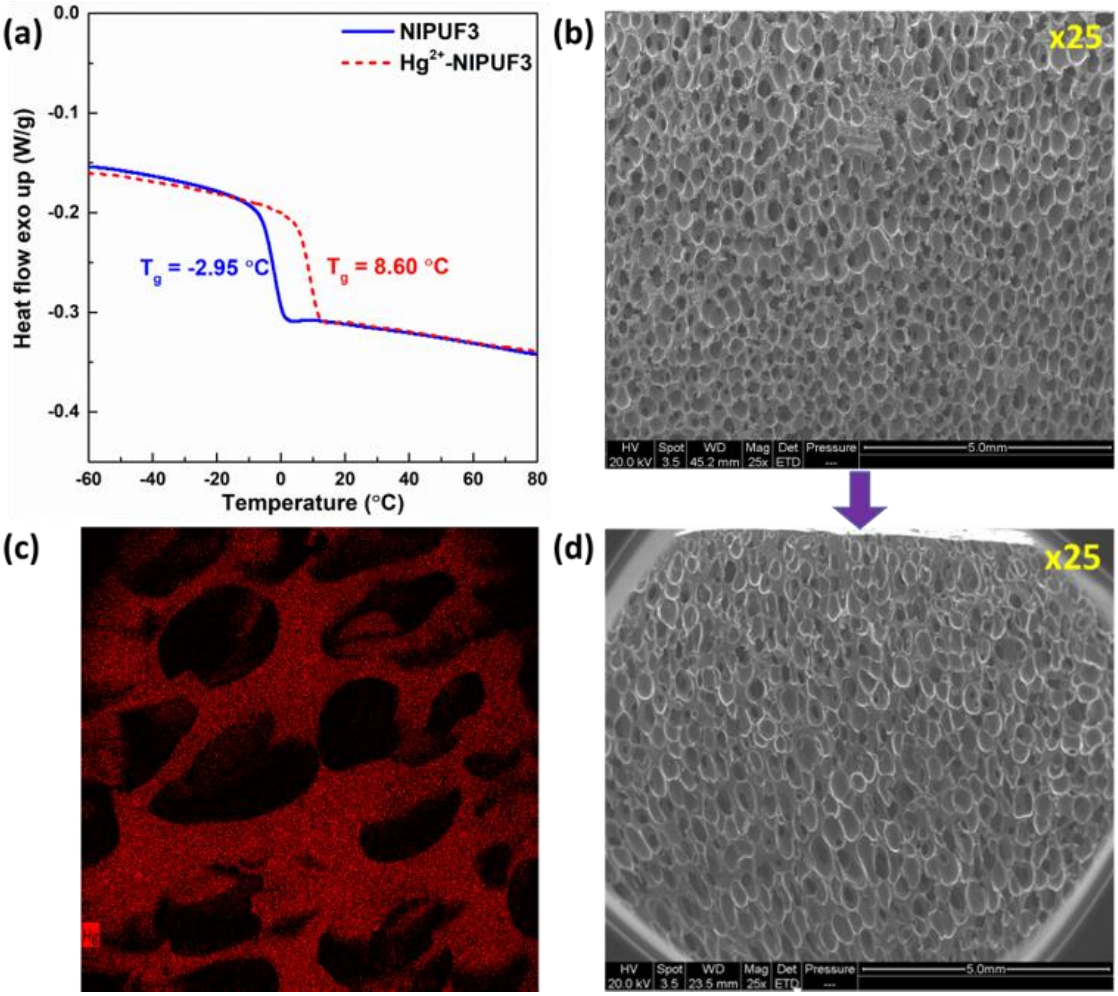

Figure S48. (a) DSC plots of **NIPUF3** and Hg(II)-**NIPUF3**; SEM photomicrographs of (b) **NIPUF3** and (d) Hg(II)-**NIPUF3**; (c) EDX mapping of Hg(II)-**NIPUF3**.

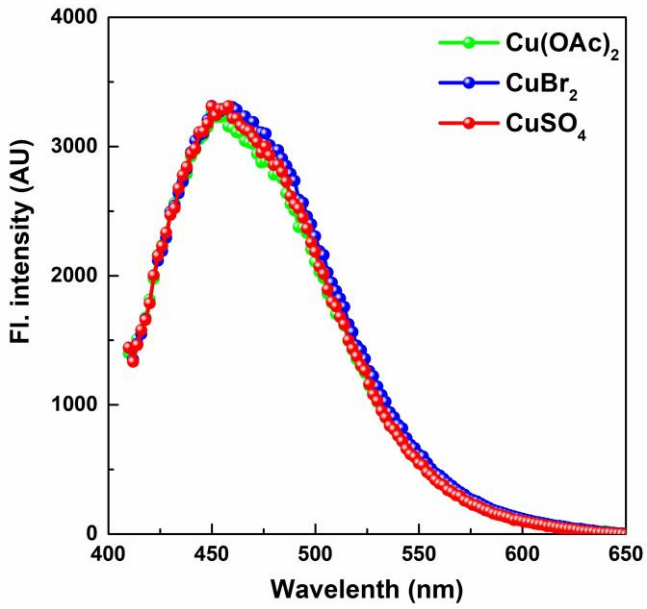

Figure S49. Fluorescence quenching of **NIPUF3** in presence of $Cu(OAc)_2$, $CuBr_2$ and $CuSO_4$ having same metal cation concentration into the foam

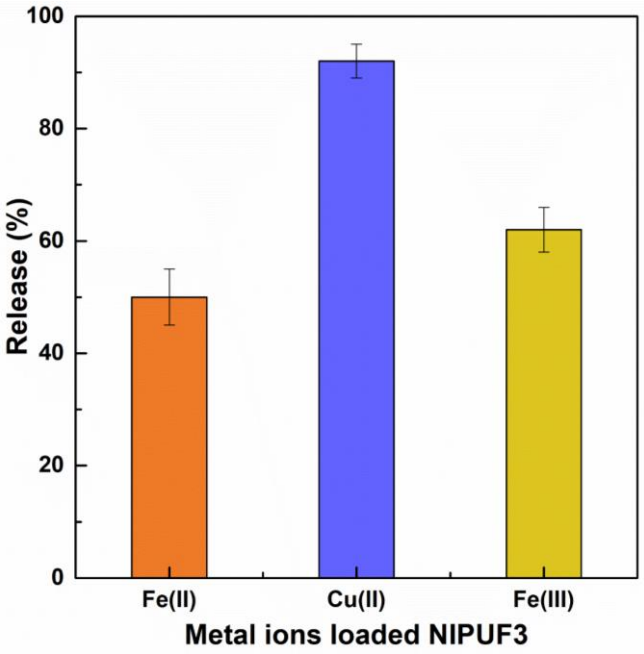

Figure S50. % Release of metal ions at pH = 1.80; It is worth mentioning that the foams still retained their network structure for 24 h dipping the foam there is no change

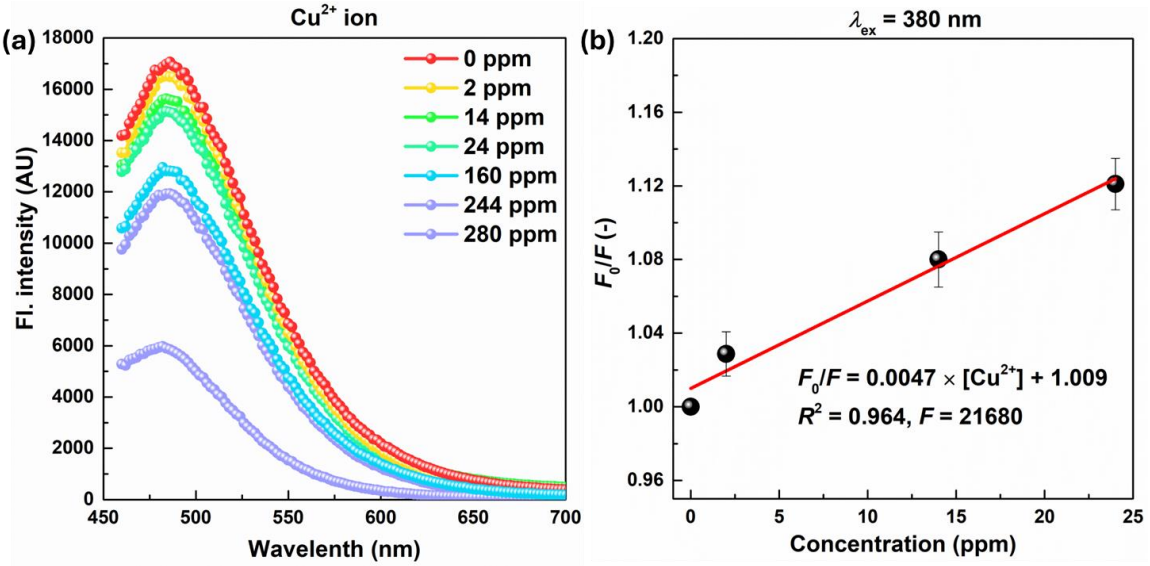

Figure S51. (a) Fluorescence quenching of non-foamed **NIPUF3** with different concentration (2, 14, 24, 244 and 280 ppm) of Cu^{2+} ion and (b) F_0/F plot of non-foamed **NIPUF3** with concentrations of Cu^{2+} ion.

7. Fluorescent sensing of antibiotics

Preparation of tetracycline solutions

Stock solution (100 ml, 1 mM) of tetracycline was prepared by dissolving 48.09 mg of tetracycline hydrochloride in distilled water. Tetracycline solutions of variable concentrations (0.5, 1.0, 5.0, 7.5, 10, 25, 35, 45, 50, 55, 75, 90 and 100 μM) were prepared by exact and subsequent dilution of 1 mM stock solution.

Fluorescence measurement for selectivity test of antibiotics

100 ml antibiotics solutions of 1 mM concentration were prepared via dissolving exact mass of antibiotics (ciprofloxacin, erythromycin, ampicillin sodium salt, bacitracin, kanamycin monosulfate, neomycin sulfate, tetracycline hydrochloride and cephalexin) in distilled water. Then 0.05 g of **NIPUF3** was added to those solutions under constant shaking at 300 rpm for 2 h. After that ,the foam was separated from antibiotics solution and dried at 60 °C for 2 h. The fluorescence intensities of antibiotics loaded **NIPUF3** were then recorded at 516 nm using the spectrofluorometer (Tecan Infinite 200Pro) at λ_{ex} = 380 nm. The UV-star® microplate, 96 well, half area, μclear®, transparent, 10 ST/BTL of Greiner Bio-One GmbH, Germany (REF: 675801) was used as sample holder. The fluorescence spectra were recorded from the bottom of the well with manual gain of 60, number of flashes of 10, integration time of 20 μs, 0 μs of lag time. The excitation and emission slit widths were 10 and 20 nm for source and detector, respectively. All the results were done twice with three replicates.

Fluorescence measurement for quantification of tetracycline

In 25 mL of 0.5, 1.0, 5.0, 7.5, 10, 25, 35, 45, 50, 55, 75, 90 and 100 μM tetracycline solutions, pieces of **NIPUF3** (0.05 g) were added under constant stirring of 300 rpm to reach equilibrium. The contact time depended on the concentration of the antibiotics. To evaluate the optimal contact time of the foam with the solution, we followed the evolution of the fluorescence spectra with time. When no more evolution of the fluorescence spectra was noted, the equilibrium was reached and the optimal contact time was known. A contact time of 6h was here used, where the equilibrium was reached for all the concentrations. The fluorescence of tetracycline loaded **NIPUF3** were recorded with 410–800 nm using the spectrofluorometer (Tecan Infinite 200Pro) using 380 nm of excitation wavelength (λ_{ex}). The UV-star® microplate, 96 well, half area, μclear®, transparent, 10 ST/BTL of Greiner Bio-One GmbH, Germany (REF: 675801) was used as sample holder. The fluorescence spectra were recorded from the bottom of the well with manual gain of 60, number of flashes of 10, integration time of 20 μs, 0 μs of lag time. The excitation and emission slit widths were 10 and 20 nm for source and detector, respectively. All the results were done twice with three replicates.

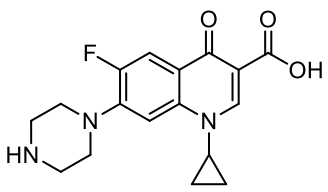

ciprofloxacin

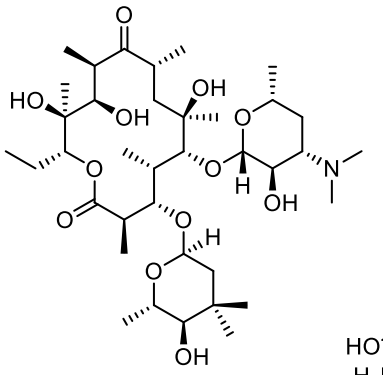

erythromycin

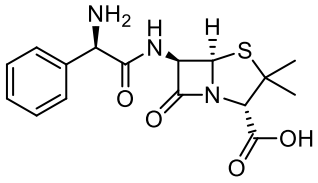

ampicillin

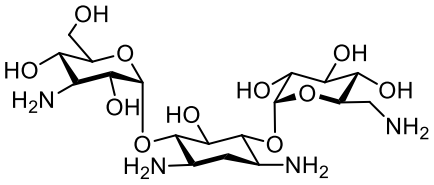

kanamycin

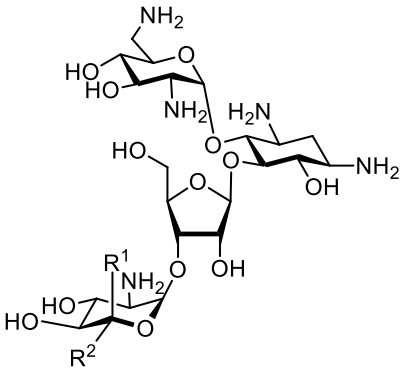

neomycin

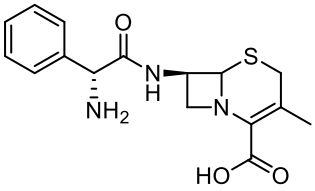

cephalexin

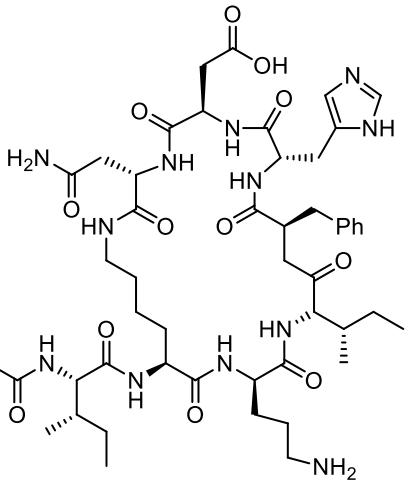

bacitracin

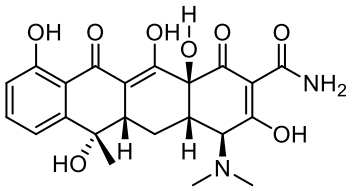

tetracycline

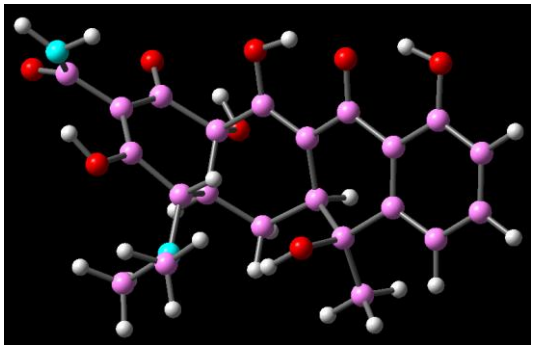

Optimized structure of tetracycline

Scheme S1. Structures of antibiotics: ciprofloxacin, erythromycin, ampicillin, bacitracin, kanamycin, neomycin, cephalexin and tetracycline

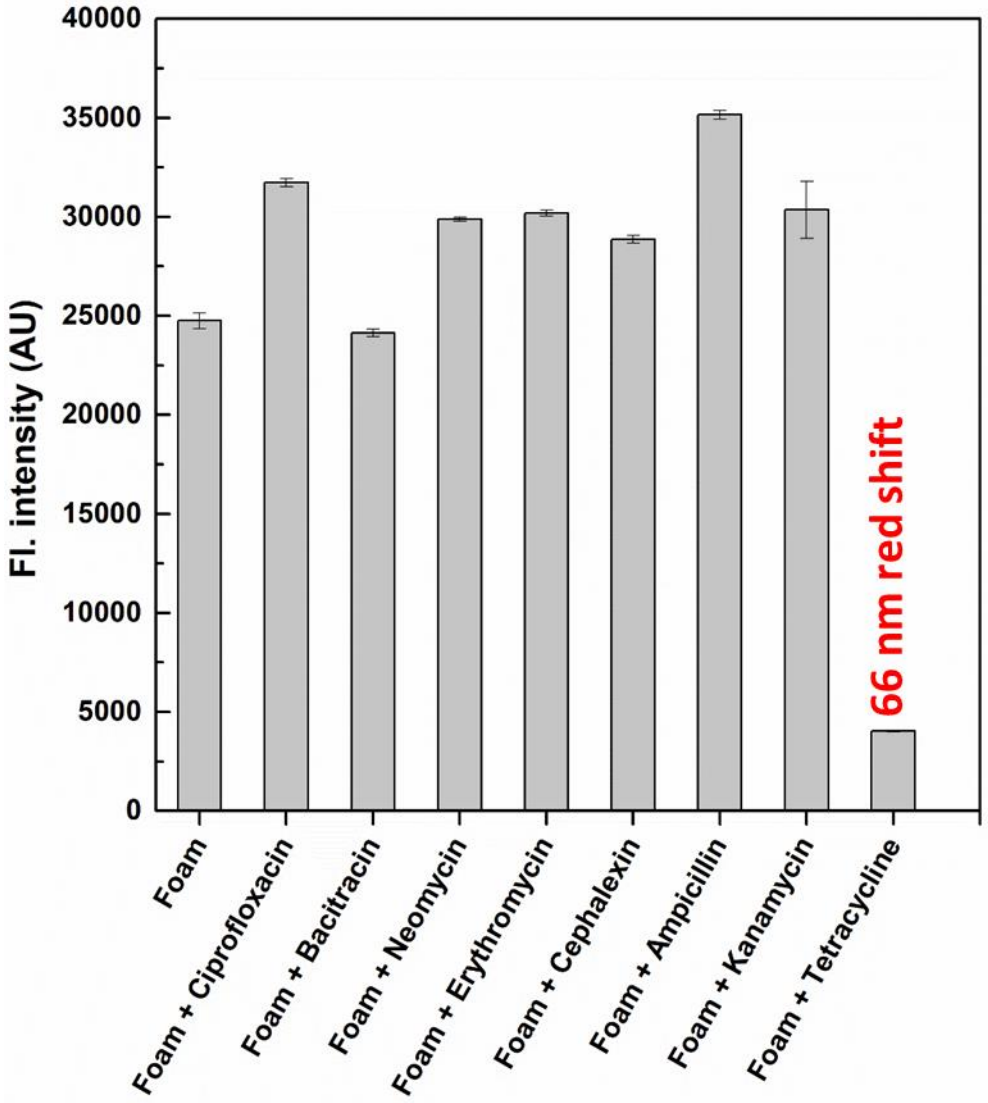

Figure S52. Bar diagram showing fluorescence intensity of control foam (**NIPUF3**) and foam (**NIPUF3**) treated with ciprofloxacin, bacitracin, neomycin, erythromycin, cephalexin, ampicillin, kanamycin and tetracycline (turn-off and 66 nm red shift in emission wavelength)

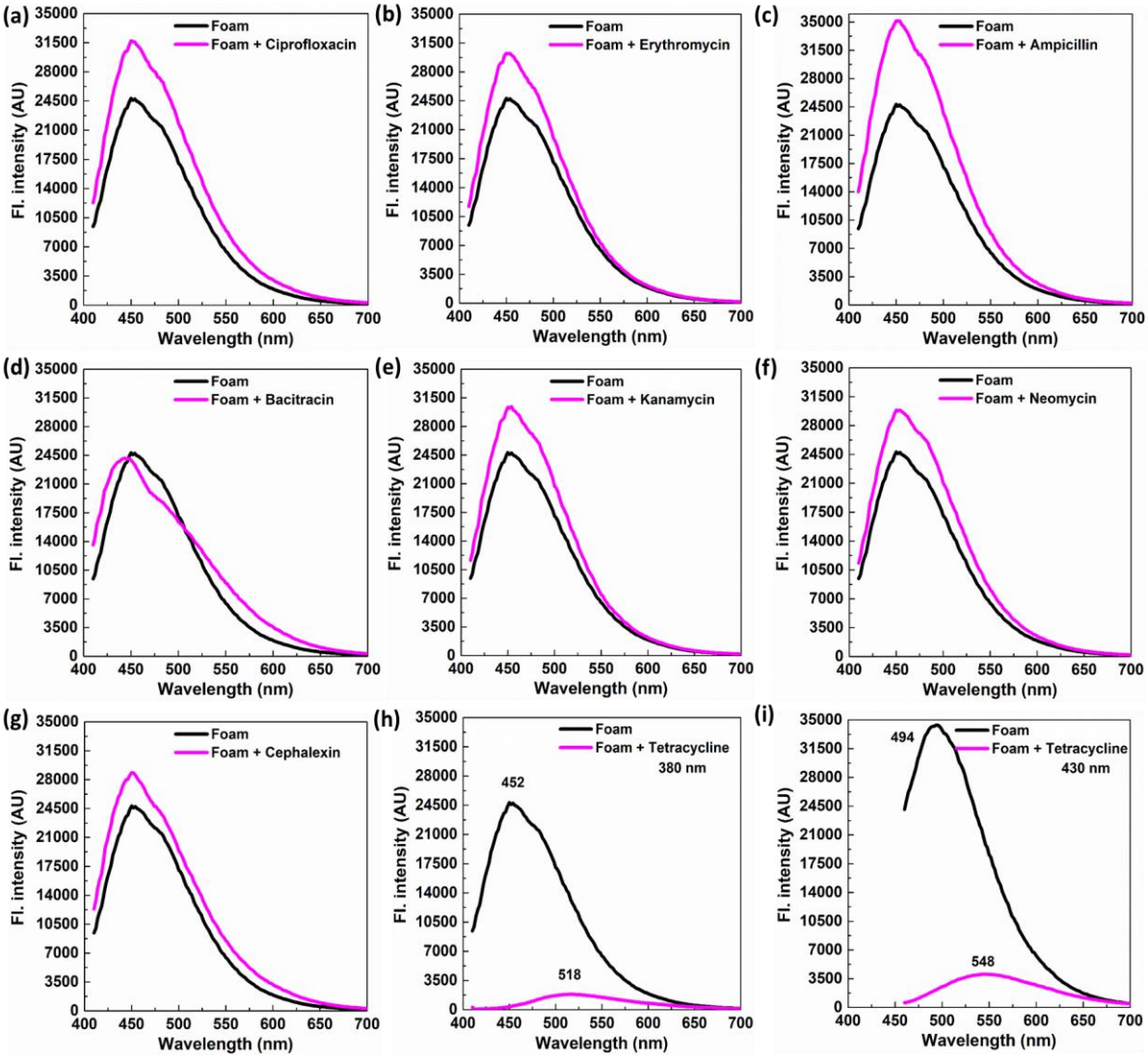

Figure S53. Full scan fluorescence spectra of foam (**NIPUF3**) after interaction with (a) ciprofloxacin, (b) erythromycin, (c) ampicillin, (d) bacitracin, (e) kanamycin, (f) neomycin, (g) cephalexin, (h) tetracycline at 380 nm and (i) tetracycline at 430 nm; for each measurement, foam (**NIPUF3**) was excited at 380 nm, and the full emission spectra were recorded within 410–700 nm using 10 nm and 20 nm bandwidths for excitation (source) and emission (detector), respectively; concentration of antibiotic = 1 mM; each antibiotic solution was prepared in distilled water and used without any further pH modification.

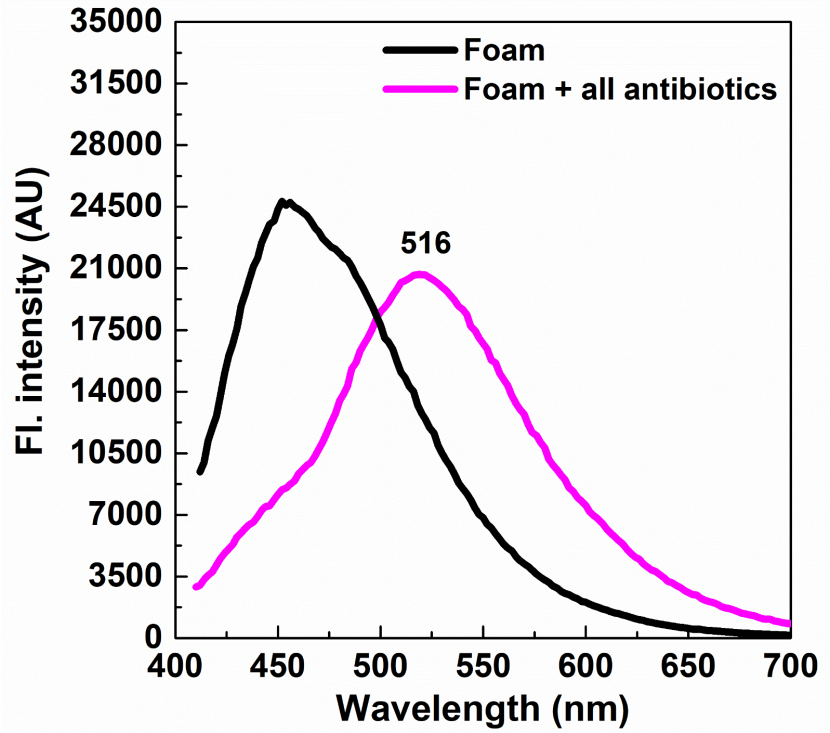

Figure S54. Full scan fluorescence spectra of (black) **NIPUF3** and (red) **NIPUF3** after interaction with mixture of antibiotics containing ciprofloxacin, erythromycin, ampicillin, bacitracin, kanamycin, neomycin, cephalexin, tetracycline; for each measurement, **NIPUF3** was excited at 380 nm, and the full emission spectra were recorded within 410–700 nm using 10 nm and 20 nm bandwidths for excitation (source) and emission (detector), respectively; concentration of antibiotics before mixing = 1 mM; concentration of antibiotics after mixing = 1.25×10^{-4} M.

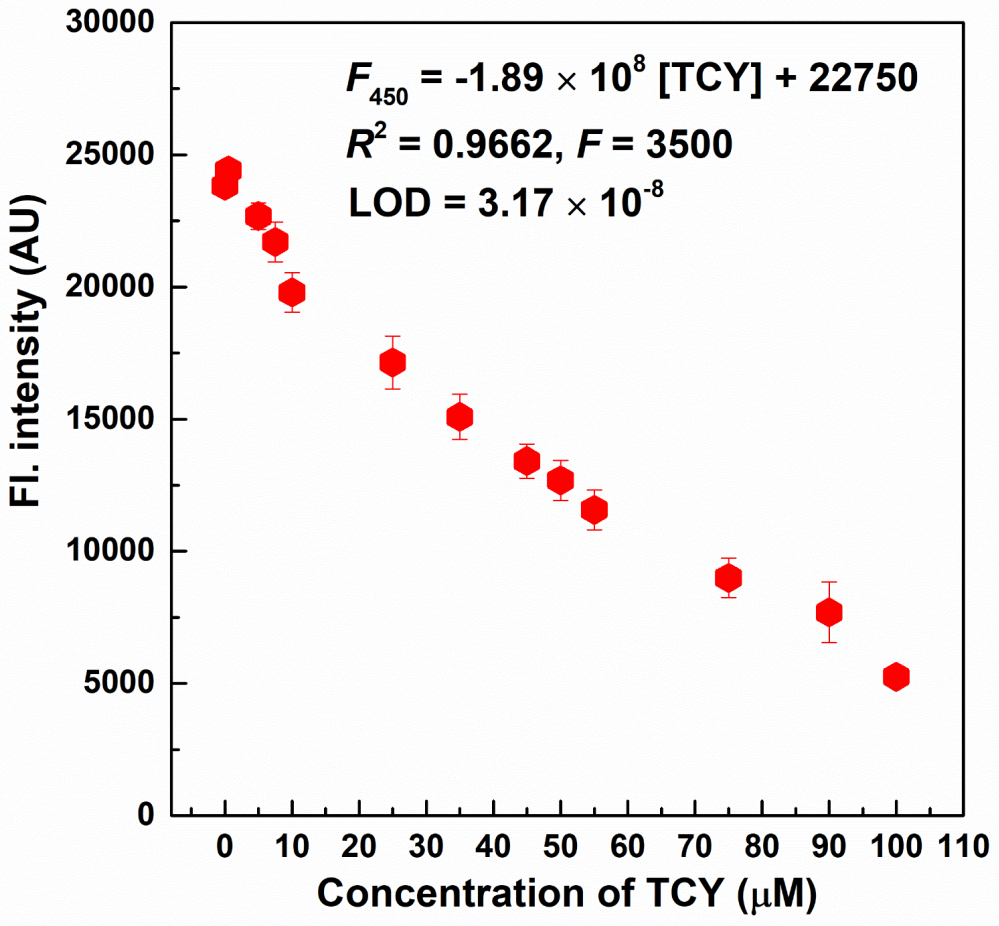

Figure S55. Plot for calculating limit of detection of tetracycline using **NIPUF3**

Table S9 Recent literature of limits of detection for tetracycline sensing

Sample	K_{SV} (M^{-1})	LOD	Type of sensing	Reference
BUT-178 [a]	8.62×10^4	188 nM	Turn-off	[1]
BUT-179 [b]	3.74×10^5	19.8 nM	Turn-off	[1]
RhB CDs@$Cu_2L(OH^-)$ [c]	4.00×10^3	777 ppb	Ratiometric	[2]
RhB@ZIF-8 [d]	7.60×10^4	0.14 μM	Ratiometric	[3]
FSS@ZIF-8 [e]	4.60×10^4	0.17 μM	Ratiometric	[3]
PCN-128Y [f]	9.85×10^5	30 nM	Turn-off	[4]
PEG [g]	1.79×10^4	1.8×10^{-8}	Turn-off	[5]
MoS_2 NPs @Gmp/Eu-Cit [h]	N/A	12.7 nM	Ratiometric	[6]
PFPT [i]	1.57×10^5	14.35 nM	Turn-off	[7]
Mg−Al LDH−Eu [j]	N/A	7.6 nM	Ratiometric	[8]
CDHis [k]	N/A	0.012 μM	Ratiometric	[9]
Cd-MOF [l]	5.98×10^3	3.61 μM	Turn-off	[10]
$CuInS_2$/ZnS QDs [m]	N/A	0.46 μM	Synchronous fluorescence	[11]
Al-MOF@Mo/Zn-MOF [n]	2.19×10^4	0.86 nM	Turn-off	[12]
NIPUF3 (solid material)	**4.36×10^4**	**3.17×10^{-8} M**	**Ratiometric; the color changes were visualized by naked eyes under the UV lamp**	**This study**

[a] BUT-178: Beijing University of Technology 178 prepared by 5′-(4-carboxyphenyl)- 2′,4′,6′-trifluoro[1,1′:3′,1″-terphenyl]-4,4″-dicarboxylic acid (H_3CTFTA); [b] BUT179: Beijing University of Technology prepared by 5′-(4-carboxyphenyl)-2′,4′,6′-trichloro- [1,1′:3′,1″-terphenyl]-4,4″-dicarboxylic acid (H_3CTCTA); [c] RhB CDs@Cu2L(OH-): RhB = rhodamine B, CDs = carbon dots, L = 1,3-bis(4′-carboxylic acid benzyloxy)benzoic acid; [d] Zeolitic imidazolate framework-8 loaded with rhodamine B (RhB) dye; [e] Zeolitic imidazolate framework-8 loaded with fluorescein disodium salt (FSS) dye; [f] Zirconium-based metal organic framework; [g] Poly(ethylene glycol); [h] MoS_2 nanoparticle@guanosine 5′-monophosphate/citric acid; [i] poly[5,5′-(((2-phenyl-9H-fluorene-9,9-diyl)bis(hexane-6,1-diyl))bis(oxy))diisophthalate] sodium; [j] Europium embedded layered double hydroxide; [k] histidine-modified cyclodextrin; [l] Cadmium-based metal organic framework; [m] Carboxyl-modified $CuInS_2$/ZnS quantum dots; [n] Aluminium-metal organic framework @Mo/Zn metal organic framework

References

[1] L. Liu, Q. Chen, J. Lv, Y. Li, K. Wang, J.-R. Li, Stable Metal–Organic Frameworks for Fluorescent Detection of Tetracycline Antibiotics, Inorg. Chem. 2022, 61, 8015−8021.

[2] K. Zhu, R. Fan, X. Zheng, P. Wang, W. Chen, T. Sun, S. Gai, X. Zhou, Y. Yang, Dual-emitting dye-CDs@ MOFs for selective and sensitive identification of antibiotics and MnO4 − in water. J. Mater. Chem. C. 2019, 7, 15057−15065.

[3] Y.-Q. Zhang, X.-H. Wu, S. Mao, W.-Q. Tao, Z. Li, Highly luminescent sensing for nitrofurans and tetracyclines in water based on zeolitic imidazolate framework-8 incorporated with dyes. Talanta. 2019, 204, 344−352.

[4] Y. Zhou, Q. Yang, D. Zhang, N. Gan, Q. Li, J. Cuan, Detection and removal of antibiotic tetracycline in water with a highly stable luminescent MOF. Sens. Actuators B Chemical. 2018, 262, 137−143

[5] S. Wang, X. Jiang, C. Sun and X. Zheng Kong, Full Green Detection of Antibiotic Tetracyclines Using Fluorescent Poly(ethylene glycol) as the Sensor and the Mechanism Study, ACS Biomater. Sci. Eng. 2022, 8, 3957−3968.

[6] Z. Sun, Y. Gao, Z. Niu, H. Pan, X. Xu, W. Zhang, and X. Zou, Programmable-Printing Paper-Based Device with a MoS2 NP and Gmp/Eu-Cit Fluorescence Couple for Ratiometric Tetracycline Analysis in Various Natural Samples, ACS Sens. 2021, 6, 4038−4047.

[7] A. H. Malik and P. K. Iyer, Conjugated Polyelectrolyte Based Sensitive Detection and Removal of Antibiotics Tetracycline from Water, ACS Appl. Mater. Interfaces 2017, 9, 4433−4439.

[8] Z. Zhou, X. Li, J. Gao, Y. Tang and Q. Wang, Tetracycline Generated Red Luminescence Based on a Novel Lanthanide Functionalized Layered Double Hydroxide Nanoplatform, J. Agric. Food Chem. 2019, 67, 3871−3878.

[9] Q. Li, X. Wang, Q. Huang, Z. Li, B. Z. Tang, S. Mao, Molecular-level enhanced clusterization-triggered emission of nonconventional luminophores in dilute aqueous solution, Nature Communications, 2023) 14:409.

[10] Q.-Q. Li, M.-J. Wen, Y.-S. Zhang, Z.-S. Guo, X. Bai, J.-X. Song, P. Liu, Y.-Y. Wan, J.-L. Li, Multiple fluorescence response behaviors towards antibiotics and bacteria based on a highly stable Cd-MOF. J. Hazard. Mater. 2022, 423, 127132.

[11] X. Chen, J. Lin, Y. Zhuang, S. Huang, J. Chen, Z. Han, Dual-mode turn-on ratiometric fluorescence sensor based on carbon dots and $CuInS_2$/ZnS quantum dots for detection of chlorotetracycline. Spectrochim. Acta. A. 2022, 270, 120851.

[12] C. Li, W. Yang, X. Zhang, Y. Han, W. Tang, T. Yue, Z. Li, A 3D hierarchical dual-metal–organic framework heterostructure up-regulating the preconcentration effect for ultrasensitive fluorescence detection of tetracycline antibiotics. J. Mater. Chem. C 2020, 8, 2054−2064.

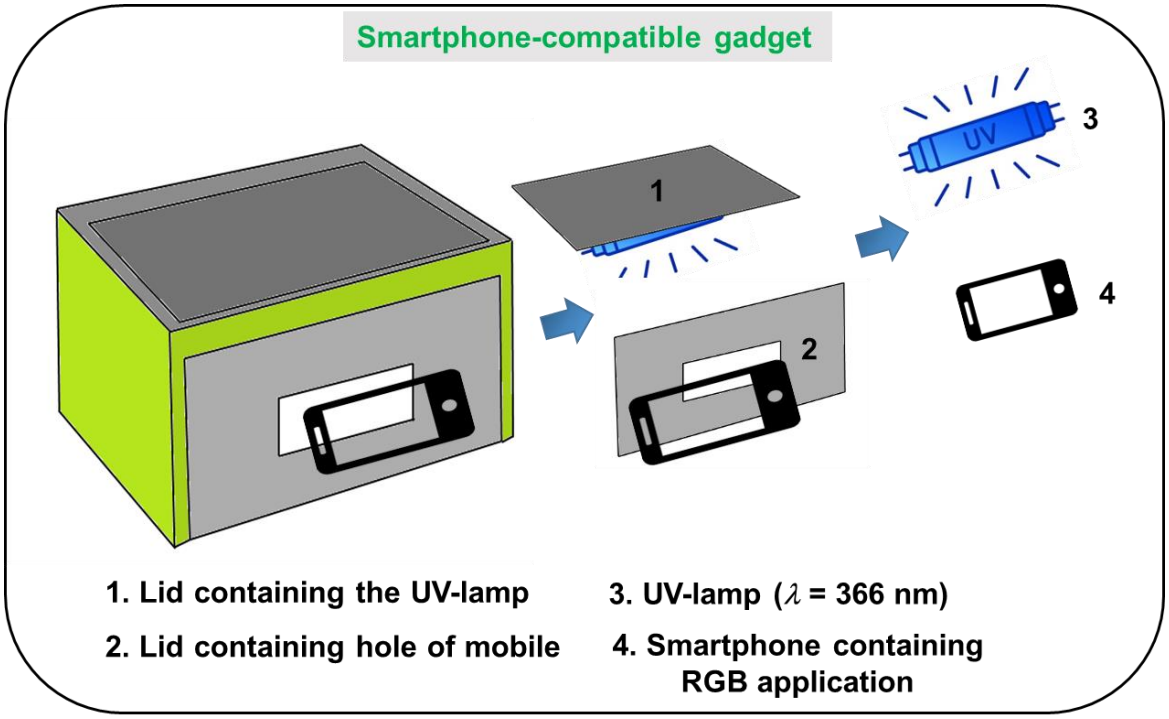

Figure S56. Smartphone-compatible gadget

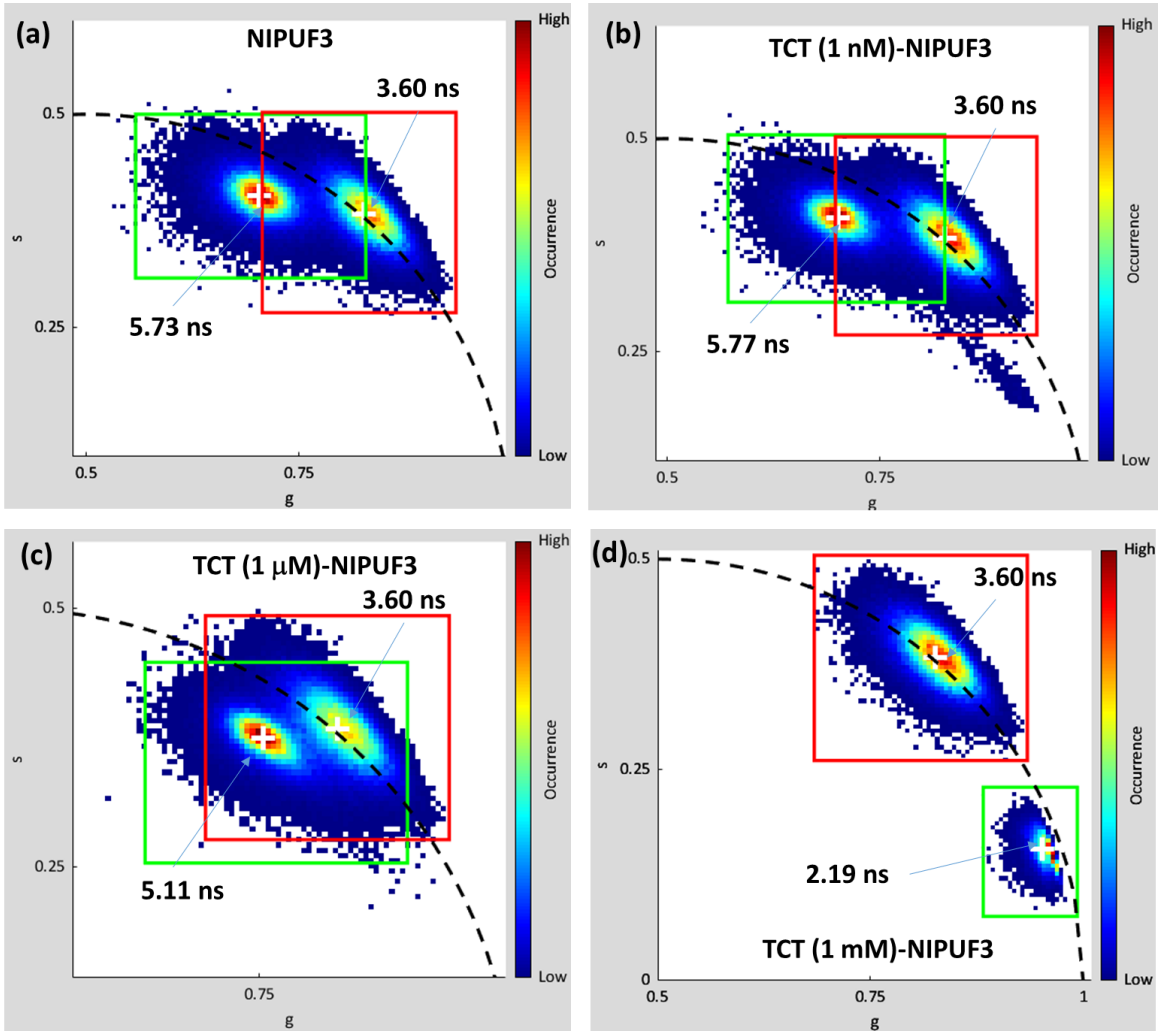

Figure S57. Phasor histogram plots of (a) **NIPUF3**, (b) **TCT (1 nM)-NIPUF3**, (c) **TCT (1 μM)-NIPUF3** and (d) **TCT (1 mM)-NIPUF3** showing lifetimes; the reference atto-425 having 3.60 ns lifetime is used as the reference; the black dotted line corresponds to the universal circle highlighting all possible phasors for monoexponential decays; JET colormaps are used for generating the p**hasor colormaps; the threshold minimum/maximum = 100/ 5000 is used**

Interactions of tetracycline with model compounds of NIPUF3 foam

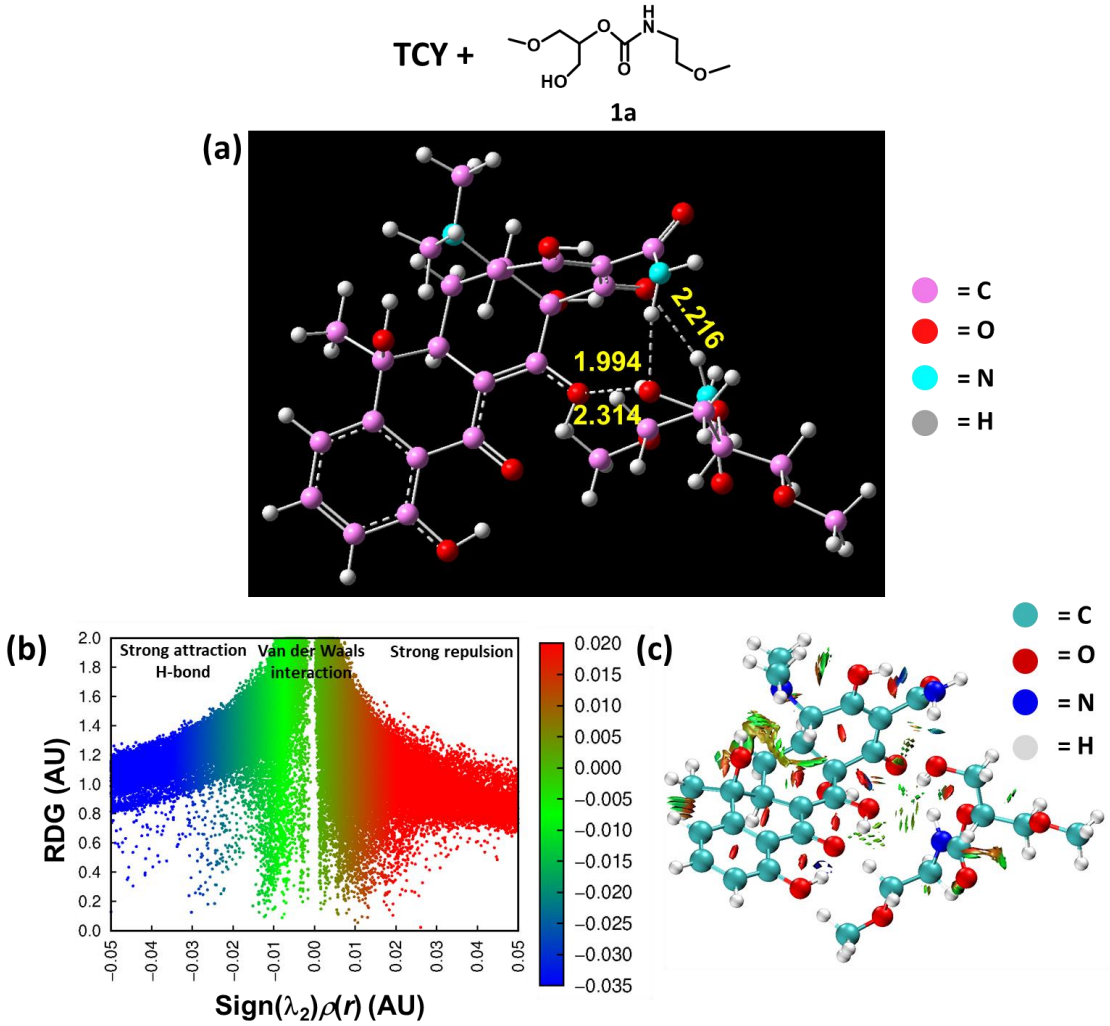

Figure S58. (a) Optimized structure of TCY-model compound 1a showing bond lengths; (b) NCI and (c) independent gradient model plots showing interactions of TCY and model compound 1a; color map −0.035 AU < sign(λ_2)ρ(r) < 0.020 AU

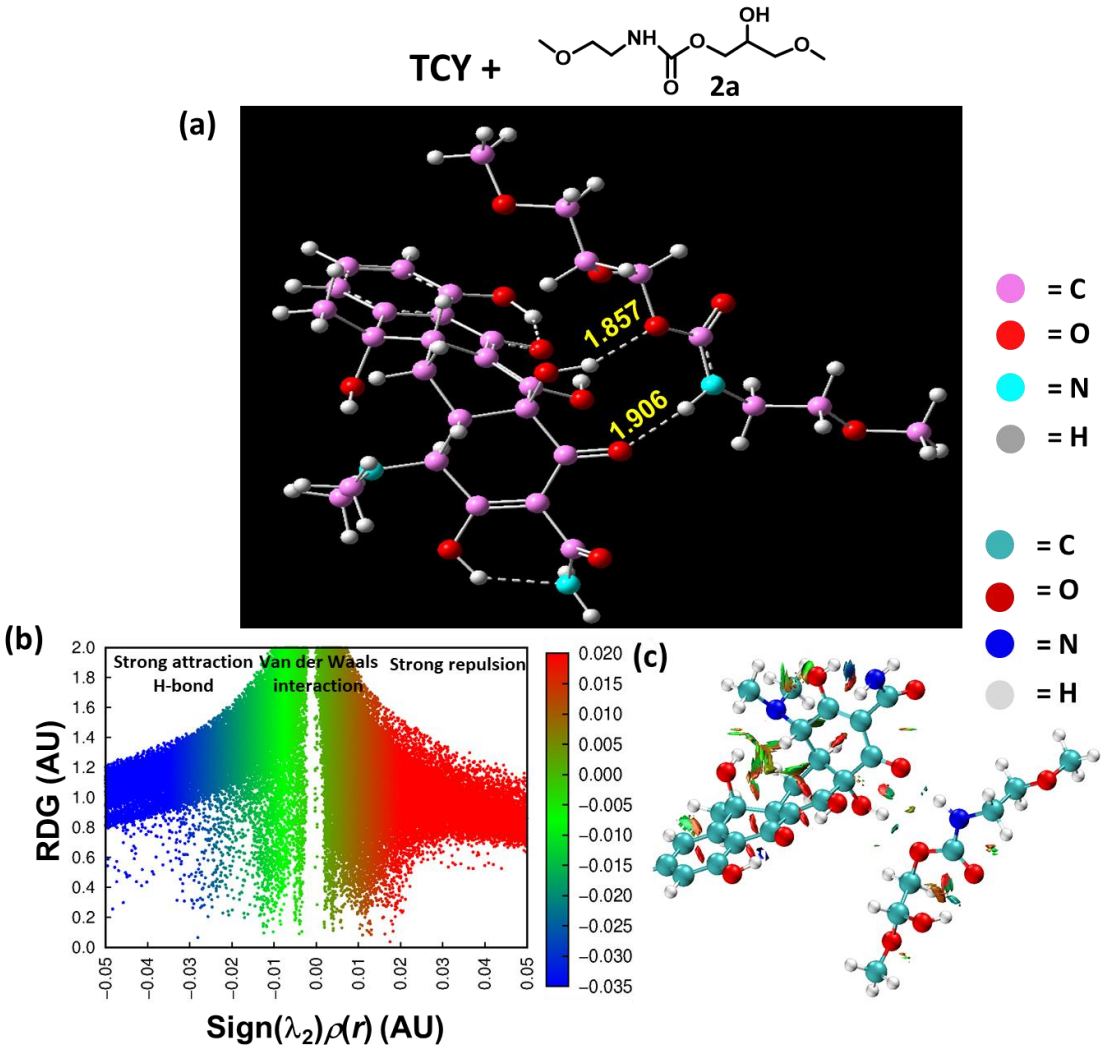

Figure S59. Optimized structures of (a) TCY-model compound 2a showing bond lengths, (b) NCI and (c) independent gradient model plots showing interactions of TCY and model compound 2a; color map −0.035 AU < sign(λ_2)ρ(r) < 0.020 AU

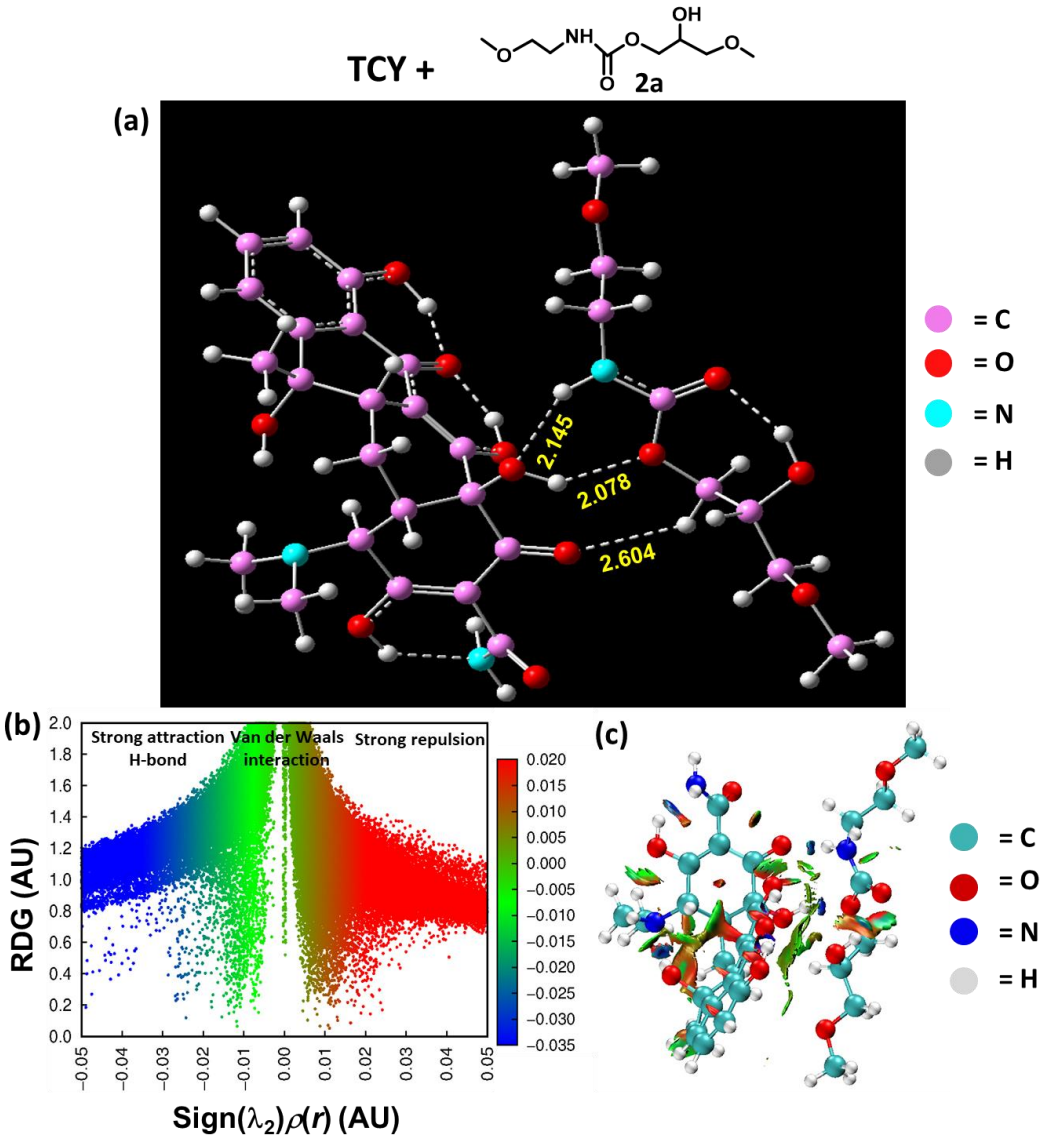

Figure S60. Optimized structures of (a) TCY-model compound 2a showing bond lengths, (b) NCI and (c) independent gradient model plots showing interactions of TCY and model compound 2a; color map −0.035 AU < sign(λ_2)ρ(r) < 0.020 AU

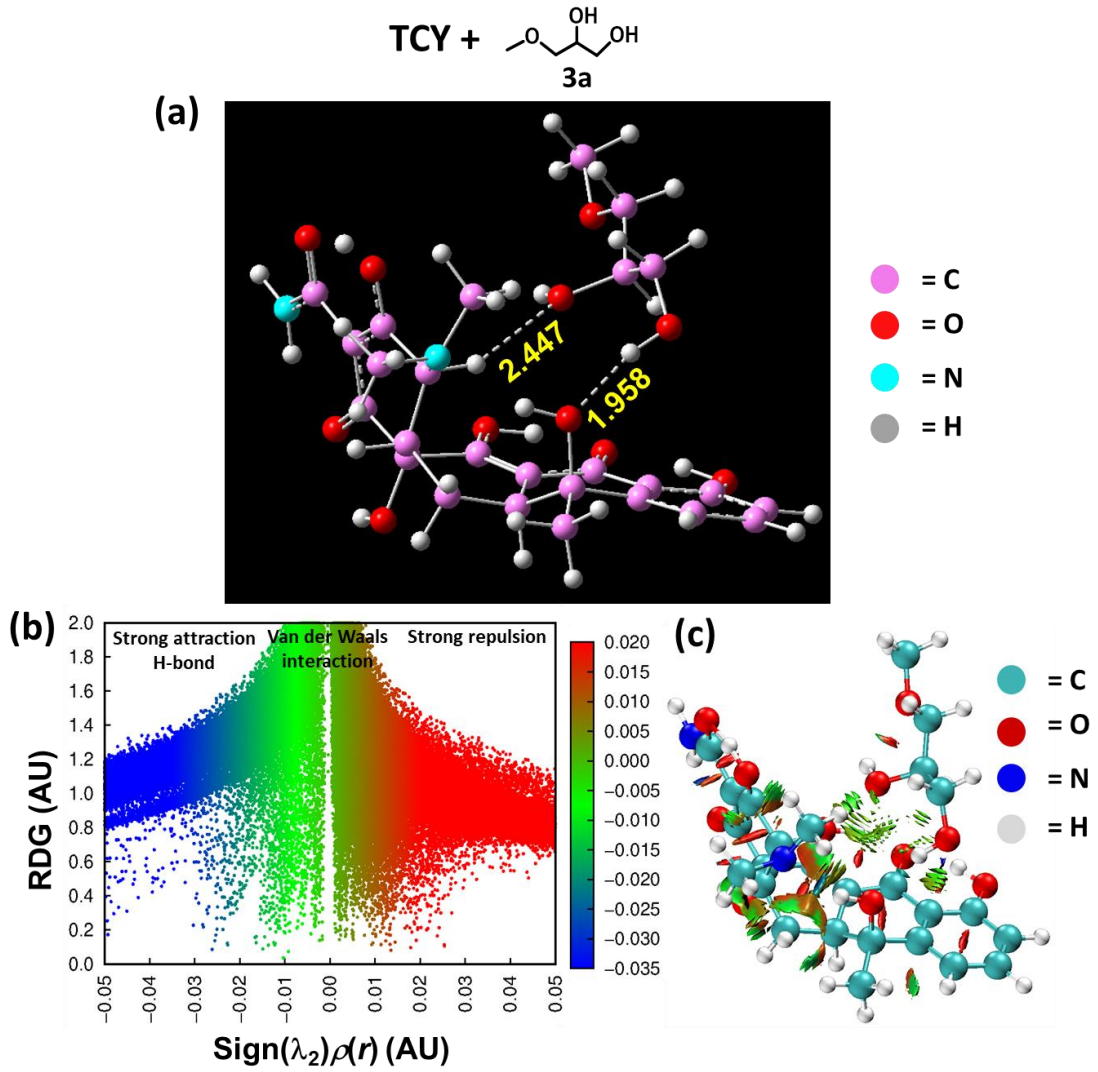

Figure S61. Optimized structures of (a) TCY-model compound 3 showing bond lengths, (b) NCI and (c) independent gradient model plots showing interactions of TCY and model compound 3; color map −0.035 AU < sign(λ_2)ρ(r) < 0.020 AU

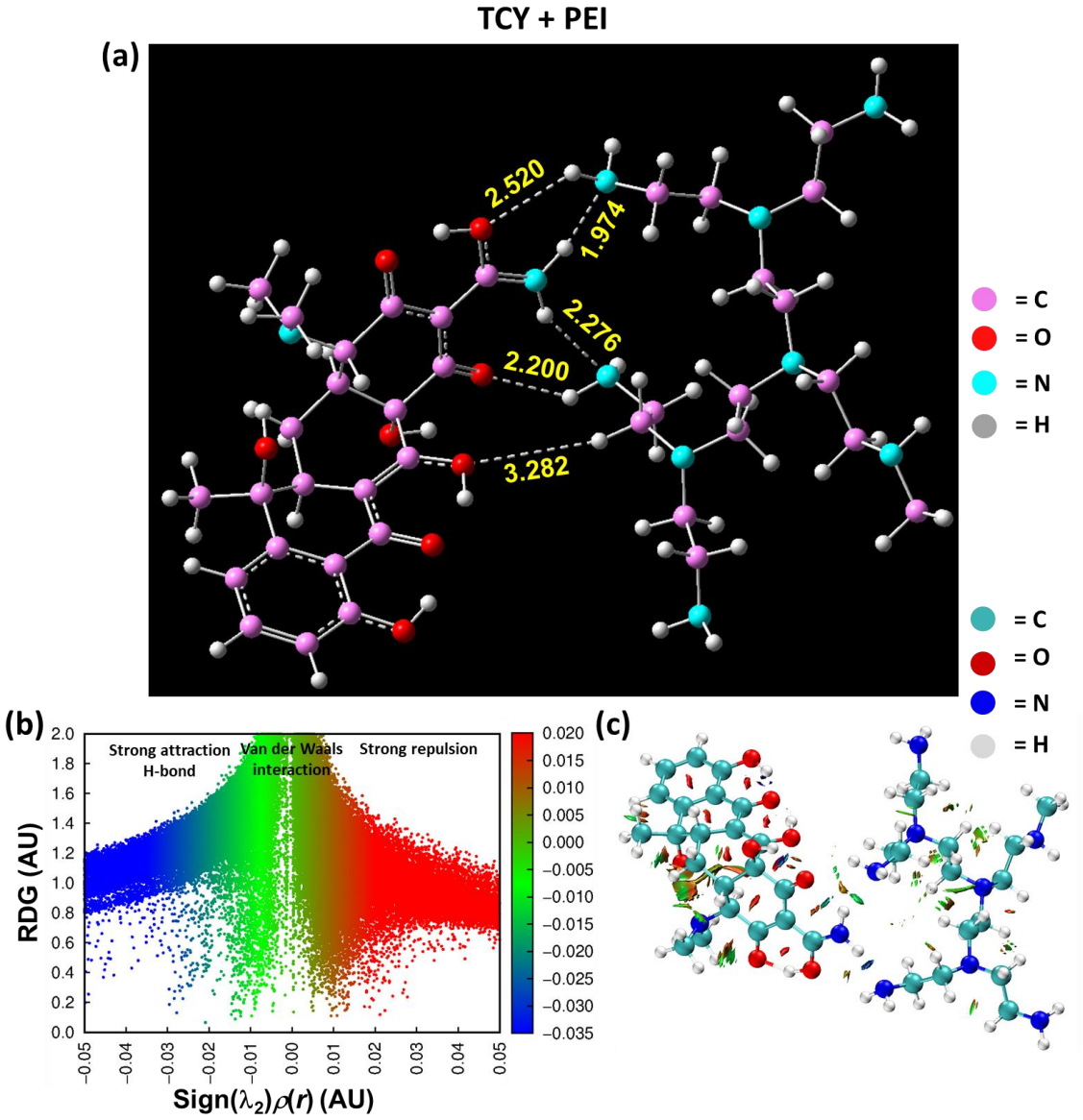

Figure S62. Optimized structures of (a) TCY-PEI showing bond lengths, (b) NCI and (c) independent gradient model (IGM) plots showing interactions of TCY and PEI; color map −0.035 AU < sign(λ_2)ρ(r) < 0.020 AU

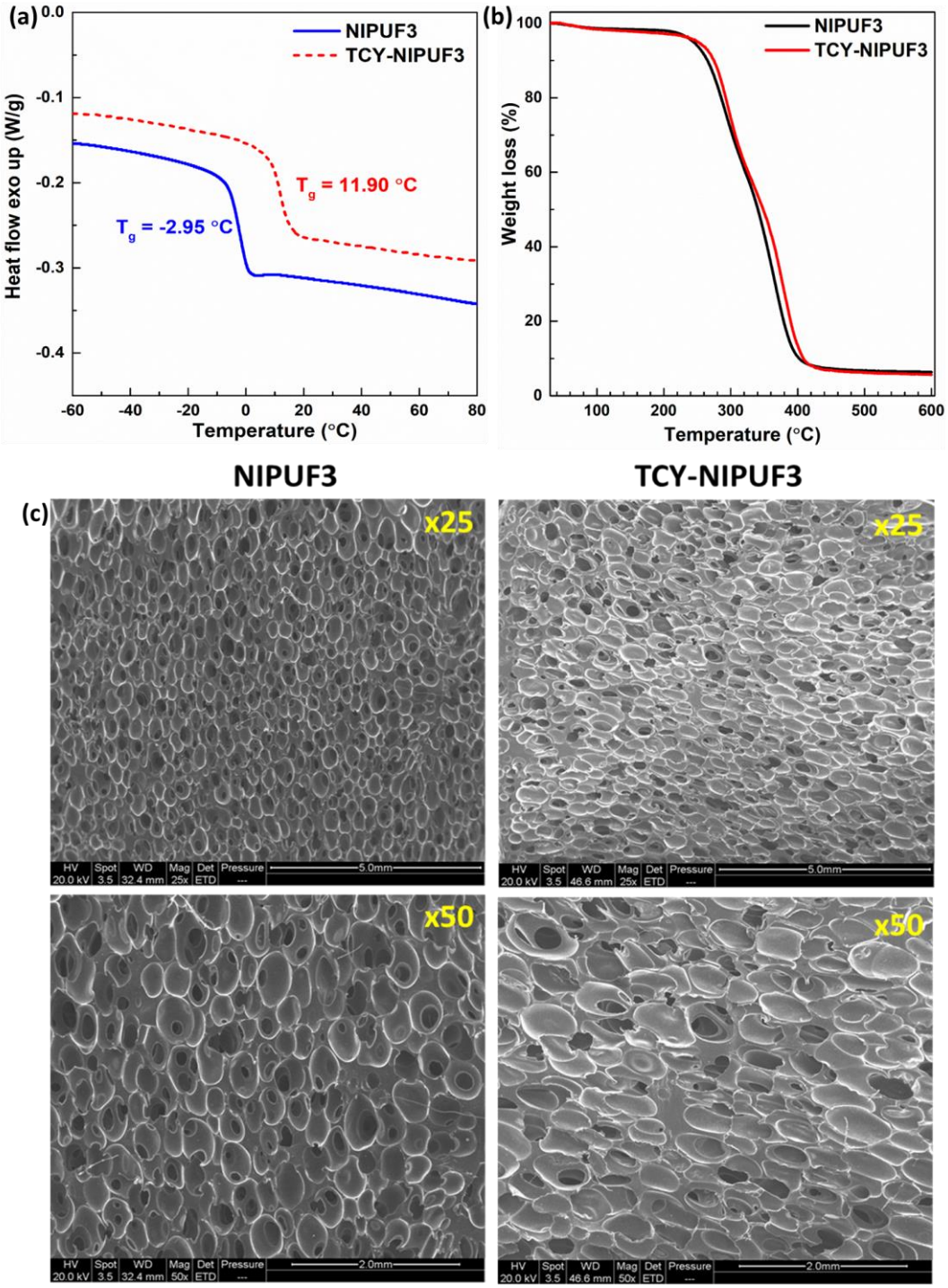

Figure S63. (a) DSC, (b) TGA and (c) SEM photomicrographs of **NIPUF3** and **TCY-NIPUF3**